Application of DLR Method to Evaluation of ATC Considering the Real Time or Predicted Weather Conditions

A Dissertation submitted in fulfillment of the requirements for the Degree
of

MASTER OF ENGINEERING
in
Power Systems

Submitted by

Vishwas Jaryal
801542026

Under the Guidance of
Dr. Amrita Sinha
Assistant Professor, EIED

2017

Electrical and Instrumentation Engineering Department
Thapar University, Patiala
(Declared as Deemed-to-be-University u/s 3 of the UGC Act., 1956)
Post Bag No. 32, Patiala – 147004
Punjab (India)

Declaration

I hereby certify that the project report entitled **"Application of DLR Method to Evaluation of ATC Considering the Real Time or Predicted Weather Conditions"** A Dissertation submitted in fulfilment of the requirements for the award of Degree of Master of Engineering in **Power Systems** submitted in Electrical & Instrumentation Engineering Department of Thapar University, Patiala is an authentic record of my own work carried out under supervision of **Dr. Amrita Sinha**, Assistant Professor, EIED, Thapar University.

The matter presented here in this thesis has not been submitted for the award of any other degree of this or any other university.

Place: Patiala

Date:

Vishwas Jaryal

801542026

It is certified that the above statement made by my student is correct to the best of our knowledge and belief

7/8/17

Dr. Amrita Sinha
Assistant Professor
Thapar University
Patiala

Acknowledgement

I express my deep gratitude and respect to my supervisor **Dr. Amrita Sinha**, Assistant Professor, Electrical & Instrumentation Engineering Department of Thapar University, Patiala for her valuable guidance, strong motivation and constant encouragement during the course of work. I thank her for his great patience, constructive criticism and useful suggestions apart from valuable guidance to me.

I would like to convey my sincere gratitude to my friends and colleagues for her support, cooperation and timely help and valuable discussions.

I owe my sincere thanks to all staff members of **Electrical & Instrumentation Engineering Department** for their support and encouragement. The meaning of my life and work is incomplete without paying regards to my respected parents whose blessings, support and continuous encouragement have shown me the path to achieve my goals.

And above all, I pay my regards to the Almighty for his love and blessings.

Date:

Vishwas Jaryal

Table of Contents

Declaration i

Acknowledgment ii

Table of Contents iii

Nomenclature v

List of tables vii

List of figures viii

Abstract x

Chapter 1. Introduction 1

1.1 Introduction 1

1.2 Literature survey 1

1.3 Thesis objective 5

1.4 Organization of dissertation 5

Chapter 2. Dynamic Line Rating Models 7

2.1 DLR models 7

2.2 ACSR Transmission Conductor 9

Chapter 3. Methodology of DLR calculation 12

3.1 Power flow method 12

3.2 Calculation for dynamic ampacity with the effect of dynamic weather conditions 14

3.3 flow chart for ATC calculation 19

Chapter 4. Methodology of DLR for 6-bus system 20

4.1 IEEE-6 bus test system 20

4.2 Industry Standard Methodology 22

4.3 Conductor MOT determination 22

4.4 Variation in current flow considering DLR 25

4.5 Graphical and Tabular representation of the ATC 26

Chapter 5. Methodology of DLR for 30-bus system 42

5.1 IEEE 30 bus test system 42

5.2 Variation in current flow considering DLR 47

5.3 Losses with and without considering DLR method 47

5.4 Results for ATC of line considering the DLR 48

Chapter 6. Conclusion and Future work 64

6.1 Conclusion 64

6.2 Future Work 65

References 66

Appendix 69

Nomenclature

A'	Area of Projection of transmission line per unit length	m^2/m
ATC	Available transfer capability	MW
C	Solar azimuth constant	degrees
D	Diameter of the Conductor	mm
DLR	Dynamic line rating	
H_c	Altitude of sun	degrees
H_e	Height of Elevation of transmission line above sea level	m
I	Altitude of sun Current Carried by conductor	A
I_f	Current before steps changes	A
I_i	Day of the year (Jan 10 = 10, Feb 12 = 43)	
K_{solar}	Solar altitude correction factor	
K_{angle}	Factor of wind direction	—
k_f	Thermal conductivity of air at temperature T_{flim}	$W/m\text{-}^0C$
Lat	Degrees of latitude	Degrees
N	Current after change in steps	A
q_{cn}, q_{c1}, q_{c2}, q_c	heat loss due to Convection per unit	W/m
q_r	heat loss rate due to Radiation per unit length	W/m
Q_s	Total sky and solar heat flux rate due to radiation	W/m^2
R_{T_c}	AC resistance of conductor at temperature, T_C	Ω/m

T_{low}	Minimum temperature of conductor for which ac resistance is specified	°C
TTC	Total transfer capability	MW
T_a	Ambient air temperature	°C
T_{flim}	$(T_c + T_a)/2$	°C
T_{high}	Max. temperature of conductor	°C
T_c	Temperature of Conductor	
W_s	Wind speed at conductor	m/s
δ	Solar declination (0 to 90)	degrees
ε	Emissivity (0.2 to 0.9)	—
c	Sun's Azimuth	
φ	Angle between conductor axis and wind	degrees
α	Solar absorptivity (0.2 to 0.9)	—
ρ_f	Density of air	kg/m^3
β	Angle between perpendicular conductor axis and wind	degrees
ω	Hours from local sun noon times 15^0	degrees
θ	sun's rays Effective angle of incidence	degrees
χ	Solar azimuth variable	—

List of Table

Table 2.1 electrical and physical properties of ACSR conductor 10
Table 2.2 Weather effect on ampacity of the line 10
Table 2.3 Specification for Overall wire diameter 11
Table 3.1 Constants for clear atmosphere 17
Table 3.2 Constants for industrial atmosphere 17
Table 4.1 Bus data and line data for IEEE 6-bus system 20
Table 4.2 Power flow in lines 21
Table 4.3 Maximum Temperature limit on which conductor can work 22
Table 4.4 Maximum Allowable Conductor temperature for IEEE 6-bus test system 23
Table 4.5 Comparison of ATC from bus 2-6 for MOOSE and ZEBRA 26
Table 4.6 Available transfer capability from bus 1-5 and 1-4 30
Table 4.7 Available transfer capability from bus 2-4, 2-3 and 2-5 34
Table 4.8 Available transfer capability from bus 3-6 and 3-5 38
Table 5.1 Bus data for IEEE-30 bus test system 42
Table 5.2 Line Data for IEEE-30 bus system 43
Table 5.3 Power Flow from generator bus to load bus 45
Table 5.4 Specified conductor temperature 45
Table 5.5 Comparison of ATC from bus 1-2 for MOOSE and ZEBRA 48
Table 5.6 Available transfer capability from bus 1-3 51
Table 5.7 Available transfer capability from bus 2-4 and 2-6 54
Table 5.8 Available transfer capability from bus 5-7 58
Table 5.9 Available transfer capability of from bus 12-13 60
Table 5.10 Available transfer capability from bus 8-28 62

List of Figure

Figure 2.1 High voltage ACSR conductor 9
Figure 3.1 Flow chart showing the ATC calculation 19
Figure 4.1 IEEE 6-bus system 20
Figure 4.2 Test line (2-6) for ATC calculation 24
Figure 4.3 Variations in current flow from line (2-4) for a whole day 25
Figure 4.4 Losses in the system from line (2-6) considering DLR method 26
Figure 4.5 Hourly Representation of ATC from line 2-6 at 45^0(MOOSE) 28
Figure 4.6 Hourly Representation of ATC from line 2-6 at 90^0(MOOSE) 28
Figure 4.7 Hourly Representation of ATC from line 2-6 at 45^0(ZEBRA) 29
Figure 4.8 Hourly Representation of ATC from line 2-6 at 90^0(ZEBRA) 29
Figure 4.9 Test line (1-4 and 1-5) for ATC calculation 30
Figure 4.10 Hourly Representation of ATC from line 1-4 at 45^0 31
Figure 4.11 Hourly Representation of ATC from line 1-4 at 90^0 32
Figure 4.12 Hourly Representation of ATC from line 1-5 at 45^0 32
Figure 4.13 Hourly Representation of ATC from line 1-5 at 90^0 33
Figure 4.14 Test line (2-3, 2-4 and 2-5) for ATC calculation 33
Figure 4.15 Hourly Representation of ATC from line 2-4 at 45^0 35
Figure 4.16 Hourly Representation of ATC from line 2-4 at 90^0 35
Figure 4.17 Hourly Representation of ATC from line 2-3at 45^0 36
Figure 4.18 Hourly Representation of ATC from line 2-3 at 90^0 36
Figure 4.19 Hourly Representation of ATC from line 2-5 at 45^0 37
Figure 4.20 Hourly Representation of ATC from line 2-5 at 90^0 37
Figure 4.21 Test line (3-5, and 3-6) for ATC calculation 38
Figure 4.22 Hourly Representation of ATC from line 3-6 at 45^0 39
Figure 4.23 Hourly Representation of ATC from line 3-6 at 90^0 40
Figure 4.24 Hourly Representation of ATC from line 3-5at 45^0 40
Figure 4.25 Hourly Representation of ATC from line 3-5 at 90^0 41
Figure 5.1 Test line (1-2 and 1-3) for ATC calculation 46
Figure 5.2 Variations in current flow from line (1-2) for a whole day 47

Figure 5.3 Losses in the system from line (1-2) considering DLR method 48
Figure 5.4 Hourly Representation of ATC from line 1-2 at 45^0(ZEBRA) 49
Figure 5.5 Hourly Representation of ATC from line 1-2 at 90^0(ZEBRA) 50
Figure 5.6 Hourly Representation of ATC from line 1-2 at 45^0(MOOSE) 50
Figure 5.7 Hourly Representation of ATC from line 1-2 at 90^0(MOOSE) 51
Figure 5.8 Hourly Representation of ATC from line 1-3 at 45^0 52
Figure 5.9 Hourly Representation of ATC from line 1-3 at 90^0 53
Figure 5.10 Test line (2-4 and 2-6) for ATC calculation 53
Figure 5.11 Hourly Representation of ATC from line 2-4 at 45^0 55
Figure 5.12 Hourly Representation of ATC from line 2-4 at 90^0 55
Figure 5.13 Hourly Representation of ATC from line 2-6at 45^0 56
Figure 5.14 Hourly Representation of ATC from line 2-6 at 90^0 56
Figure 5.15 Test lines (5-7, 12-13 and 8-28) for ATC calculation 57
Figure 5.16 Hourly Representation of ATC from line 5-7 at 45^0 59
Figure 5.17 Hourly Representation of ATC from line 5-7 at 90^0 59
Figure 5.18 Hourly Representation of ATC from line 12-13 at 45^0 61
Figure 5.19 Hourly Representation of ATC from line 12-13 at 90^0 61
Figure 5.20 Hourly Representation of ATC from line 8-28 at 45^0 63
Figure 5.21 Hourly Representation of ATC from line 8-28 at 90^0 63

Abstract

In order to obtain the optimal usage of maximum already present transmission structure is more preferable than reconstruction of already existing transmission lines (TLs). Advancements in, technologies, sensors and communication system make possible to calculate the real time thermal capacity of transmission lines and that rating is called dynamic rating. For this competitive energy market, transmission capability of line and condition of the system in real time is necessary to predict for future operations. In this thesis the dynamic transmission line rating (DLR) method is considered, rather than static rating for the calculation. The DLR of line is done by considering repetitive calculation of the line current based on dynamic environmental conditions. It reflects that use of DLR has a vast effect for the calculation of available transfer capability (ATC) of TLs. A MATLAB program has been developed for calculating the dynamic rating using IEEE standard 738. The aim of this work is to minimize the difference between Actual power flow in the line and the power i.e. calculated with considering the effect of dynamic weather conditions. With this it has been trying to predict that at what wind speed, Temperature, and wind angle the power transfer will be maximum. Online or predicted weather data can also be fetched and calculate that at what time of the day the line has been able to transfer the maximum power to the load. IEEE 6-bus system and 30-bus system have been used as test system.

Chapter1. Introduction

1.1 Introduction

Due to increase in demand of electric energy in last few years, increasing the capacity of existing transmission lines (TL) has been facing economical constraint. The transfer of power through TL has stability, thermal and voltage constraints out of which the thermal constraint has maximum effect on it. In the thermal constraint has been emphasized for calculating the power transfer for north paths of California's bus system over thermal and voltage constraint [3]. The power transfer capability of TL has been traditionally calculated using static rating method. This is fixed rating method and is calculated based on some assumptions related to fixed weather parameters while the Dynamic line rating (DLR) method, considers the real time or predicted weather conditions for determining the ampacity of the conductor which approaches to its maximum power transfer capability. DLR method calculates the maximum power transfer of TL and helps the utility to update the system on the basis of real time ambient data without violation of the design limits. To explain the dynamic nature of power transfer through overhead conductor following parameters are considered: -

1. Wind speed
2. Ambient temperature
3. Wind speed angle with respect to the conductor's axis
4. Solar radiation
5. Line loading
6. The Assumed maximum allowable conductor temperature
7. Conductor characteristics.

1.2 Literature survey

Bahadoor sinsh *et al* [1] developed studies for actual monitoring of transmission line throughout the last thirty years, and also some case studies around the world, and brings out the advantages

and technical limitations of using dynamic line rating on overhead lines. Further, the utilization of those DLR systems in wind integration is reviewed

Fernandez. E *et al* [2] discussed the significance of DLR method from the viewpoint of available transfer capability (ATC) and apply that system for wind power integration.

M.mahmoudian and G.R.yousefi [3] discussed the significant effect of using of dynamic resistance in loss estimation, and also the optimal use of conductor's thermal capacity without considering real thermal lines capacity is impossible. Static ratings can be improved by forecasting day ahead weather conditions. Conventionally, the worst weather conditions are used for determination of static ratings and try to improve the ATC of TLs. ATC improvement means increasing the capability of power transferring.

Abdalla *et al* [4] developed a model in MATLAB to solved the dynamic ampacity of the TLs. The ambient temperature and speed of the wind is taken at different instants to verify the ampacity of line with tolerable limits. The burden of the transmission lines improves with the speed of wind, i.e. it allows extra power to be transmitted

Tony yip *et al* [5] discussed that the dynamic line rating is also very useful for protection and load management of a 132kV system line. The line rating has been determined dynamically using local environmental condition measurements to compare the specified generation automatically.

Igor albizu *et al* [6] discussed an approach of improving the power carrying capability of the line by designing the transmission conductor with a much higher working temperature. Which needs the allowable temperature of the conductor to be raised to 70^{o}C and above. Also, the life span of transmission lines, strength of the conductor and other parameters has been studied.

Marija bockarjova and Goran andersson [8] have studied that the change of overhead line resistances due to ambient temperature have high impact on state estimation accuracy. The state estimation has been improved if resistance of transmission model is corrected to particular loading and weather conditions.

IEEE Std. 738 [11] has described the methodology (formulas) for the calculation of effect of change in ambient temperature and wind speed on ampacity of transmission line network. And also describe the methodology to solve the current carrying capability of conductor using which it

has been also possible to calculate the power transfer capability of TL. For an overhead transmission line, if the conductor's temperature (Tc) and the static environmental parameters (Ws, Ta, etc.) are known; the solar heat gain (qs), the heat losses due to radiation and convection (qr and qc), and the dynamic conductor resistance R(Tc) can be calculated. Under these environmental conditions the analogous current of the conductor is known using steady state techniques. Whereas this calculation is often done for any conductor temperature and any environmental conditions, i.e. "conservative" weather conditions (e.g., 0.6 m/s to 1.2 m/s wind speed, 30°C to 45°C summer ambient) are often used to find a static thermal rating for the conductor and a maximum allowable conductor temperature (e.g., 75 °C to 150 °C).

Maski miura *et al* [12] discussed the validity of DLR method from the view point of ATC. Dynamic rating which varies operation constraints dynamically has been introduced to increase and attain efficiency in operation of power system. Tie-line ATC has been proposed or discussed as a test system.

Central Electricity Authority[13] has described the ampacity and MW loading (assuming nominal voltage and unity power factor) for normally used conductors, i.e. ACSR Moose, ACSR Bersimis, Zebra and Panther, for every 2^0C temperature drop below 40^0C and for every 2^0C temperature drop below 45^0C between 45^0C and 40^0C, for maximum temperature of 75^0C and consider the variable wind speed as per the practical historical conditions and suggest the power which has been effected with the change in weather conditions ampacity calculations has been performed with the help of IEEE standard 738[11]

Marco merante [14] discussed that the monitoring of overhead lines has been necessary to avoid clearance to ground matters caused by overheating of conductor. The different weather data has been studied in order to find conductor temperature. This calculation confirmed the significant influence that convicted cooling has on the overall conductor thermal balance and showed that stranded conductor cannot be exactly related with perfect cylinders.

Douglass *et al* [15] discussed the dynamic line rating of TLs on the basis of real time weather data or real time tension data. For the weather based calculation the wind angle should be considered fixed and near parallel to the TL.

Dale.A.douglass el al [16] discussed a SCADA/EMS based dynamic thermal circuit rating (DTCR) system. The equipment has been connected in series and parallel combinations and finding the most limiting ampacity for each rating situation.

Mai Ruikun *et al* [17] presents a DLR estimator with synchronized phasor measurement to attain the actual conductor temperature and predict the current carrying capability of the transmission lines, the time to violate the conductors' thermal limits and the final conductor temperature. Such information has been helpful to find the increased power transfer capability of the lines.

S.S.mousavi-seyedi *et al* [18] has described the two type of DTR (dynamic thermal rating) methods, namely environment conditions based method and on-line monitoring of TL ambient temperature. The second method contributes the major part of the work and first method has been only reviewed. For the estimation process NWLS (non-linear weighted least square) based algorithm have been adopted. MATLAB simulation has been used to simulate a typical TL and further the performance of the proposed method has been demonstrated on this simulated system.

H.D. chiang *et al* [20] discussed the method for continuous power flow to devolved a tool for tracing the steady-state behavior of power system due to variation in generation and load.

Wijethunga A.H. *et al* [21] developed a MATLAB based model to assess the dynamic ampacity of a transmission line with change of wind speed and temperature. The sampling rate of wind speed and temperature profiles has been taken from real time measurements of the previous year and its effect on only line's ampacity has been evaluated.

Black W.Z. and R.L. rehberg [22] recognized that the equations and the parameters which used to calculate the DLR method shows that the convective mode of heat transfer completely dominates the heat transfer leaving the conductor. Therefore, those factors which dictate the value of the convective heat transfer coefficient have the greatest influence on the ampacity of an overhead conductor as well as how that conductor responds thermally to a change in current. While the conductor emissivity, absorptivity and incident solar flux affect the temperature of the conductor, the influence of these parameters on thermal behavior of the conductor has been secondary to the influence produced by the convection parameters.

W.Z.black and W.R.byrd [23] discussed that the convected heat transfer have been more significant than the radiated heat transfer in determining the temperature of conductor. The wind speed and wind direction are the two supreme factors which specify the convection from the surface of the conductor. Therefore, an information of the wind speed and direction of the wind at the line location is important if the computer program has to precisely forecast the conductor temperature.

Cigre [29] has explained that the application of the real time monitoring system will depend on the type of constraint the utility or system operator has been facing. It may not always be the solution for uprating of a line; however, it can assist in delaying new construction or accommodating new build delays as shown in the case studies. A particularly interesting and more and more frequent application of a direct real time monitoring system has been on-line that are congested due to the integration of renewable production. Currently this production has been often reduced to remain below the static limits of the adjacent network.

1.3 Thesis objective

The proposed system of IEEE standard 738 has been implemented on MATLAB to study the nature of transmission line Parameters at dynamic atmospheric conditions.

i. Find the wind speed, ambient temperature and time of the day at which the difference between TTC (total transfer capability) and ATC (available transfer capability) of line is minimum or the time at which ATC exceeds the TTC
ii. Variation in dynamic current flow in line and compare with actual current flow in the line.
iii. Try to find the minimum losses with dynamic weather conditions and compare with actual losses in the line.
iv. Predict the value of ATC as per predicted or real time weather conditions.

1.4 Organization of dissertation

The dissertation structure has been organized as follows:

Chapter-1 gives a brief overview of dynamic line rating method, background, thesis objective and literature survey.

Chapter-2 covers a brief discussion on DLR methods and algorithm used for the calculation of DLR method.

Chapter-3 covers the results for IEEE 6-bus test system.

Chapter-4 covers the results for IEEE 30-bus test system.

Chapter-5 covers the conclusion and future scope.

Chapter2. Dynamic Line Rating Models

2.1 DLR models

The heat transfer process of a transmission conductor can be designed starting with different parameters. The purpose of this is to achieve the trade-off between system costs and precision. Different arrangements can achieve the goal basing on the different conditions where DLR (Dynamic Line Rating) has to be applied. Overhead line (OHL) parameters can be considered in real time by different devices connected to the operational center in different ways. The main line's characteristics that are monitored are sag, temperature and tension [15]. Dynamic Line rating can be calculated by computer programs if environmental conditions and load on a line are also known. From singular input it is difficult to calculate the line's rating. To rate means to have an understanding of how the component behaves on the different conditions it will experience. This means that different parameters should be calculated and crossed-verified to obtain a reliable forecast on the Transmission conductor behavior under different environmental conditions [23]. The early software that has been developed to calculate different measurement inputs and obtain the rating of grid components is EPRIS's DTCR (Dynamic Thermal Circuit Rating) [16]. This software contains three different models for evaluation. These models represent a classification of all the different set-ups that have been worked and are still used nowadays. These are:

- Temperature Based DLR
- Tension/ Sag Based DLR
- Weather Based DLR

Temperature based DLR

With this method the score is received starting from an instantaneous size of the conductor temperature in mixture with the line present day, air temperature and sun heating values [15]. The update conductor temperature is converted to an equivalent wind speed perpendicular to the line. Then knowing the entire climate parameters, the score can subsequently be obtained through the identical heat balance equation used inside the weather-primarily based approach. This method as

the benefit that a right away dimension of the temperature is available. in this way a fast feedback of the line situations is available. The temperature is generally measured by means of devices located immediately on the conductor. Some other technique to estimate the conductor temperature is through phase measurement devices as it's far analyzed in [17], [18].

Sag/Tension based DLR

The majority of transmission and distribution lines are constrained by clearance to ground limits and not by annealing issues [16]. In these cases, a direct determination of the sag amplitude is important. Sag is directly related to the line tension. Line's tension magnitude depends on the average weather conditions present along all the spans between two tension poles. The consequence is that ratings based on a single sag-tension monitor are comparable with ratings obtained through several weather stations along all the line sections. Tension monitors are normally installed when the line is de-energized. This means that commonly to apply this device an outage is required.

Weather- Based DLR

This method estimates the rating from load data and environmental conditions. Through one of the heat balance of the conductor it is possible to calculate the temperature of a conductor and therefore rate the overhead transmission line [21]. It represents the simplest approach and it is the cheapest also since no devices have to be installed directly on the line and survive an environment of high electromagnetism. The accuracy of the calculation depends on the number and proximity of weather stations to the overhead line. The higher the number and the closer to the line, the better will be the temperature estimation. The measured data have to be the closer possible to the ones experienced by the conductor itself. The main advantages of this method are: Independency from line current, the equipment used for monitoring is relatively cheap, not requiring line outages to install and maintenance operations of expensive equipment and environmental data may also be used to rate all the close grid equipment.

2.2 ACSR Transmission Conductor

Because of the increase in the use of these transmission conductors, ACSR (Aluminum conductor steel reinforced) has been chosen for the analysis [24], however it doesn't actually represent the conductor used by international standards. Other conductor options are all aluminum copper and alloy of aluminum. Copper is a good conductor than aluminum, however the copper is expensive than aluminum and has a higher density, and it also requiring extra reinforcement on Transmission towers. ACSR's most required property is its high ratio of strength-to-weight, while maintaining the conductivity of conductor at a good level. For this reason, it is common to use ACSR in medium and high-voltage transmission lines. These conductors are not a single wire but comprised of several aluminum and steel strands built in a spiraled configuration. The stranded design is used to give flexibility in the cable. Figure below shows a schematic of 54/7 ACSR cable; it consists of 54 outer strands of aluminum wire and 7 center strands of steel wire. Throughout this thesis work Starling 26/7 ACSR conductor is used for the analysis. Table 2.1 gives the electrical and physical properties of the ACSR conductor [24]. The effect of weather on ampacity of hawk ACSR overhead line with static line rating for morning time at 30^0C and wind speed of 0.6m/s has been tabulated in Table 2.2. The static resistance for different types and cross-sectional area of overhead conductor has been tabulated in Table 2.3.

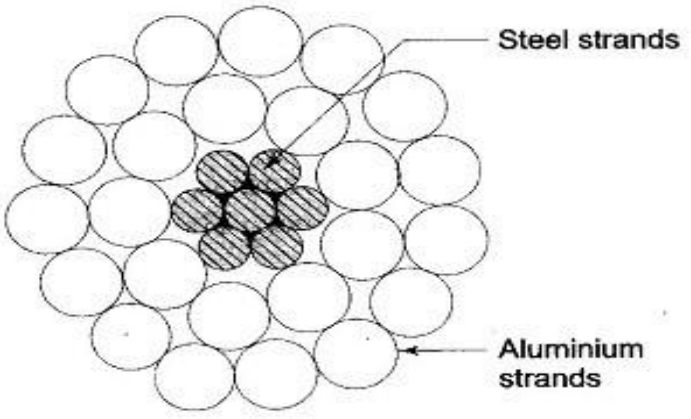

Figure 2.1 High voltage ACSR conductor

Table 2.1 electrical and physical properties of ACSR conductor

Property	Value	Unit
Conductor nominal diameter	2.667	[cm]
Aluminum wire diameter	4.214	[mm]
Steel wire diameter	3.277	[mm]
Resistance at 25°C	8.00525	[ohm/m]
Resistance at 75°C	9.58005	[ohm/m]
Aluminum specific heat	955	[J/kg°C]
Steel specific heat	476	[J/kg^{0}C]

Table 2.2 Weather effect on ampacity of the line

Hawk ACSR Over Head-line (thirty km) with Static Line Rating consideration: 30°C, 0.6 m/sec and morning-time	
Changes in environmental Parameter (s)	Variation in Conductor ampacity
Ambient Temperature (°C) + 5°C Variation - 5°C Variation	 21.7 % Capacity is decrease 17.7 % Capacity is Increase
Speed of wind (m/sec) at line corridor 1 m/sec Increase 45^{0}angle 90^{0}angle	 24.8 % Capacity is Increase 36.9 % Capacity is Increase

Table 2.3 Specification for Overall wire diameter

Code name	Nominal Area [mm]	Al No. of wires/c/s of wires	Steel wires/c/s of wires	Overall Diameter[mm]	Resistance [Ω/km]
Ibis	234	26/3.14	7/2.44	19.9	0.1430
Dove	**329**	**26/3.72**	**7/2.89**	**23.6**	**0.1020**
Al 59	241	19/4.02	0	20.1	0.1230
Al 59	**454**	**61/3.08**	**0**	**27.7**	**0.0654**
Al 59	**593**	**61/3.52**	**0**	**31.7**	**0.0501**

Macro Merante [14] performed a laboratory test to find the accurate maximum conductor temperature. The highlight yellow conductors are the one that have been tested in the 13 days long test.

The procedure consisted on heating up the pieces until the steady state temperature value. Once the equilibrium in steady air is achieved the fan is powered and the wind cooling process is traced until a new equilibrium temperature is reached. The new temperature allows to obtain the increase in the wind convective forced cooling. The procedure is then repeated for different wind speeds, conductors and angles.

Chapter3. Methodology of DLR calculation

3.1 Power flow method

The preliminary idea of any analysis of power system will be the calculation of complex voltages at all the busses. After the complex voltages have been calculated the power coming out of a bus and the power flowing in all the TLs can be calculated. Power flow calculation have been generally used in forecasting studies when a power network undergoes planning and expansion.

There are many methods of expressing the power flow equations. The most common formulation of the equations has been based on the nodal admittance form. The equations are nonlinear and therefore no direct solution is possible. As an alternative, iterative methods have to be employed to obtain a solution. Hence good initial approximations of the solution are essential. There are many numerical solution methods for solving the power flow problem. The one that has found extensive use is the Newton-Raphson method.

Calculation for actual power flow in the line

Let the power system consists n-number of buses. First bus i.e. bus1 is a swing bus. buses 2, are x number of Voltage buses and the remaining Buses x+2, x+3.....n are load buses [20].

Step 1- Read bus data and line data of the given system.

Step 2- Line data is taken by using Y_{bus} .

Step 3- Assume the values of phase angles and bus voltages, Set V(0)= 1 p.u. and $\delta(0) = 0^0$

Step 4- Calculate the real and reactive power injection in line using the most recent updated values of phase angle and voltages and for the calculation purpose following equations are used.

$$P_i = n_k = 1 \times V_i V_k Y_{ik} \cos(\delta_i - \delta_k + \gamma_{ik}) \quad (1.1)$$

$$Q_i = n_k = 1 \times V_i V_k Y_{ik} \sin(\delta_i - \delta_k + \gamma_{ik}) \quad (1.2)$$

Step 5- Check limits of reactive power injection in line $Q_{min} \leq Q_i \leq Q_{max}$ for voltage buses. If Qi is within the limits, go to Step 6 Else set $Q_i = Q_{min}$ or Q_{max} as the case and treat this i^{th} bus as load bus. Re-designate the bus number and return to step-1.

Step 6- Calculate the mismatch in real and reactive power.

$$\Delta P_r = P_r(s) - P_r(c) \tag{2.1}$$

for i=2, 3....., n

$$\Delta Q_i = Q_i(s) - Q_i(c) \tag{2.2}$$

for i=x+2, x+3....., n

Step 7- Calculate the Jacobian Matrix elements.

Step 8- Calculate the increment matrix as.

$$\begin{bmatrix} \Delta\delta \\ \Delta|V|/|V| \end{bmatrix} = [J]^{-1} \begin{bmatrix} \Delta P \\ \Delta Q \end{bmatrix} \tag{3}$$

Step 9- Update magnitudes of voltage and phase angles using the increments as:

$$V_{r+1} = V_r + \Delta V_r \tag{4.1}$$

$$\delta_{r+1} = \delta_r + \Delta\delta_r \tag{4.2}$$

Step 10- Bus Current Injections.

$$I_i = Y_{bus} \times V \tag{5}$$

Step 11- Line Current Flows

$$I_{ij}(p,q) = (V_q - V_p) Y_{bus}(p,q) \tag{6}$$

Where p = from bus and q = to bus

Step 12- Line Power Flows

$$P_{ij}(p,q) = V \times \text{conj}(I_{ij}(p,q)) \tag{7}$$

3.2 Calculation for dynamic ampacity with the effect of dynamic weather conditions

IEEE Standard 738-2006

In work towards engineering, thermal ratings of transmission lines i.e. overhead conductors are normally found with the help of one of two standards: the IEEE (Institute of Electrical and Electronics Engineers) [11] or CIGRE [9]. Both use the same standards or concept to calculate the heat balance equation. In this study for the calculation purpose, the IEEE (Institute of Electrical and Electronics Engineers) standard 738-2006 are used for the calculation of the ampacity of the bare overhead conductors. The temperature of conductor is a function of the properties of it's material, diameter, surface texture and ambient environmental conditions.

IEEE made a study on different methods for calculating the heat equation to find the ampacity of overhead line conductor. The mathematical calculation decided in the IEEE 738 standard is based on the House and Tuttle method. Formulas consider all of the important parameters without the simplifications that were made in other formulas

Equations used to find the dynamic line rating considers the effect of dynamic weather conditions i.e. real time weather data has been adapted and incorporated in the power flow solution.

Now, with the help of the equations (based on IEEE-738 standard) shown below, the power carrying capability of transmission line can be easily calculated.

According to the law of conservation of energy, there should be balance between heat loss rate and heat gain rates, i.e. the heat balance equation [11].

$$Heat_{gain} = Heat_{loss} \quad (8)$$

The balance between heat gain and heat loss is representing the following heat balance equation.

$$P_{loss} + Q_{solar} = Q_{convection} + Q_{radation} \quad (9)$$

Conductor electric resistance

The resistance has been calculated solely the function of temperature of conductor, however the resistance may be the function of current density and frequency. The value of resistance for highest temperature T_{high} and lowest value of resistance T_{low} is taken from the Handbook for aluminum electric conductor [24]**,** and for any other value of the conductor resistance at any other temperature is obtained[25] according to the equation.

$$R_{TC} = \frac{\left(R(T_{high}) - R(T_{low})\right)}{T_{high} - T_{low}} (T_c - T_{low}) + (R_{Tlow}) \quad (10)$$

The solar heat gain is calculated from which it is found that this heat gain (Q_{solar}) depends upon mainly five factors and that factors are power of conductor to absorbing sun's ray, latitude of the conductor, projected area of conductor, the timing and the number of the day.

$$Q_{solar} = \beta \varphi \sin(\theta) A_{p,I} \quad (11)$$

The heat loss in conductor is classified into two types i.e., loss of heat due to radiation and loss of heat due to convection [24]**.** The classification of convected heat loss is of two types; the forced convection and natural convection. The natural convection loss of heat is depending upon the difference between the ambient temperature and conductor temperature, diameter of conductor and density of air.

$$Q_{Nc} = 0.0205 \sigma^2 D_i (T_{c,I} - T_A)^{1.25} \quad (12)$$

The forced convected loss of heat is mainly wind dependent i.e. speed and direction. The forced convicted heat loss is calculated for two cases (i) low speed of the wind and (ii) high speed of wind. The equation for both is as follows .

At low wind speed

$$Q_1 = 1.01+0.0372 \left(\frac{D_i * \sigma * W_s}{\epsilon}\right)^2 K_{angle} \alpha T_B \quad (13)$$

Where $T_B = (T_c - T_A)$

At high wind speed

$$Q_2 = 0.0119 \left(\frac{D_i * \sigma * W_s}{\epsilon}\right)^{0.6} \alpha K_{angle} T_B \quad (14)$$

Where $T_B = (T_c - T_A)$

To find the forced convection heat loss, wind direction factor (K_{angle}) [26] has been considered by equation

$$K_{angle}=1.194 - \cos(\varphi) + 0.194\times\cos(2\varphi)+0.368 \sin(2\varphi) \quad (15)$$

The thermal conductivity of air(α) at T_{flim} temperature is given as.

$$\alpha =2.424\times10^{-2}+7.477\times10^{-5} T_{flim} - 4.407\times10^{-9}(T_{flim})^2 \quad (16)$$

The dynamic viscosity of the ambient air is given as.

$$\epsilon = 0.00353 \times\frac{(T_{flim}+273)}{T_{flim}+383.4}^{1.5} \quad (17)$$

Average value of temperature of conductor and ambient temperature (T_{flim}) is represented as.

$$T_{flim} =\frac{(\mathbf{Tc + TA})}{\mathbf{2}} \quad (18)$$

Now the density of air is calculated as.

$$\sigma = \frac{1.293 - h_e\ 1.525\times10^{-4} + {h_e}^2 6.379\times10^{-9}}{F_r} \quad (19)$$

Where $F_r = (1 + (0.00367\ T_{flim}))$

From IEEE standard [11] the radiated heat loss is calculated as

$$Q_r=0.0178\ D \left[\frac{(T_c+273)^4}{100} - \frac{(T_a+273)^4}{100}\right] \epsilon \quad (20)$$

Rate of solar heat gain

$$q_s = S_a\ Q_{se} \sin(\theta)\ A' \quad (21)$$

Where $A' = \frac{D}{100}$ and $\theta = \cos^{-1}[\cos(H_c)\times\cos(Z_c - Z_1)]$

Qse is the heat flux elevation correction factor which is calculated as.

$$Q_{se} = K_{solar}\ Q_s \quad (22)$$

Where $K_{solar} = A_s + B_s\ (h_e) + C_s\ (h_e)^2$

h_e elevation of conductor above sea level & A_s, B_s, C_s are the constants.

Q_s the total flux received by a surface at sea level.

The total solar heat flux density at sea level is dependent on the atmospheric conditions and solar altitude [27]. The heat flux density received by a surface at sea level for clear atmosphere and industrial atmosphere has been tabulated in table 3-1 and table 3-5 respectively.

Table 3.1 Constants for clear atmosphere

A	-42.2391
B	63.8044
C	-1.9220
D	3.46921×10^{-2}
E	-3.61118×10^{-6}
F	1.94318×10^{-9}
G	-4.07608×10^{-8}

Table 3.2 Constants for industrial atmosphere

A	53.1821
B	14.2110
C	6.6138×10^{-1}
D	-3.1658×10^{-2}
E	5.4654×10^{-4}
F	-4.3446×10^{-6}
G	1.3236×10^{-8}

Total flux received by a surface at sea level is given by the equation

$$Q_s=A+B(h_e)+C(h_e)^2 + D(h_e)^3 + E(h_e)^4 + F(h_e)^5 + G(h_e)^6 \quad (23)$$

Altitude of the sun(Hc) is calculated as.

$$H_c = \sin^{-1}[(\cos(Lat)\cos(\delta)\cos(\omega)) + (\sin(Lat)\sin(\delta))] \quad (24)$$

The hour angle 'ω' is number of hours from noon times 15^0. For example for 11a.m. $\omega = -15^0$

12 p.m. $\omega = -15+15 = 0^0$, 1p.m. $\omega = 0+15 = 15^0$,2p.m. $\omega = 15+15 = 30^0$

The solar declination has been calculated as (δ)

$$\delta = 23.4583\times\sin[(284+\frac{N}{365}) 360] \quad (25)$$

Where N = Number of day of the year

Azimuth of the sun is calculated as.

$$Z_c = C + \tan^{-1}(\chi) \quad (26)$$

Where $\chi = \frac{\sin(\omega)}{(\sin(Lat)\cos(\omega) - \cos(Lat)\tan(\delta))}$

Now, Calculate the Current flow in the line.

$$I = \sqrt{\frac{Qi+Qr-qs}{R(Tc)}} \quad (27)$$

Hence with the help of current 'I' new power flow in the line will be calculated

$$NP_{ij} = I\,(V_{(j)} - V_{(i)}) \quad (28)$$

Where i = from bus, j = to bus

3.3 flow chart for ATC calculation

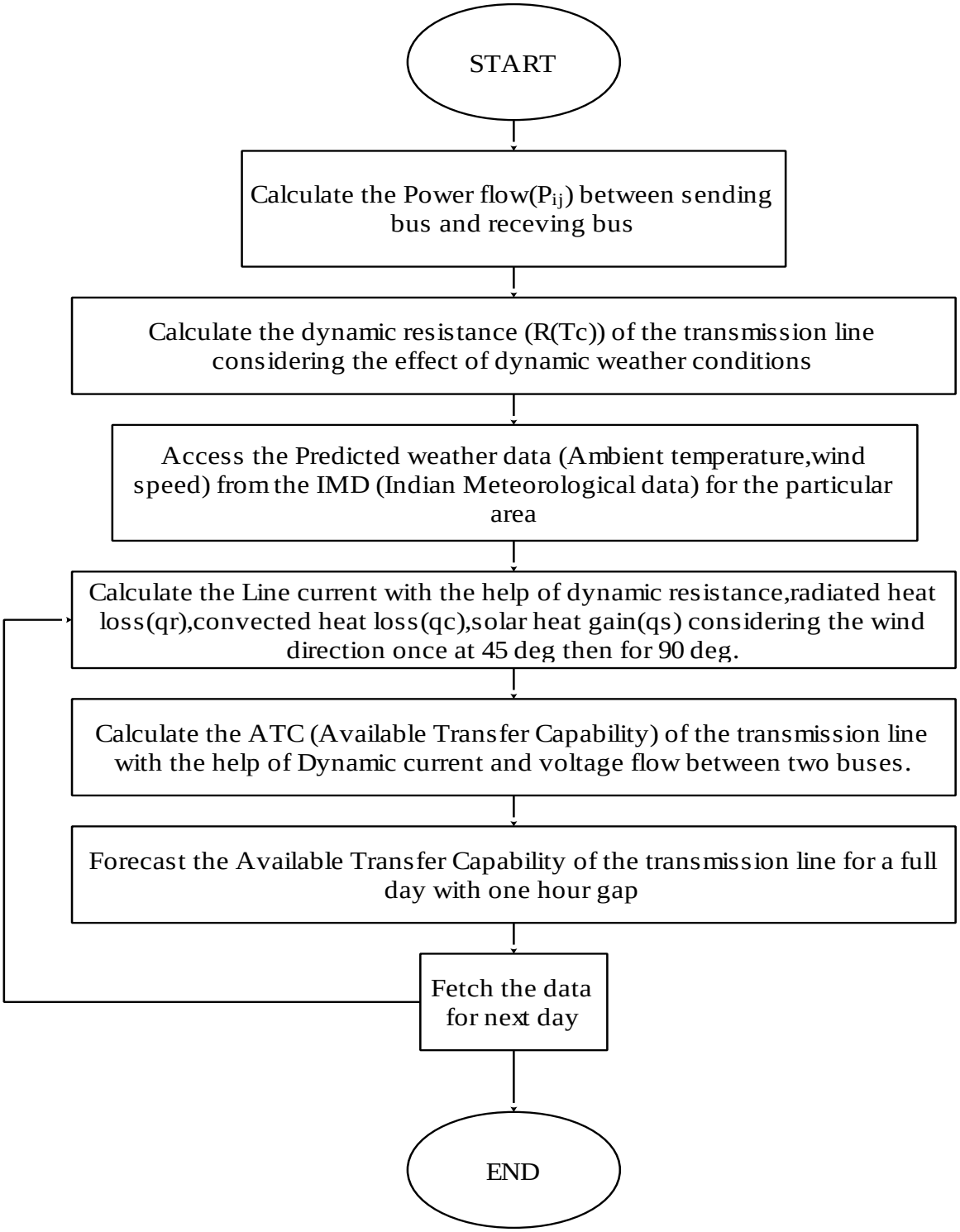

Figure 3.1 Flow chart showing the ATC calculation

Chapter4. Methodology of DLR for 6-bus system

4.1 IEEE-6 bus test system

IEEE 6-bus system has been used as the test system to demonstrate the calculation of power carrying capability of transmission line. In this system consider the dynamic weather condition or real time weather conditions to estimate the real power carrying capability of transmission line. In previous researches static weather conditions or worst weather conditions has been considered to estimate the power flow [3]. But with the use of dynamic weather conditions it has been possible to get the accurate data. IEEE 6-bus system with 11 transmission line has been shown in Fig 4.1. In Table 4.1 bus data and line data for six bus system has been tabulated and the power flow in the system from one bus to another has been tabulated in Table 4.2.

Data used for IEEE 6-bus system

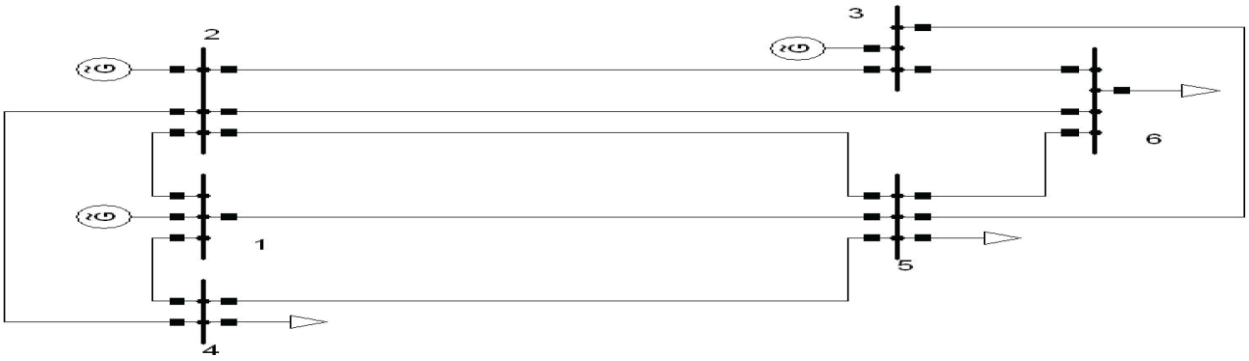

Figure 4.1 IEEE 6-bus system

Table 4.1 Bus data and line data for IEEE 6-bus system

Bus No.	Bus Type	Voltage	P_{gen}	P_{load}	Q_{load}
1	Swing	1.05			
2	Gen	1.05	0.50	0.0	0.0
3	Gen	1.07	0.60	0.0	0.0
4	Load		0.0	0.7	0.7

5	Load		0.0	0.7	0.7
6	Load		0.0	0.7	0.7

From Bus	To Bus	R(pu)	X(pu)	BCAP(pu)
1	2	0.10	0.20	0.02
1	4	0.05	0.20	0.02
1	5	0.08	0.30	0.03
2	3	0.05	0.25	0.03
2	4	0.05	0.10	0.01
2	5	0.10	0.30	
2	6	0.07	0.20	0.025
3	5	0.12	0.30	0.025
3	6	0.02	0.10	0.01
4	5	0.20	0.40	0.04
5	6	0.10	0.30	0.03

Table 4.2 Power flow in lines

Line	MW Limit
1-2	28.8025
1-4	43.3573
1-5	35.4112
2-4	33.1848
2-6	26.2514
3-6	43.8212
4-5	4.0488
2-3	3.0
2-5	15.6246
3-5	19.0847
5-6	1.5348

Parameters used for the test system

Available Transfer Capability ratings are calculated to define the current so as to not exceed the thermal limit of a transmission line i.e. above the maximum operating temperature (MOT) for a recommended set of working and ambient conditions. The Maximum Operating Temperature may be better for ambient conditions rather than the define power carrying capability of line at extreme conditions, which also defines that the power carrying capability of the line will also increase as it predicted before.

4.2 Industry Standard Methodology

This thesis work uses the calculations and terminology that are shown in IEEE Standard 738, has been considered as guide line to find the capacity (amps) for a given conductor under maximum operating temperature and not the clear atmospheric conditions as tabulated in Table 3.1&3.2.

4.3 Conductor MOT determination

Maximum operating temperature (MOT) of a conductor is depended on each of two the physical conditions of the conductor or the sag limit of the conductor, whichever controls. The conductor actual condition limitation has been loss of strength due to annealing, which for aluminum begins to occur at temperatures greater than 200°F (93°C). ATC has calculated as an acceptable loss of durability based on temperature as briefed in Table 4.3.

Table 4.3 Maximum Temperature limit on which conductor can work

Material of Conductor	Limits of Temperature	
	Normal Rating	Emergency Rating
ACSR, steel > 7.5% area	93^0C	149^0C
ACSR, steel < 7.5% area	93^0C	135^0C
AAAC, AAC, & ACAR	93^0C	110^0C

Material of Conductor	Limits of Temperature	
	Normal Rating	Emergency Rating
ACSS, steel < 7.5% area	200^0C	200^0C
Copper	75^0C	85^0C
Copper weld	75^0C	85^0C
Alumo weld	93^0C	135^0C

Table 4.4 Maximum Allowable Conductor temperature for IEEE 6-bus test system

Line	Conductor Temperature(Tc)
1-4	100
1-5	70
2-3	70
2-6	75
3-6	100
2-4	85
2-5	100
3-5	100

Cooling due to convection of a bare transmission conductor is dependent on both the direction of wind and wind speed. In the thesis course work, the main objective is to take the real time weather conditions and verify the power carrying capability of line at different wind angles i.e. K_{angle}. This parameter has been employed in the forced convective cooling calculation of the IEEE standard. The following sensitivity study has been conducted in order to estimate the influence magnitude of K_{angle} on the conductor cooling. Results shows that the coefficient substantially influences the conductor's rating. A 20 % increase of K_{angle} make the ampacity increase (for the investigated overhead line corresponds to an increase of maximum 10 MW in the allowed power transmission) [15]. It has been concluded that the effect of K_{angle} have an important role on overhead lines rating

and further investigations should be conducted in order to better estimate the conductor conditions when the wind does not flow in a perpendicular direction.

taking the real time data from Indian metrological data [28] (IMD), now update the function by just updating the data again and again. Information about the ambient temperature (Ta), Wind speed (Ws) and time of a day is take from the real time data. The data has been for one-hour gap for a full day. Now, by set the wind direction with conductor axis once at 45^0 i.e. the worst wind angle and then for 90^0 i.e. the best wind angle by this we are able to predict the Power carrying capability of that line for a full day and also Predict the best time of the day at which it has been possible to transfer the maximum power to the load side. Real time weather data for 20/5/17 has been fetched online for different places [28] from where to where we suppose to transmit the power and check the power transfer capability at both wind angles (90^0 and 45^0). The conductors considered for this test system is moose and zebra as it has been the most popular type of conductors used for transmission system. Technical specification for Moose and zebra conductor used in transmission system has been taken from Gujrat energy transmission corporation limited.

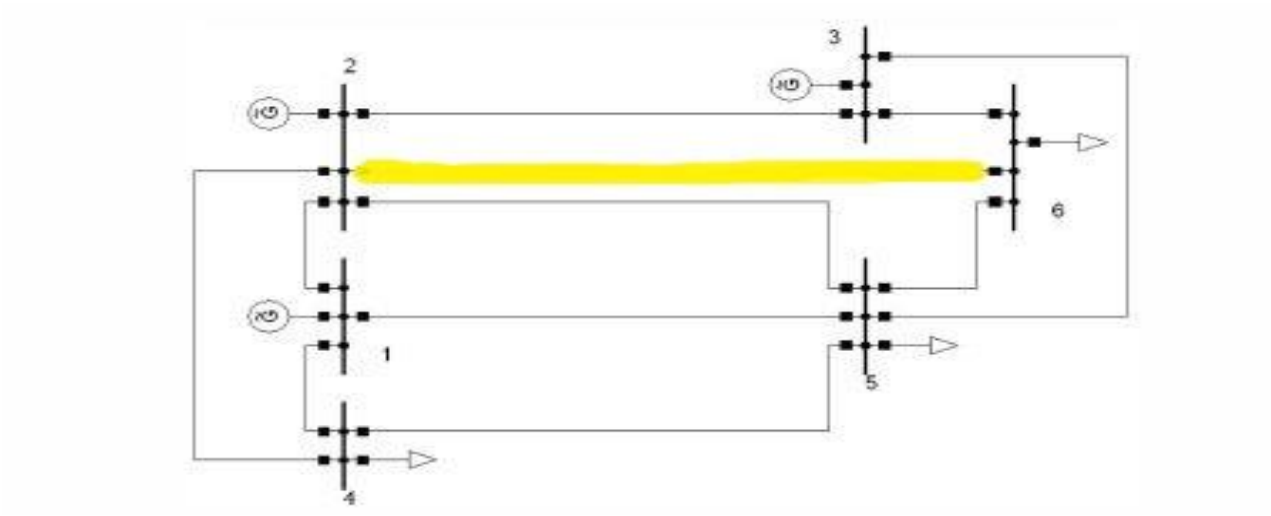

Figure 4.2 Test line (2-6) for ATC calculation

The line for which ATC has calculated i.e. generating to load end has been highlighted in Fig 4.2. Bus 2 has been the generating bus so; weather conditions has been considered for the area of bus

2 (the generator bus is considering in the Kullu area of Himanchal Pradesh, India). Comparison for Moose and Zebra conductor, Losses, ampacity and change in ATC for a full day has been shown in Fig 4.3 to Fig 4.8 and the data for wind speed, ambient temperature has been tabulated in Table 4.5 .

4.4 Variation in current flow considering DLR

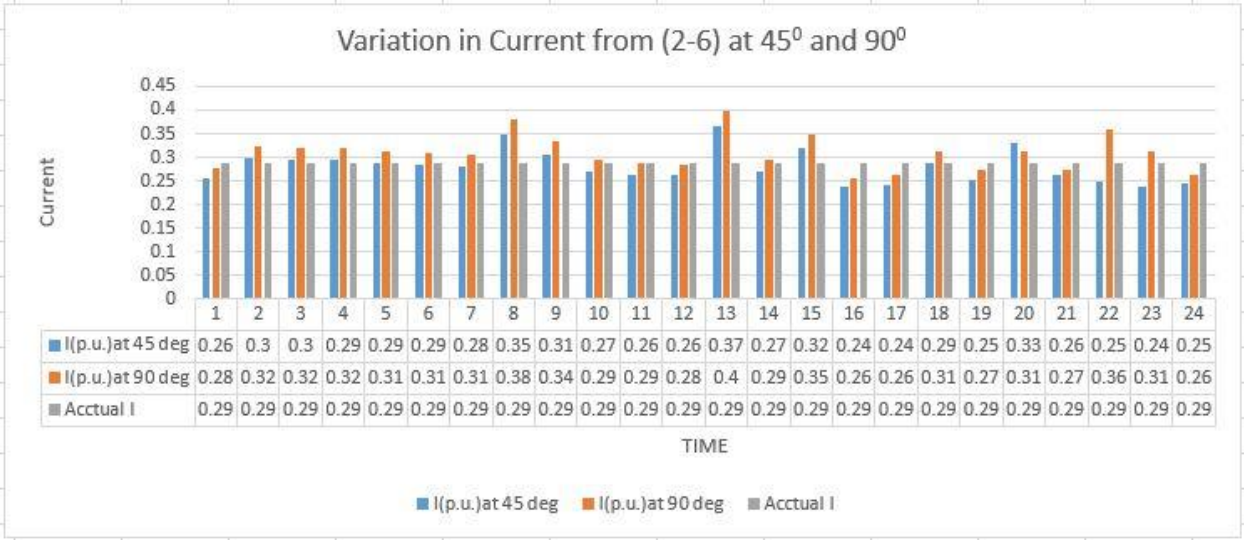

	1	2	3	4	5	6	7	8	9	10	11	12	13	14	15	16	17	18	19	20	21	22	23	24
I(p.u.)at 45 deg	0.26	0.3	0.3	0.29	0.29	0.29	0.28	0.35	0.31	0.27	0.26	0.26	0.37	0.27	0.32	0.24	0.24	0.29	0.25	0.33	0.26	0.25	0.24	0.25
I(p.u.)at 90 deg	0.28	0.32	0.32	0.32	0.31	0.31	0.31	0.38	0.34	0.29	0.29	0.28	0.4	0.29	0.35	0.26	0.26	0.31	0.27	0.31	0.27	0.36	0.31	0.26
Acctual I	0.29	0.29	0.29	0.29	0.29	0.29	0.29	0.29	0.29	0.29	0.29	0.29	0.29	0.29	0.29	0.29	0.29	0.29	0.29	0.29	0.29	0.29	0.29	0.29

Figure 4.3 Variations in current flow from line (2-4) for a whole day

Actual current flow in the line is 0.287(p.u.) considering the DLR method for calculation of dynamic current the mean dynamic current for whole day is 0.27(p.u.) for 45^0 and 0.31(p.u.) at 90^0 so, by considering the DLR current it has been possible to transfer more current to the load side which means power transfer has been also increased Fig 4.2 shows the variation in current with considering the DLR and compare that with static rating.

Losses with and without considering DLR method

Losses for the line without DLR is 0.0058 and after considering the effect of DLR the mean losses for a whole day is 0.00529 which means with the consideration of dynamic conditions on the

system or line it has been possible to minimize the losses on the system or line variation in losses with DLR method and comparison with SLR method has been shown in Fig 4.3.

Figure 4.4 Losses in the system from line (2-6) considering DLR method

4.5 Graphical and Tabular representation of the ATC

Showing the variation in power carrying capability of transmission. ATC from bus (2-6) (Comparison between **moose** and **zebra** Conductor)

ATC for different type of conductors i.e. moose and zebra has been calculated and the results for both conductors at different wind angle has been tabulated in Table 4.5

Table 4.5 Comparison of ATC from bus 2-6 for MOOSE and ZEBRA

Time	Ws(m/s)	Ta(^{0}C)	ATC at $\Phi=45^0$ (MOOSE)	ATC at $\Phi=90^0$(MOOSE)	ATC at $\Phi=45^0$(ZEBRA)	ATC at $\Phi=90^0$(ZEBRA)
1	1	9.5000	22.8547	25.3478	21.8956	28.6412
2	2	8.6000	24.9371	27.1470	24.2151	26.3706
3	1	8.4000	21.3208	23.1397	20.6875	22.4634
4	1	8.8000	21.2524	23.0662	20.6213	22.3922

Time	Ws(m/s)	Ta(^{0}C)	ATC at $\Phi=45^0$ (MOOSE)	ATC at $\Phi=90^0$(MOOSE)	ATC at $\Phi=45^0$(ZEBRA)	ATC at $\Phi=90^0$(ZEBRA)
5	1	9.4000	21.1494	22.9554	20.5217	22.2848
6	1	10.5000	20.9590	22.7505	20.3374	22.0865
7	1	11.6000	20.7664	22.5435	20.1510	21.8860
8	5	12.6000	30.0359	32.7963	29.1888	31.8788
9	4	13.9000	28.1448	30.7157	27.3475	29.8534
10	7	14.9000	31.9821	34.9514	31.0870	33.9799
11	6	15.8000	30.5540	33.3812	29.6968	32.4515
12	3	16.6000	25.6484	27.9732	24.9180	27.1844
13	5	18.8000	28.4381	31.0621	27.6388	30.1957
14	6	19.4000	29.5695	32.3121	28.7416	31.4137
15	6	20.3000	29.3178	32.0389	28.4974	31.1485
16	5	20.4000	28.0096	30.5974	27.2232	29.7448
17	5	19.3000	28.3049	30.9177	27.5096	30.0556
18	1	17.4000	19.7132	21.4128	19.1324	20.7914
19	3	16.5000	21.5231	23.4587	21.4582	22.3654
20	3	14.3000	26.1764	28.5447	25.4298	27.7387
21	2	12.8000	24.0928	26.2344	23.3970	25.4858
22	2	10.0000	24.6594	26.8467	23.9459	26.0794
23	2	7.5000	25.1529	27.3803	24.4242	26.5969
24	1	5.3000	21.8416	23.7004	21.1916	23.0065

The power carrying capability of the transmission lines has increased as the temperature has been decreased and wind speed has increased. The relation between diameter of the conductor and the variation of the ATC has been found. The direct relationship between the ATC and the diameter of conductor is shown in table 4-5.

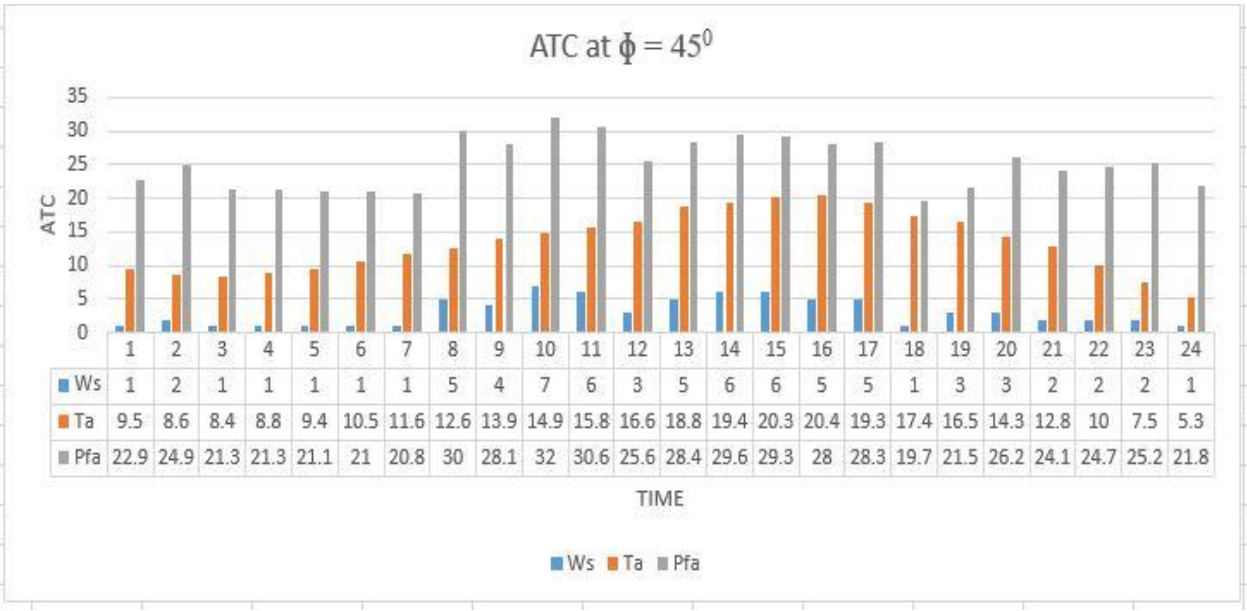

	1	2	3	4	5	6	7	8	9	10	11	12	13	14	15	16	17	18	19	20	21	22	23	24
Ws	1	2	1	1	1	1	1	5	4	7	6	3	5	6	6	5	5	1	3	3	2	2	2	1
Ta	9.5	8.6	8.4	8.8	9.4	10.5	11.6	12.6	13.9	14.9	15.8	16.6	18.8	19.4	20.3	20.4	19.3	17.4	16.5	14.3	12.8	10	7.5	5.3
Pfa	22.9	24.9	21.3	21.3	21.1	21	20.8	30	28.1	32	30.6	25.6	28.4	29.6	29.3	28	28.3	19.7	21.5	26.2	24.1	24.7	25.2	21.8

Figure 4.5 Hourly Representation of ATC from line 2-6 at 45^0(MOOSE)

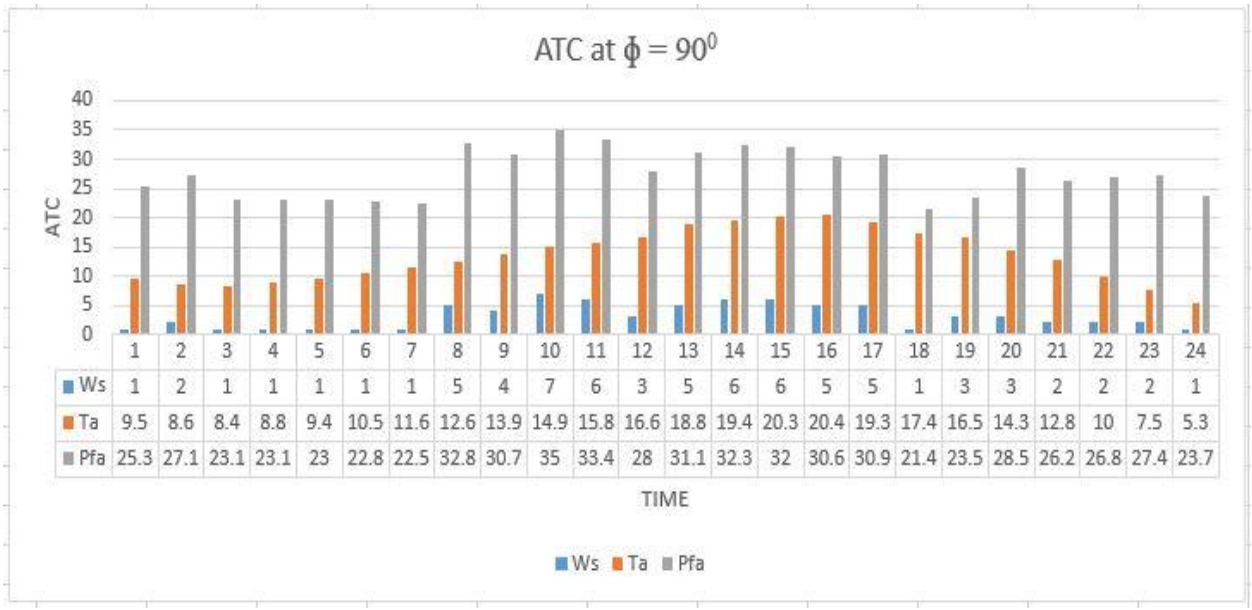

	1	2	3	4	5	6	7	8	9	10	11	12	13	14	15	16	17	18	19	20	21	22	23	24
Ws	1	2	1	1	1	1	1	5	4	7	6	3	5	6	6	5	5	1	3	3	2	2	2	1
Ta	9.5	8.6	8.4	8.8	9.4	10.5	11.6	12.6	13.9	14.9	15.8	16.6	18.8	19.4	20.3	20.4	19.3	17.4	16.5	14.3	12.8	10	7.5	5.3
Pfa	25.3	27.1	23.1	23.1	23	22.8	22.5	32.8	30.7	35	33.4	28	31.1	32.3	32	30.6	30.9	21.4	23.5	28.5	26.2	26.8	27.4	23.7

Figure 4.6 Hourly Representation of ATC from line 2-6 at 90^0(MOOSE)

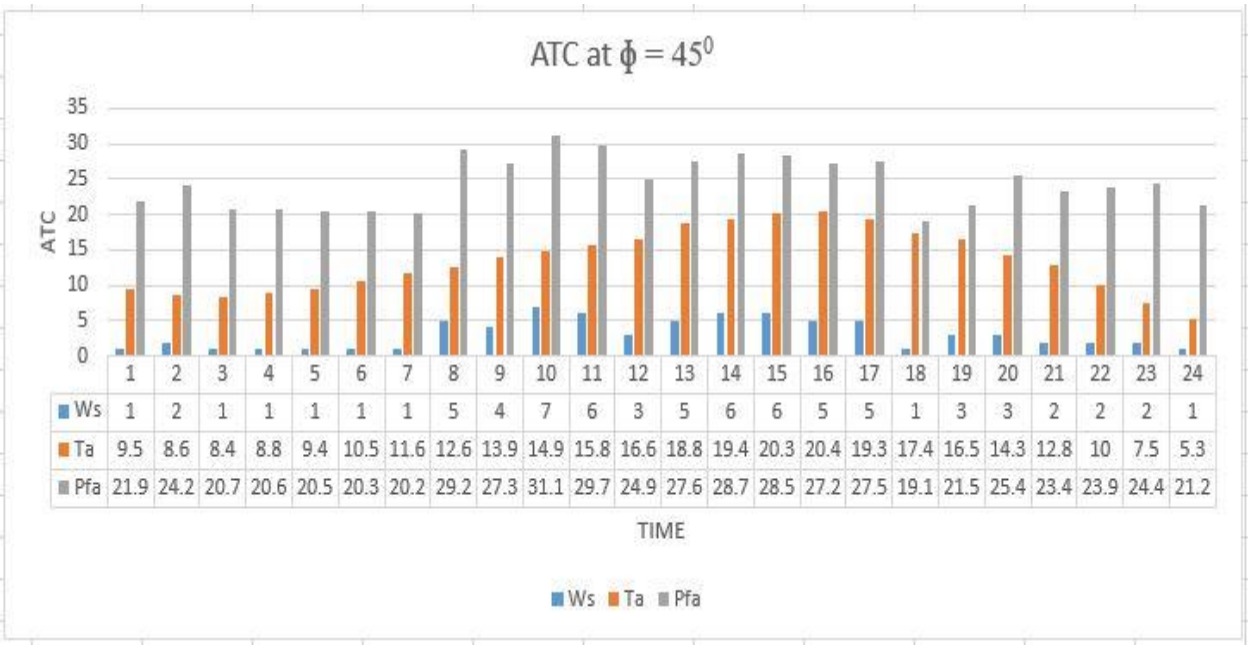

Figure 4.7 Hourly Representation of ATC from line 2-6 at 45^0(ZEBRA)

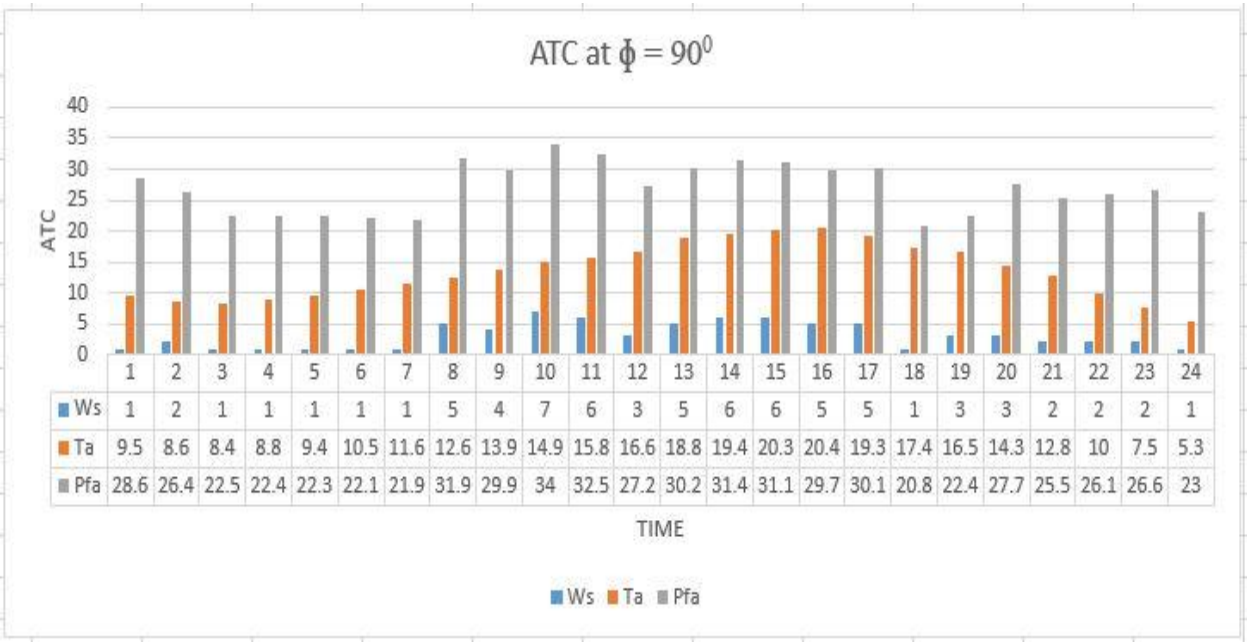

Figure 4.8 Hourly Representation of ATC from line 2-6 at 90^0(ZEBRA)

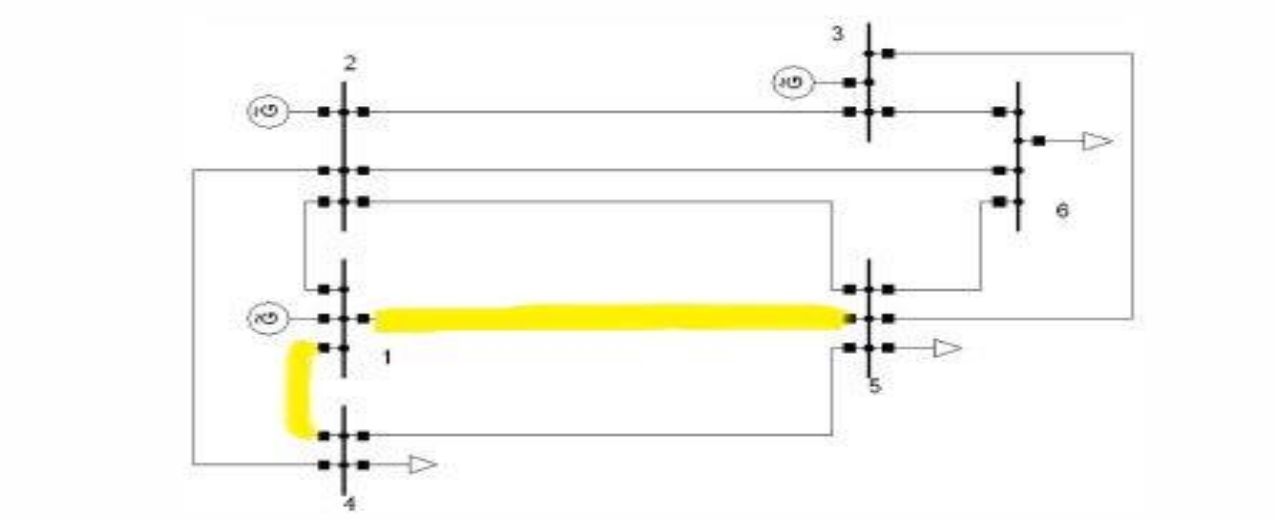

Figure 4.9 Test line (1-4 and 1-5) for ATC calculation

The line for which ATC has calculated i.e. generating to load end has been highlighted in Fig 4.9. Bus 1 is the generating bus so; weather conditions has been considered for the area of bus 1 (generator bus is considering in the Spiti area of Himachal Pradesh, India) change in ATC of the line for a full day has been shown in Fig 4.10 to Fig 4.13 and the data for wind speed, ambient temperature has been tabulated in Table 4.6 .

ATC from bus (1-5) and (1-4)

Table 4.6 Available transfer capability from bus 1-5 and 1-4

Time	Ws(m/s)	Ta(^{0}C)	ATC at $\Phi=45^0$ (1-5)	ATC at $\Phi=90^0$ (1-5)	ATC at $\Phi=45^0$ (1-4)	ATC at $\Phi=90^0$ (1-4)
1	2	17.0000	31.5623	34.2156	35.8942	38.0124
2	1	16.8000	26.1132	28.1022	29.6100	32.0023
3	1	16.9000	26.2042	28.5109	29.7170	32.0822
4	2	17.2000	30.7400	33.5275	34.4161	37.3138
5	2	18.7000	30.2609	33.0115	34.1002	36.9715
6	2	19.0000	30.1641	32.9072	34.0366	36.9026
7	2	21.1000	29.4761	32.1669	33.5871	36.4159
8	2	22.9000	28.8718	31.5170	33.1960	35.9925

Time	Ws(m/s)	Ta(^{0}C)	ATC at $\Phi=45^0$ (1-5)	ATC at $\Phi=90^0$ (1-5)	ATC at $\Phi=45^0$ (1-4)	ATC at $\Phi=90^0$ (1-4)
9	2	24.7000	28.2530	30.8520	32.7993	35.5631
10	5	24.4000	35.5148	38.8501	40.5063	44.1020
11	3	24.0000	31.4538	34.3739	36.0930	39.2133
12	2	28.8000	26.7840	29.2754	31.8731	34.5617
13	2	31.5000	25.7658	28.1846	31.2451	33.8833
14	2	32.4000	25.4165	27.8106	31.0324	33.6536
15	8	31.9000	36.2836	39.7564	42.9390	46.8294
16	2	29.0000	26.7100	29.1961	31.8271	34.5120
17	4	28.5000	31.9220	34.9300	37.3782	40.6631
18	1	26.5000	23.3796	25.4938	27.9169	30.1425
19	1	24.0000	24.1522	26.3175	28.4000	30.6625
20	2	21.5000	29.3430	32.0237	33.5007	36.3223
21	1	19.2000	25.5604	27.8220	29.2988	31.6310
22	3	16.4000	34.1658	37.3017	37.8751	41.1476
23	1	13.6000	27.0966	29.4671	30.3040	32.7159
24	2	13.0000	29.5214	32.6816	34.2658	35.8819

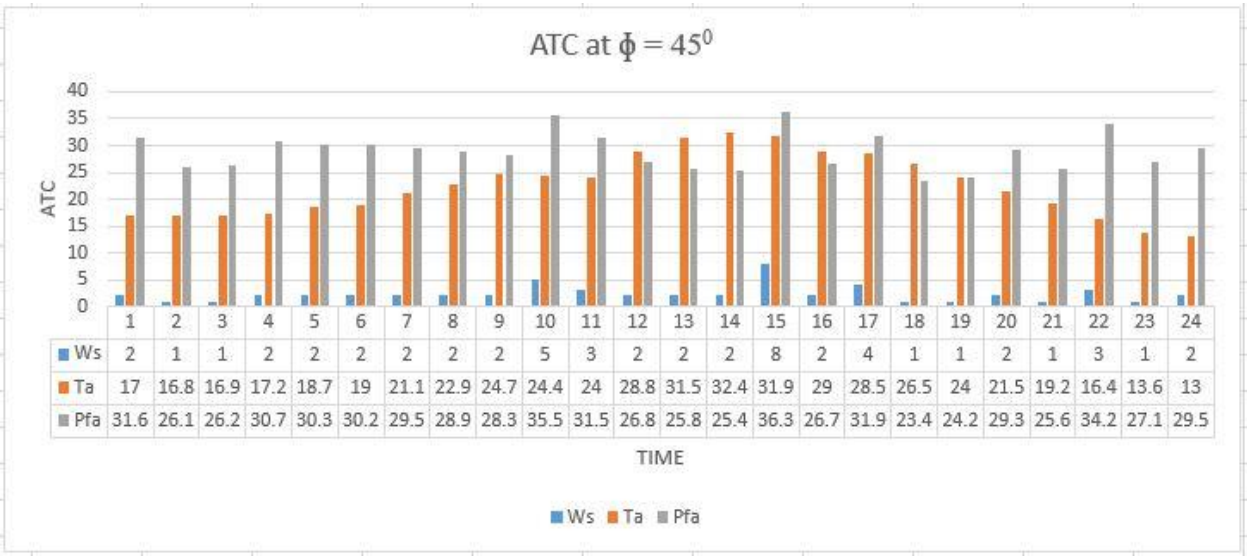

Figure 4.10 Hourly Representation of ATC from line 1-4 at 45^0

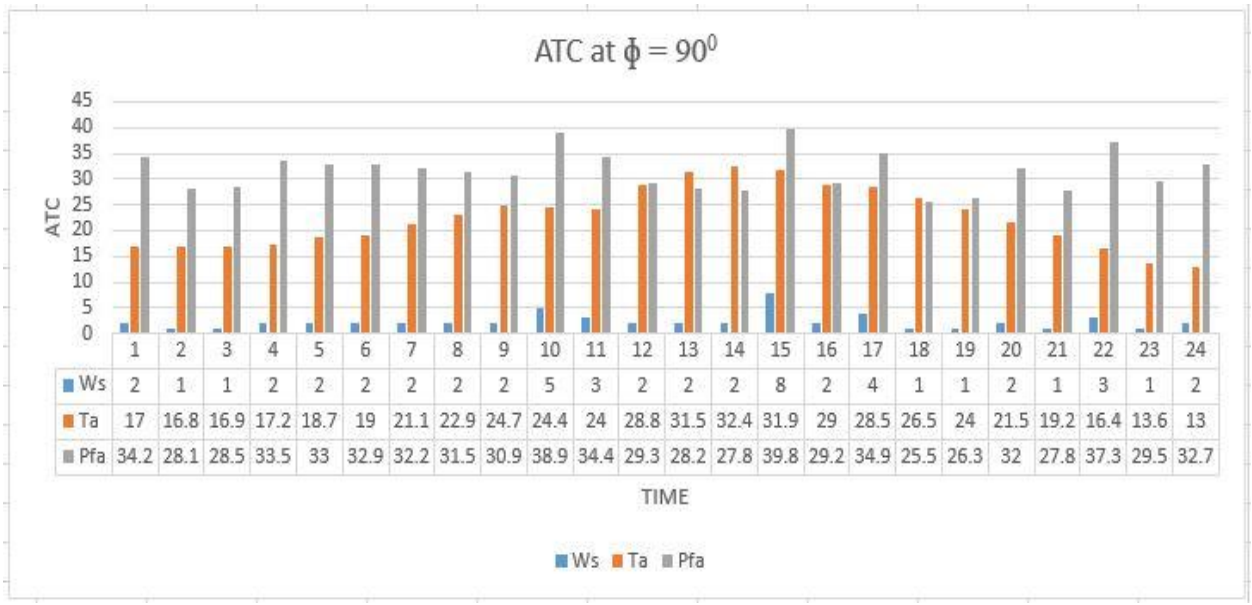

	1	2	3	4	5	6	7	8	9	10	11	12	13	14	15	16	17	18	19	20	21	22	23	24
Ws	2	1	1	2	2	2	2	2	2	5	3	2	2	2	8	2	4	1	1	2	1	3	1	2
Ta	17	16.8	16.9	17.2	18.7	19	21.1	22.9	24.7	24.4	24	28.8	31.5	32.4	31.9	29	28.5	26.5	24	21.5	19.2	16.4	13.6	13
Pfa	34.2	28.1	28.5	33.5	33	32.9	32.2	31.5	30.9	38.9	34.4	29.3	28.2	27.8	39.8	29.2	34.9	25.5	26.3	32	27.8	37.3	29.5	32.7

Figure 4.11 Hourly Representation of ATC from line 1-4 at 90^0

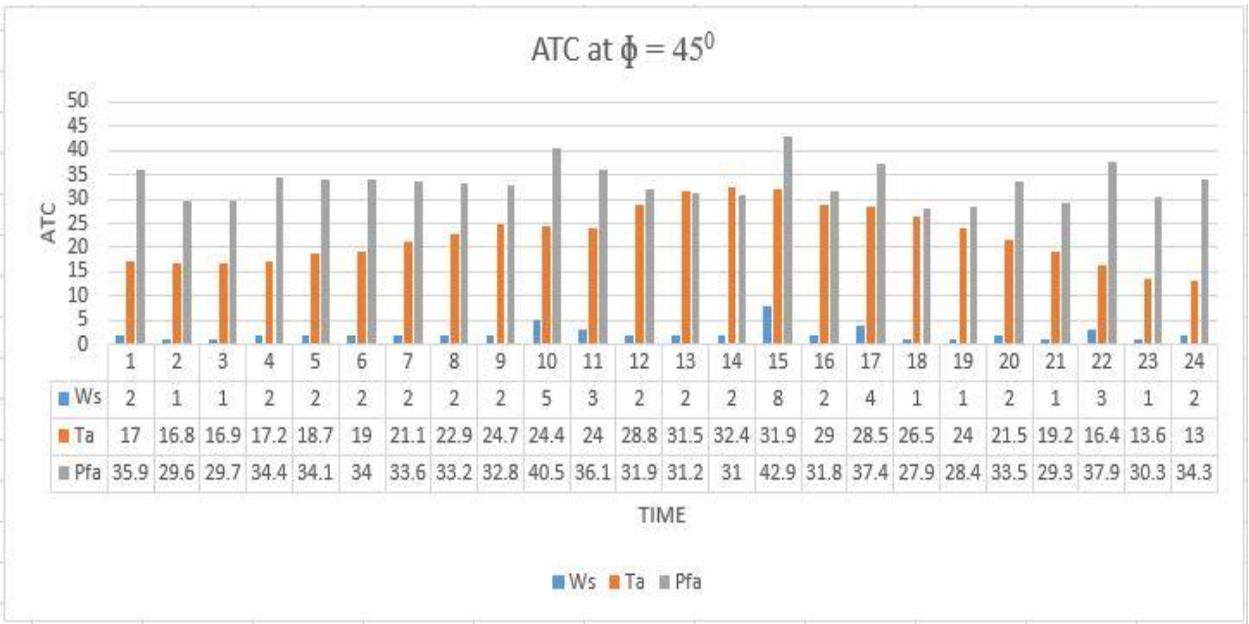

	1	2	3	4	5	6	7	8	9	10	11	12	13	14	15	16	17	18	19	20	21	22	23	24
Ws	2	1	1	2	2	2	2	2	2	5	3	2	2	2	8	2	4	1	1	2	1	3	1	2
Ta	17	16.8	16.9	17.2	18.7	19	21.1	22.9	24.7	24.4	24	28.8	31.5	32.4	31.9	29	28.5	26.5	24	21.5	19.2	16.4	13.6	13
Pfa	35.9	29.6	29.7	34.4	34.1	34	33.6	33.2	32.8	40.5	36.1	31.9	31.2	31	42.9	31.8	37.4	27.9	28.4	33.5	29.3	37.9	30.3	34.3

Figure 4.12 Hourly Representation of ATC from line 1-5 at 45^0

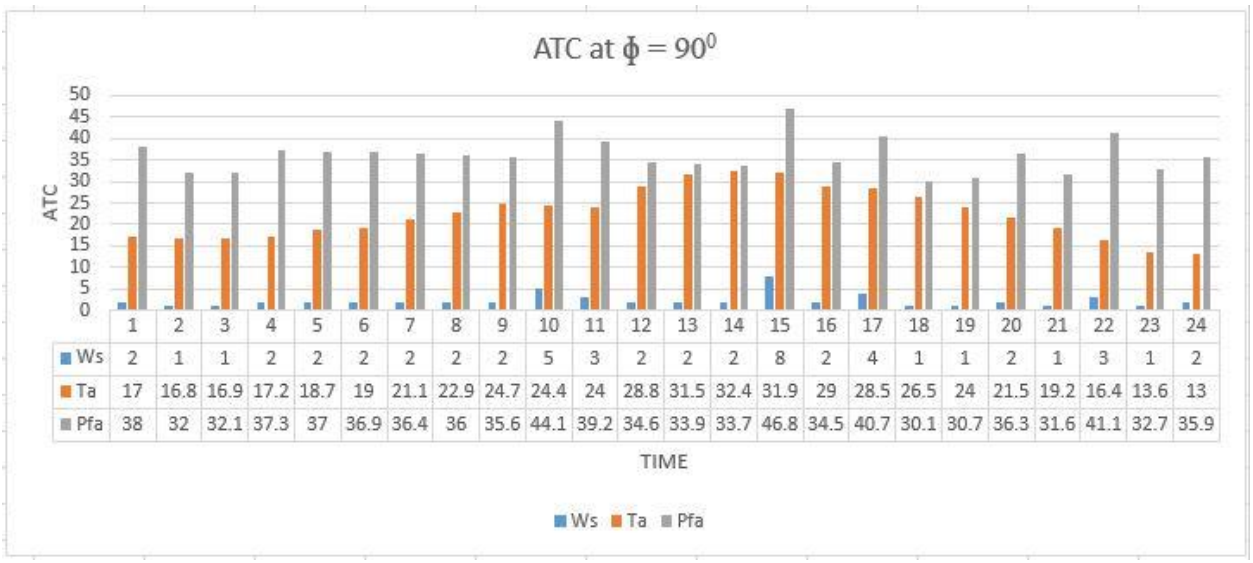

	1	2	3	4	5	6	7	8	9	10	11	12	13	14	15	16	17	18	19	20	21	22	23	24
Ws	2	1	1	2	2	2	2	2	2	5	3	2	2	2	8	2	4	1	1	2	1	3	1	2
Ta	17	16.8	16.9	17.2	18.7	19	21.1	22.9	24.7	24.4	24	28.8	31.5	32.4	31.9	29	28.5	26.5	24	21.5	19.2	16.4	13.6	13
Pfa	38	32	32.1	37.3	37	36.9	36.4	36	35.6	44.1	39.2	34.6	33.9	33.7	46.8	34.5	40.7	30.1	30.7	36.3	31.6	41.1	32.7	35.9

Figure 4.13 Hourly Representation of ATC from line 1-5 at 90^0

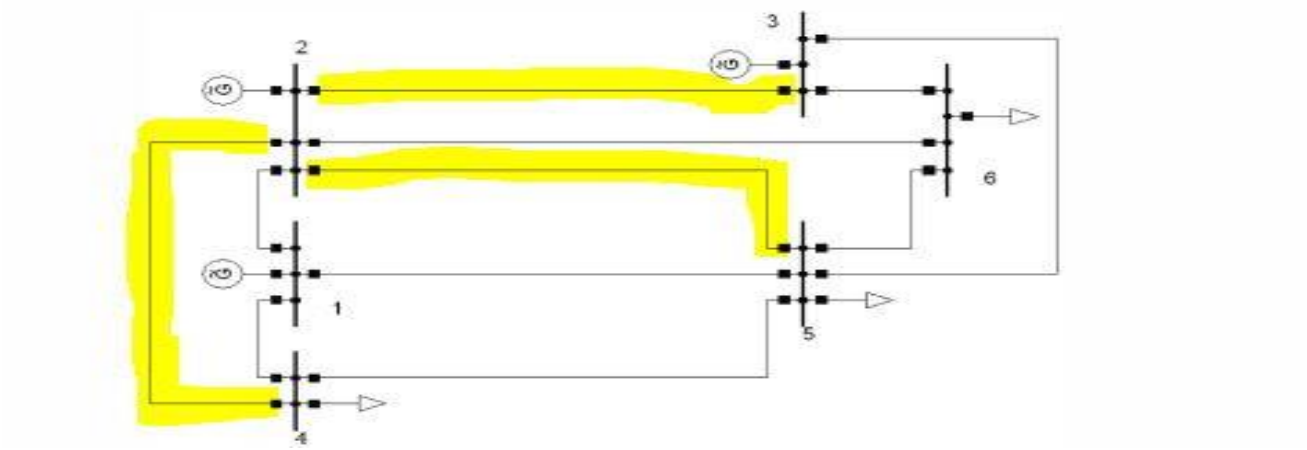

Figure 4.14 Test line (2-3, 2-4 and 2-5) for ATC calculation

The line for which ATC has calculated i.e. generating to load end has been highlighted in Fig 4.14. Bus 2 is the generating bus so; weather conditions has been considered for the area of bus 2 (generator bus has been considering in the Kullu area of Himachal Pradesh, India) change in ATC of the line for a full day has been shown in Fig 4.15 to Fig 4.20 and the data for wind speed, ambient temperature has been tabulated in Table 4.7 .

ATC from bus (2-4), (2-3) and (2-5)

Table 4.7 Available transfer capability from bus 2-4, 2-3 and 2-5

Time	Ws(m/s)	Ta(^{0}C)	ATC at $\Phi=45^0$ (2-4)	ATC at $\Phi=90^0$ (2-4)	ATC at $\Phi=45^0$ (2-3)	ATC at $\Phi=90^0$ (2-3)	ATC at $\Phi=45^0$ (2-5)	ATC at $\Phi=90^0$ (2-5)
1	1	9.5000	24.5214	27.2348	2.7542	2.5478	10.2458	10.5894
2	2	8.6000	27.9550	30.3774	3.1938	3.4805	12.4333	13.4806
3	1	8.4000	23.9979	25.9837	2.7242	2.9607	10.7269	11.5811
4	1	8.8000	23.9331	25.9138	2.7146	2.9504	10.7037	11.5559
5	1	9.4000	23.8355	25.8086	2.7001	2.9348	10.6686	11.5180
6	1	10.5000	23.6553	25.6142	2.6733	2.9060	10.6040	11.4482
7	1	11.6000	23.4733	25.4181	2.6461	2.8769	10.5388	11.3777
8	5	12.6000	33.6922	36.7407	3.8444	4.2009	14.9836	16.3131
9	4	13.9000	31.6538	34.4943	3.5964	3.9284	14.1183	15.3574
10	7	14.9000	35.9373	39.2279	4.0887	4.4713	16.0073	17.4480
11	6	15.8000	34.3943	37.5288	3.9017	4.2659	15.3502	16.7231
12	3	16.6000	28.9971	31.5695	3.2666	3.5665	13.0064	14.1301
13	5	18.8000	32.1781	35.0951	3.6194	3.9569	14.4392	15.7204
14	6	19.4000	33.4631	36.5163	3.7629	4.1153	15.0160	16.3591
15	6	20.3000	33.2258	36.2584	3.7273	4.0768	14.9312	16.2668
16	5	20.4000	31.7743	34.6566	3.5588	3.8913	14.2949	15.5634
17	5	19.3000	32.0525	34.9587	3.6006	3.9365	14.3943	15.6715
18	1	17.4000	22.4830	24.3521	2.4971	2.7172	10.1862	10.9969
19	2	16.5000	31.2489	34.1054	3.8462	4.5217	15.2486	16.7125
20	3	14.3000	29.4965	32.1109	3.3410	3.6470	13.1855	14.3247
21	2	12.8000	27.1531	29.5091	3.0751	3.3523	12.1446	13.1672
22	2	10.0000	27.6907	30.0912	3.1548	3.4384	12.3380	13.3771
23	2	7.5000	28.1605	30.6001	3.2241	3.5132	12.5076	13.5612
24	1	5.3000	24.4927	26.5176	2.7974	3.0394	10.9051	11.7739

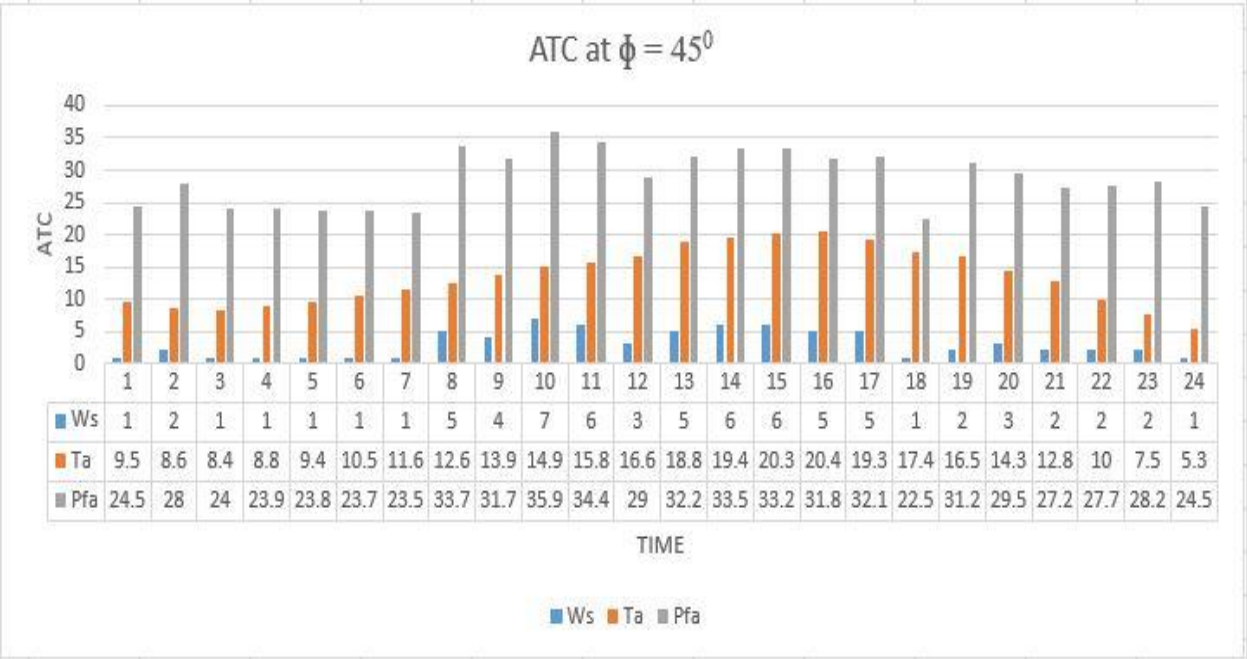

Figure 4.15 Hourly Representation of ATC from line 2-4 at 45^0

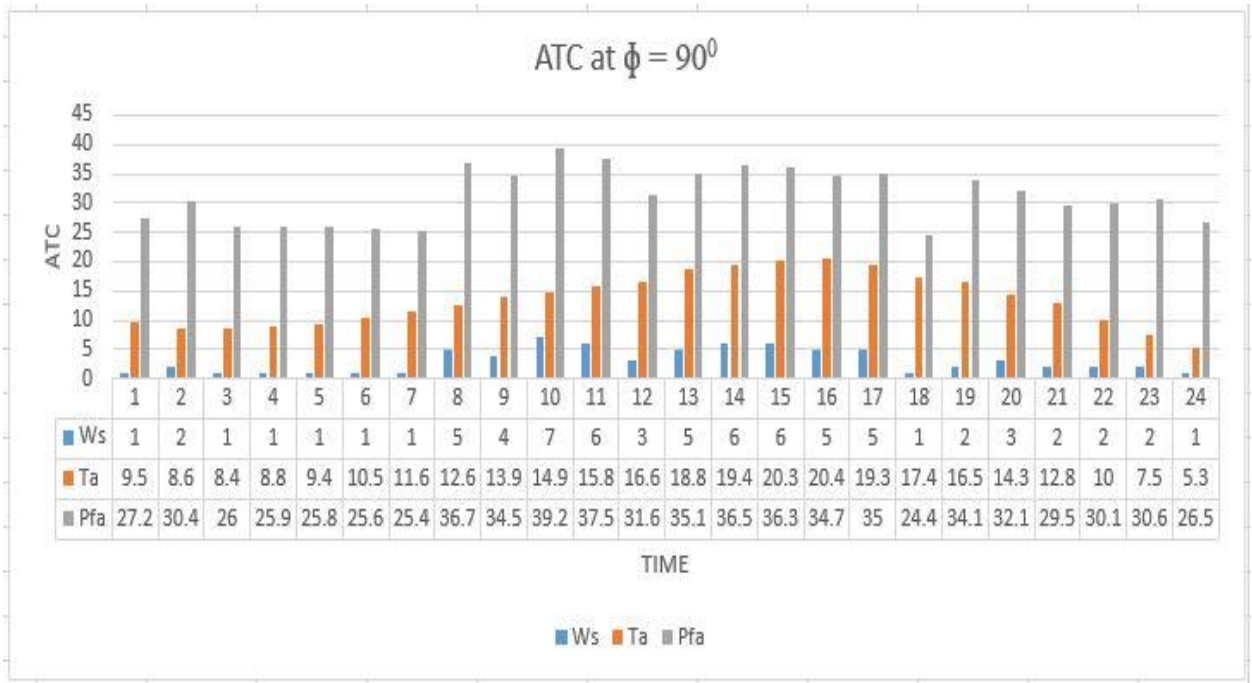

Figure 4.16 Hourly Representation of ATC from line 2-4 at 90^0

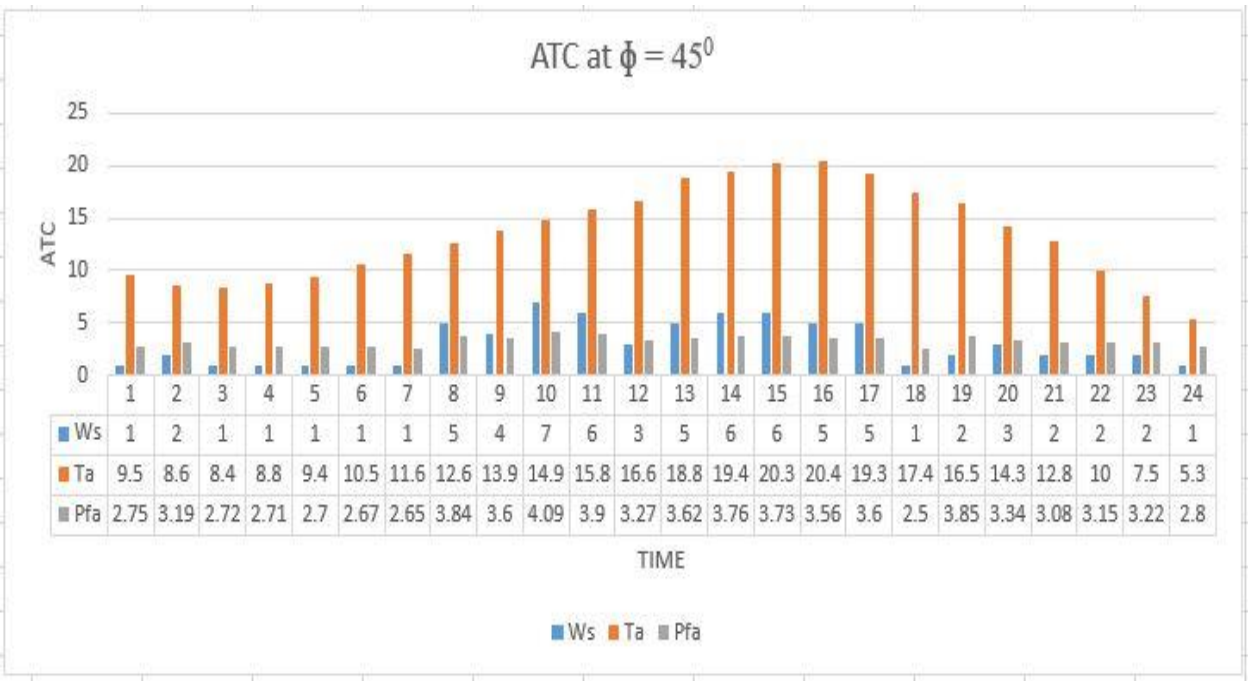

	1	2	3	4	5	6	7	8	9	10	11	12	13	14	15	16	17	18	19	20	21	22	23	24
Ws	1	2	1	1	1	1	1	5	4	7	6	3	5	6	6	5	5	1	2	3	2	2	2	1
Ta	9.5	8.6	8.4	8.8	9.4	10.5	11.6	12.6	13.9	14.9	15.8	16.6	18.8	19.4	20.3	20.4	19.3	17.4	16.5	14.3	12.8	10	7.5	5.3
Pfa	2.75	3.19	2.72	2.71	2.7	2.67	2.65	3.84	3.6	4.09	3.9	3.27	3.62	3.76	3.73	3.56	3.6	2.5	3.85	3.34	3.08	3.15	3.22	2.8

Figure 4.17 Hourly Representation of ATC from line 2-3at 45^0

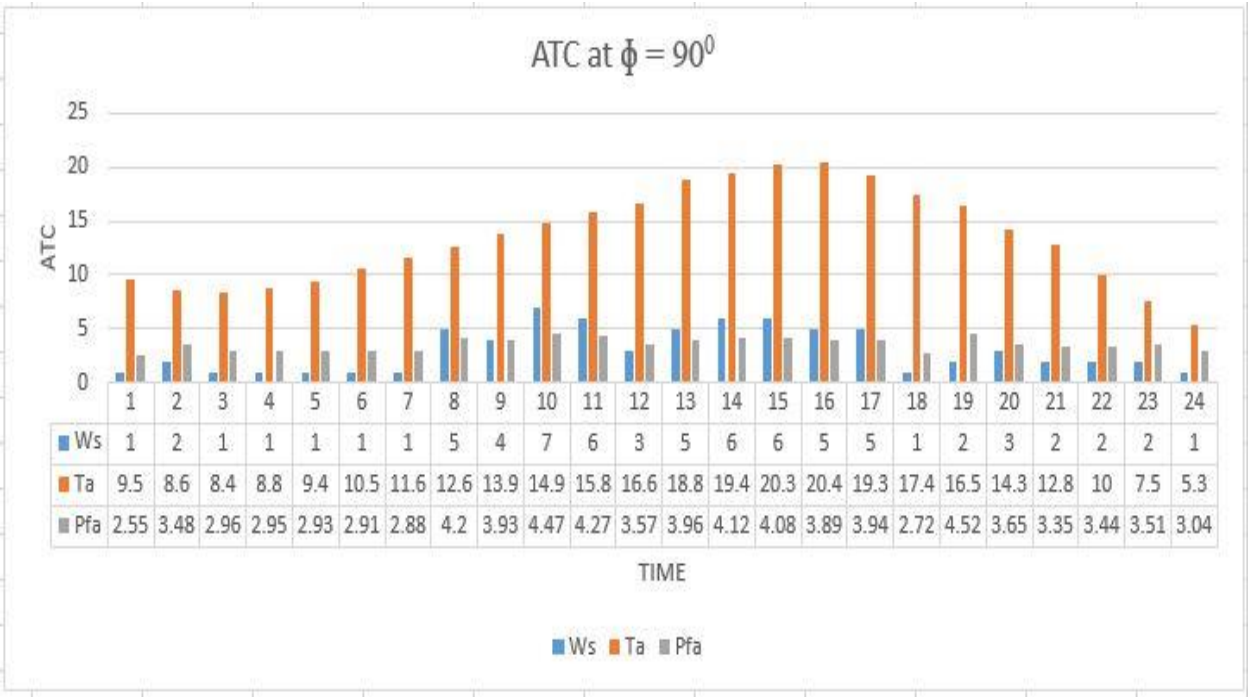

	1	2	3	4	5	6	7	8	9	10	11	12	13	14	15	16	17	18	19	20	21	22	23	24
Ws	1	2	1	1	1	1	1	5	4	7	6	3	5	6	6	5	5	1	2	3	2	2	2	1
Ta	9.5	8.6	8.4	8.8	9.4	10.5	11.6	12.6	13.9	14.9	15.8	16.6	18.8	19.4	20.3	20.4	19.3	17.4	16.5	14.3	12.8	10	7.5	5.3
Pfa	2.55	3.48	2.96	2.95	2.93	2.91	2.88	4.2	3.93	4.47	4.27	3.57	3.96	4.12	4.08	3.89	3.94	2.72	4.52	3.65	3.35	3.44	3.51	3.04

Figure 4.18 Hourly Representation of ATC from line 2-3 at 90^0

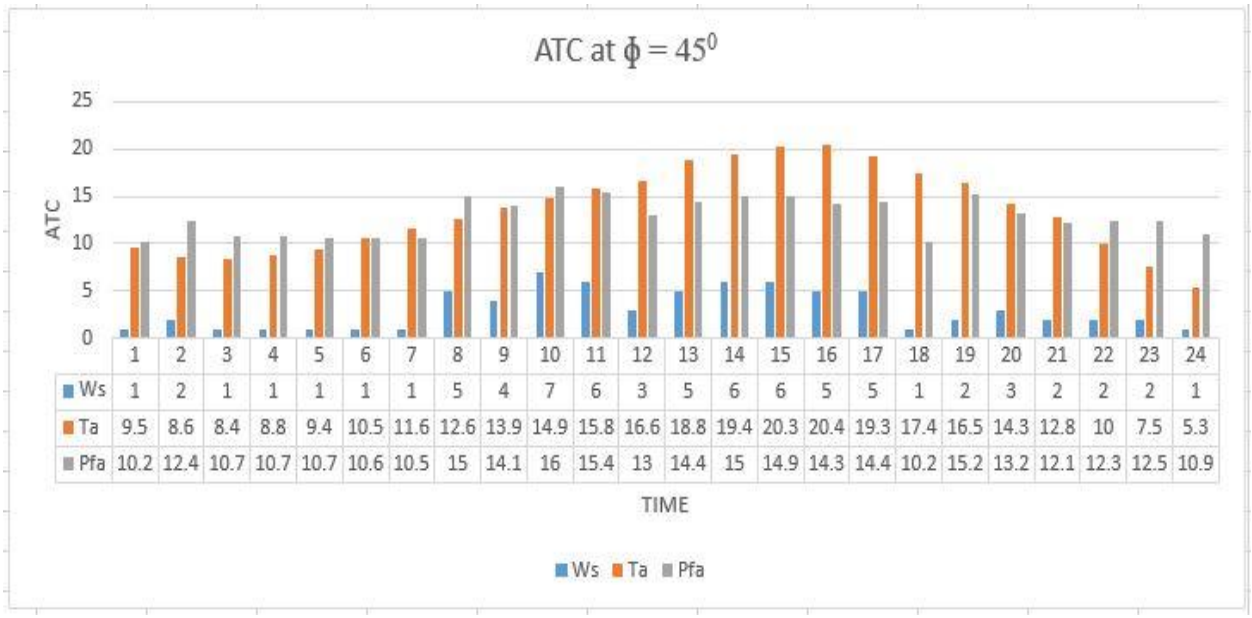

	1	2	3	4	5	6	7	8	9	10	11	12	13	14	15	16	17	18	19	20	21	22	23	24
Ws	1	2	1	1	1	1	1	5	4	7	6	3	5	6	6	5	5	1	2	3	2	2	2	1
Ta	9.5	8.6	8.4	8.8	9.4	10.5	11.6	12.6	13.9	14.9	15.8	16.6	18.8	19.4	20.3	20.4	19.3	17.4	16.5	14.3	12.8	10	7.5	5.3
Pfa	10.2	12.4	10.7	10.7	10.7	10.6	10.5	15	14.1	16	15.4	13	14.4	15	14.9	14.3	14.4	10.2	15.2	13.2	12.1	12.3	12.5	10.9

Figure 4.19 Hourly Representation of ATC from line 2-5 at 45^0

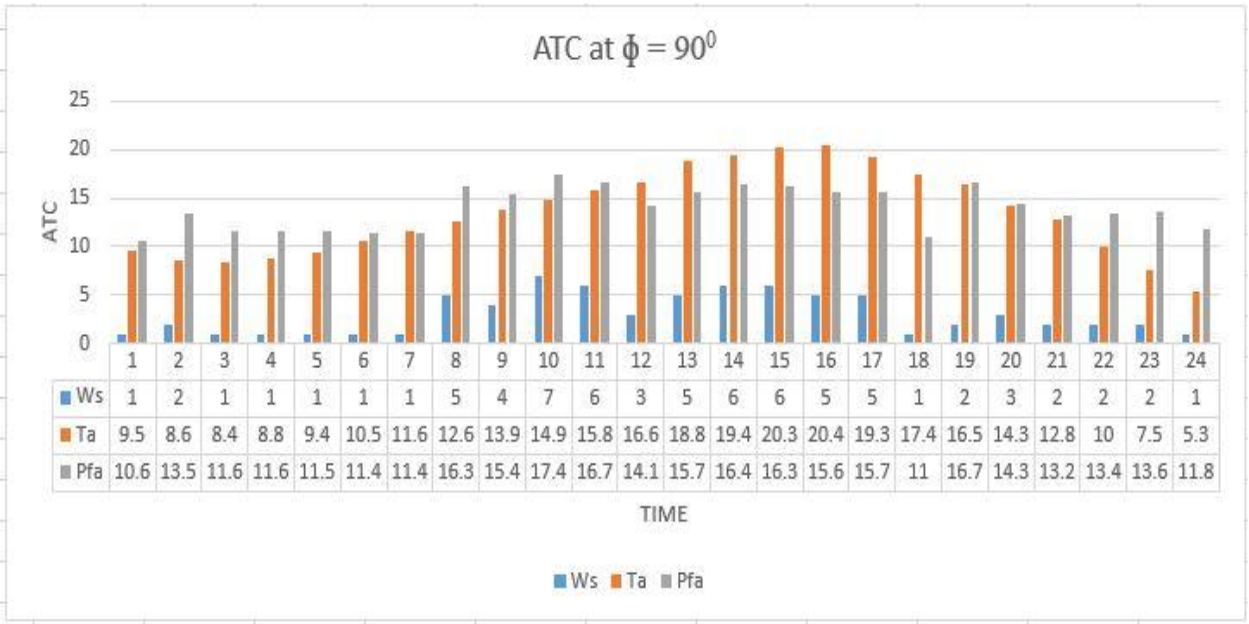

	1	2	3	4	5	6	7	8	9	10	11	12	13	14	15	16	17	18	19	20	21	22	23	24
Ws	1	2	1	1	1	1	1	5	4	7	6	3	5	6	6	5	5	1	2	3	2	2	2	1
Ta	9.5	8.6	8.4	8.8	9.4	10.5	11.6	12.6	13.9	14.9	15.8	16.6	18.8	19.4	20.3	20.4	19.3	17.4	16.5	14.3	12.8	10	7.5	5.3
Pfa	10.6	13.5	11.6	11.6	11.5	11.4	11.4	16.3	15.4	17.4	16.7	14.1	15.7	16.4	16.3	15.6	15.7	11	16.7	14.3	13.2	13.4	13.6	11.8

Figure 4.20 Hourly Representation of ATC from line 2-5 at 90^0

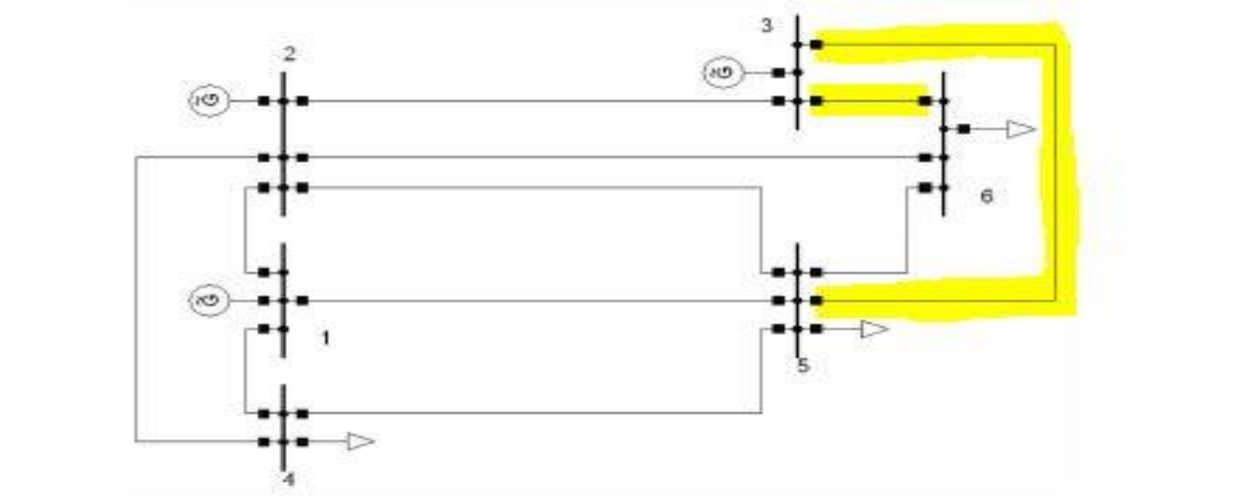

Figure 4.21 Test line (3-5, and 3-6) for ATC calculation

The line for which ATC has calculated i.e. generating to load end has been highlighted in Fig 4.21. Bus 3 is the generating bus so; weather conditions has been considered for the area of bus 3 (generator bus is considering in the Lahaul area of Himachal Pradesh, India) change in ATC of the line for a full day has been shown in Fig 4.22 to Fig 4.25 and the data for wind speed, ambient temperature has been tabulated in Table 4.8

ATC from bus (3-6) and (3-5)

Table 4.8 Available transfer capability from bus 3-6 and 3-5

Time	Ws(m/s)	Ta(^{0}C)	ATC at Φ = 45^0 (3-6)	ATC at Φ = 90^0 (3-6)	ATC at Φ = 45^0 (3-5)	ATC at Φ = 90^0 (3-5)
1	4	28.5000	36.1783	39.3577	16.7361	18.2069
2	1	27.5000	27.7512	30.1234	12.1102	13.3542
3	1	16.9000	28.7630	31.0523	13.3058	14.3648
4	2	17.2000	33.3112	36.1160	15.4098	16.7073
5	2	18.7000	33.0055	35.7846	15.2683	16.5540
6	2	19.0000	32.9439	35.7179	15.2399	16.5231
7	2	21.1000	32.5089	35.2468	15.0386	16.3052
8	2	22.9000	32.1304	34.8370	14.8635	16.1156
9	2	24.7000	31.7463	34.4215	14.6859	15.9234

Time	Ws(m/s)	Ta(^{0}C)	ATC at Φ = 45^0 (3-6)	ATC at Φ = 90^0 (3-6)	ATC at Φ = 45^0 (3-5)	ATC at Φ = 90^0 (3-5)
10	5	24.4000	39.2059	42.6862	18.1367	19.7466
11	3	24.0000	34.6998	37.7002	16.0522	17.4401
12	2	28.8000	30.8499	33.4522	14.2712	15.4750
13	2	31.5000	30.2421	32.7955	13.9900	15.1712
14	2	32.4000	30.0362	32.5732	13.8948	15.0684
15	5	30.8000	43.2671	47.5248	22.0154	22.1204
16	8	31.9000	41.5606	45.3260	19.2259	20.9678
17	2	29.0000	30.8054	33.4041	14.2506	15.4527
18	3	27.0000	32.4723	35.8619	16.2753	18.2441
19	1	26.5000	27.0207	29.1749	12.4998	13.4963
20	1	24.0000	27.4883	29.6781	12.7161	13.7291
21	2	21.5000	32.4252	35.1563	14.9999	16.2633
22	1	19.2000	28.3582	30.6156	13.1185	14.1628
23	3	16.4000	36.6592	39.8266	16.9586	18.4238
24	1	13.6000	29.3312	31.6656	13.5686	14.6485

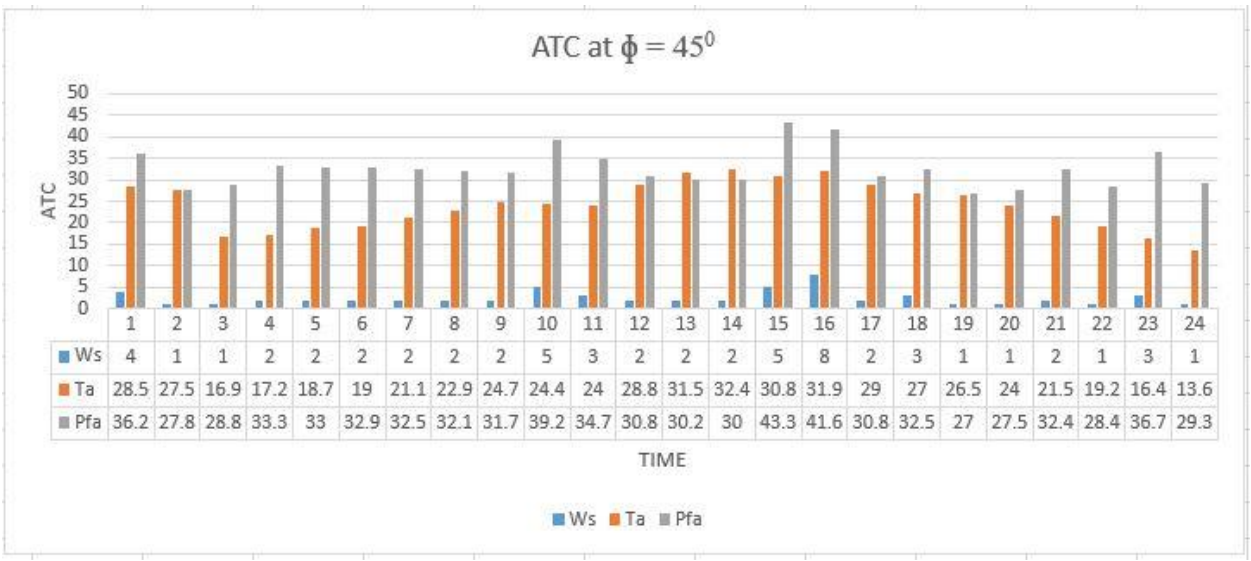

Figure 4.22 Hourly Representation of ATC from line 3-6 at 45^0

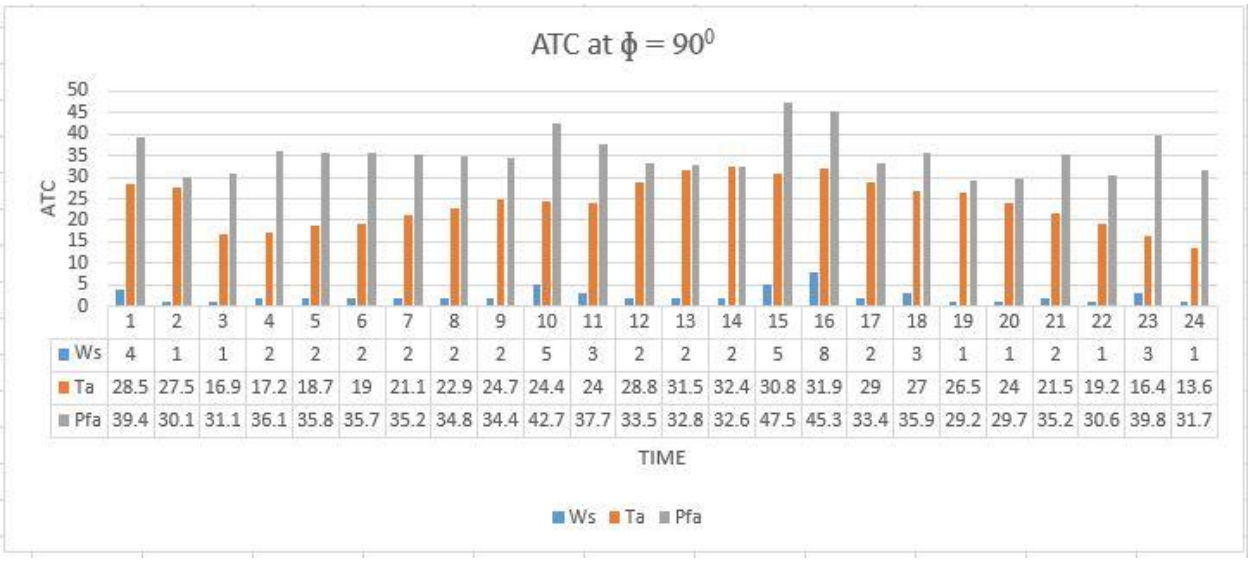

	1	2	3	4	5	6	7	8	9	10	11	12	13	14	15	16	17	18	19	20	21	22	23	24
Ws	4	1	1	2	2	2	2	2	2	5	3	2	2	2	5	8	2	3	1	1	2	1	3	1
Ta	28.5	27.5	16.9	17.2	18.7	19	21.1	22.9	24.7	24.4	24	28.8	31.5	32.4	30.8	31.9	29	27	26.5	24	21.5	19.2	16.4	13.6
Pfa	39.4	30.1	31.1	36.1	35.8	35.7	35.2	34.8	34.4	42.7	37.7	33.5	32.8	32.6	47.5	45.3	33.4	35.9	29.2	29.7	35.2	30.6	39.8	31.7

Figure 4.23 Hourly Representation of ATC from line 3-6 at 90^0

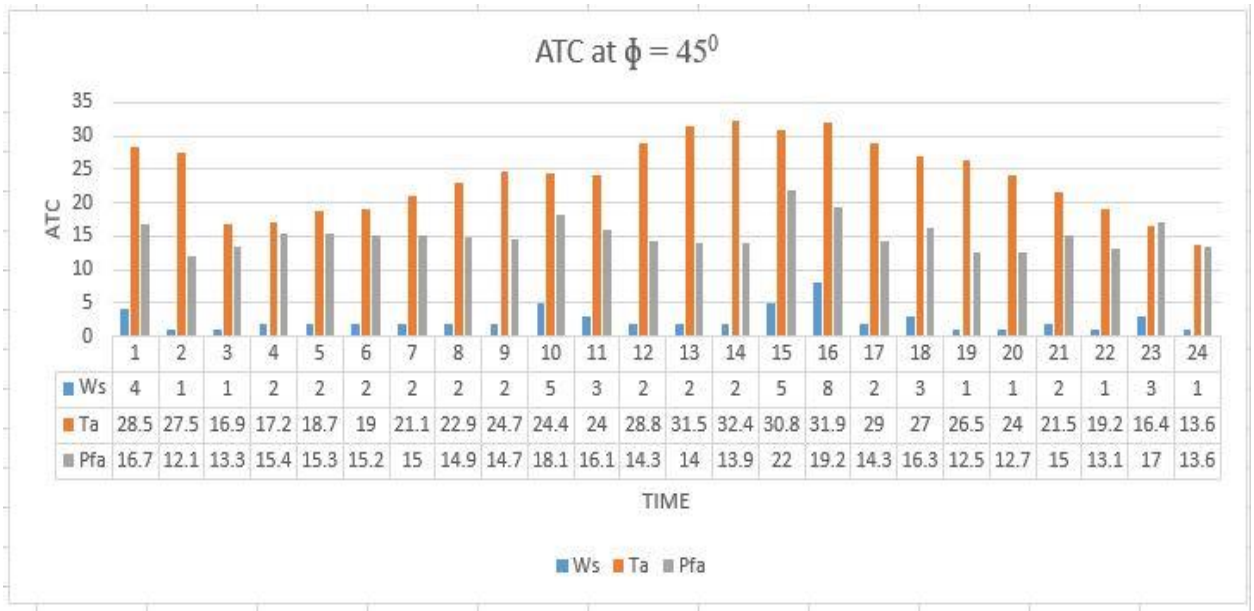

	1	2	3	4	5	6	7	8	9	10	11	12	13	14	15	16	17	18	19	20	21	22	23	24
Ws	4	1	1	2	2	2	2	2	2	5	3	2	2	2	5	8	2	3	1	1	2	1	3	1
Ta	28.5	27.5	16.9	17.2	18.7	19	21.1	22.9	24.7	24.4	24	28.8	31.5	32.4	30.8	31.9	29	27	26.5	24	21.5	19.2	16.4	13.6
Pfa	16.7	12.1	13.3	15.4	15.3	15.2	15	14.9	14.7	18.1	16.1	14.3	14	13.9	22	19.2	14.3	16.3	12.5	12.7	15	13.1	17	13.6

Figure 4.24 Hourly Representation of ATC from line 3-5at 45^0

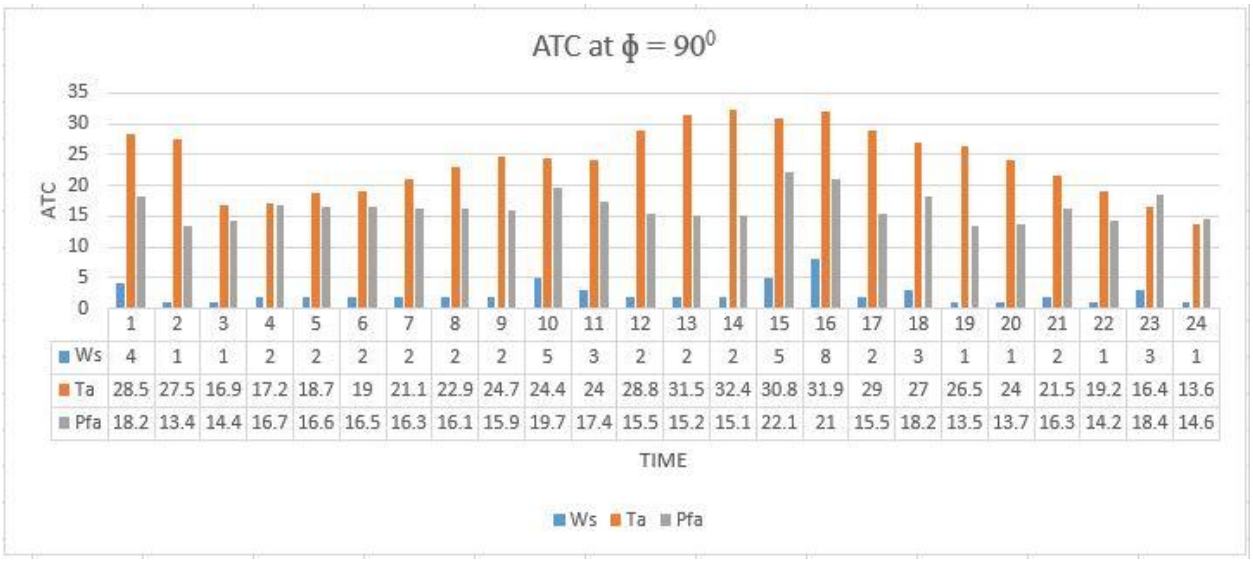

	1	2	3	4	5	6	7	8	9	10	11	12	13	14	15	16	17	18	19	20	21	22	23	24
Ws	4	1	1	2	2	2	2	2	2	5	3	2	2	2	5	8	2	3	1	1	2	1	3	1
Ta	28.5	27.5	16.9	17.2	18.7	19	21.1	22.9	24.7	24.4	24	28.8	31.5	32.4	30.8	31.9	29	27	26.5	24	21.5	19.2	16.4	13.6
Pfa	18.2	13.4	14.4	16.7	16.6	16.5	16.3	16.1	15.9	19.7	17.4	15.5	15.2	15.1	22.1	21	15.5	18.2	13.5	13.7	16.3	14.2	18.4	14.6

Figure 4.25 Hourly Representation of ATC from line 3-5 at 90^0

Chapter5. Methodology of DLR for 30-bus system

5.1 IEEE 30 bus test system

IEEE 30-bus system has been used as the test system to demonstrate the calculation of power carrying capability of transmission line. In this system consider the dynamic weather condition, Predicted or real time weather conditions to estimate the real power carrying capability of transmission line. In previous researches they consider static weather conditions or worst weather conditions to estimate the power [3]. But with the use of dynamic weather conditions it has been possible to get the accurate data. IEEE 30-bus system with 38 transmission line in this system from which generator has been connected on the six buses. The effect of dynamic weather conditions has been considering only on the power flow from generator bus to the load bus.to estimate the time of a day when the transmission line has been capable to carry the power to its maximum capability towards the load. If the transmission line has been not able to transfer the maximum power to the load, then extra demand has been fulfilling by another transmission line. For that we have to find the shortest path to transfer the power. The bus data and line data for 30 bus system has been shown Table 5-1 and table 5-2 respectively and the power flow between the buses has been demonstrated in table 5-3.

Table 5.1 Bus data for IEEE-30 bus test system

Bus	Type	Vsp	Theta	PGen	QGen	Pload	Qload
1	Swing	1.06	0	138	-2.79	0	0
2	Gen	1.043	0	57.6	2.47	21.7	12.7
3	Load	1.0	0	0	0	2.4	1.2
4	Gen	1.06	0	0	0	7.6	1.6
5	Gen	1.01	0	24.6	22.6	94.2	19.0
6	Load	1.0	0	0	0	0	0.0
7	Load	1.0	0	0	0	22.8	10.9
8	Gen	1.0	0	35.0	34.8	30.0	30.0
9	Load	1.0	0	0	0	0	0.0

10	Load	1.0	0	0	0	5.8	2.0
11	Load	1.082	0	17.9	30.8	0	0.0
12	Load	1.0	0	0		11.2	7.5
13	Gen	1.071	0	16.9	37.8	0.0	0.0
14	Load	1.0	0	0	0	6.2	1.6
15	Load	1.0	0	0	0	8.2	2.5
16	Load	1.0	0	0	0	3.5	1.8
17	Load	1.0	0	0	0	9.0	5.8
18	Load	1.0	0	0	0	3.2	0.9
19	Load	1.0	0	0	0	9.5	3.4
20	Load	1.0	0	0	0	2.2	0.7
21	Load	1.0	0	0	0	17.5	11.2
22	Load	1.0	0	0	0	0.0	0.0
23	Load	1.0	0	0	0	3.2	1.6
24	Load	1.0	0	0	0	8.7	6.7
25	Load	1.0	0	0	0	0.0	0.0
26	Load	1.0	0	0	0	3.5	2.3
27	Load	1.0	0	0	0	0.0	0.0
28	Load	1.0	0	0	0	0.0	0.0
29	Load	1.0	0	0	0	2.4	0.9
30	Load	1.0	0	0	0	10.6	1.9

Table 5.2 Line Data for IEEE-30 bus system

From Bus	To Bus	R(pu)	X(pu)	B/2(pu)	T/F Tap
1	2	0.0192	0.0575	0.0528	1
1	3	0.0452	0.1652	0.0408	1
2	4	0.0570	0.1737	0.0368	1

From Bus	To Bus	R(pu)	X(pu)	B/2(pu)	T/F Tap
3	4	0.0132	0.0379	0.0084	1
2	6	0.0581	0.1763	0.0374	1
5	7	0.0460	0.1160	0.0204	1
6	7	0.0267	0.0820	0.0170	1
6	8	0.0120	0.0420	0.0090	1
6	9	0.0	0.2080	0	0.978
6	10	0.0	0.5560	0	0.969
9	10	0.0	0.1100	0	1
4	12	0.0	0.2560	0	0.932
12	13	0.0	0.1400	0	1
12	14	0.1231	0.2559	0	1
12	15	0.0662	0.1304	0	1
12	16	0.0945	0.1987	0	1
14	15	0.2210	0.1997	0	1
16	17	0.0824	0.1923	0	1
15	18	0.1073	0.2185	0	1
18	19	0.0639	0.1292	0	1
19	20	0.0340	0.0680	0	1
10	20	0.0936	0.2090	0	1
10	17	0.0324	0.0845	0	1
10	21	0.0348	0.0749	0	1
10	22	0.0727	0.1499	0	1
21	23	0.0116	0.0236	0	1
15	23	0.1000	0.2020	0	1
22	24	0.1150	0.1790	0	1
23	24	0.1320	0.2700	0	1
24	25	0.1885	0.3292	0	1

From Bus	To Bus	R(pu)	X(pu)	B/2(pu)	T/F Tap
25	26	0.2544	0.3800	0	1
25	27	0.1093	0.2087	0	1
28	27	0.0	0.3960	0	0.968
27	29	0.2198	0.4153	0	1
27	30	0.3202	0.6027	0	1
29	30	0.2399	0.4533	0	1
8	28	0.0636	0.2000	0.4028	1
6	28	0.0169	0.0599	0.0130	1

Table 5.3 Power Flow from generator bus to load bus

Line	Power flow (MW)
1-2	88.0995
1-3	50.7483
2-4	28.4190
2-6	37.6148
4-12	30.9634
5-7	13.9183
12-13	18.1304
8-28	7.6167

Table 5.4 Specified conductor temperature

Line	Conductor Temp.(Tc)
1-2	75
1-3	100

Line	Conductor Temp.(Tc)
2-4	100
2-6	100
5-7	70
12-13	70
8-28	70

Results for the estimation of power carrying capability of transmission line considering the effect of dynamic environmental conditions are shown in tabular or graphical form. The following graphical reports are the results obtained for the Al59 241mm^2 conductor. The graphs show the comparison between two different wind angles (90^0 and 45^0) for the test and model cases. The considered wind speeds and temperatures are variable and predicted on the bases of real predicted data [19]

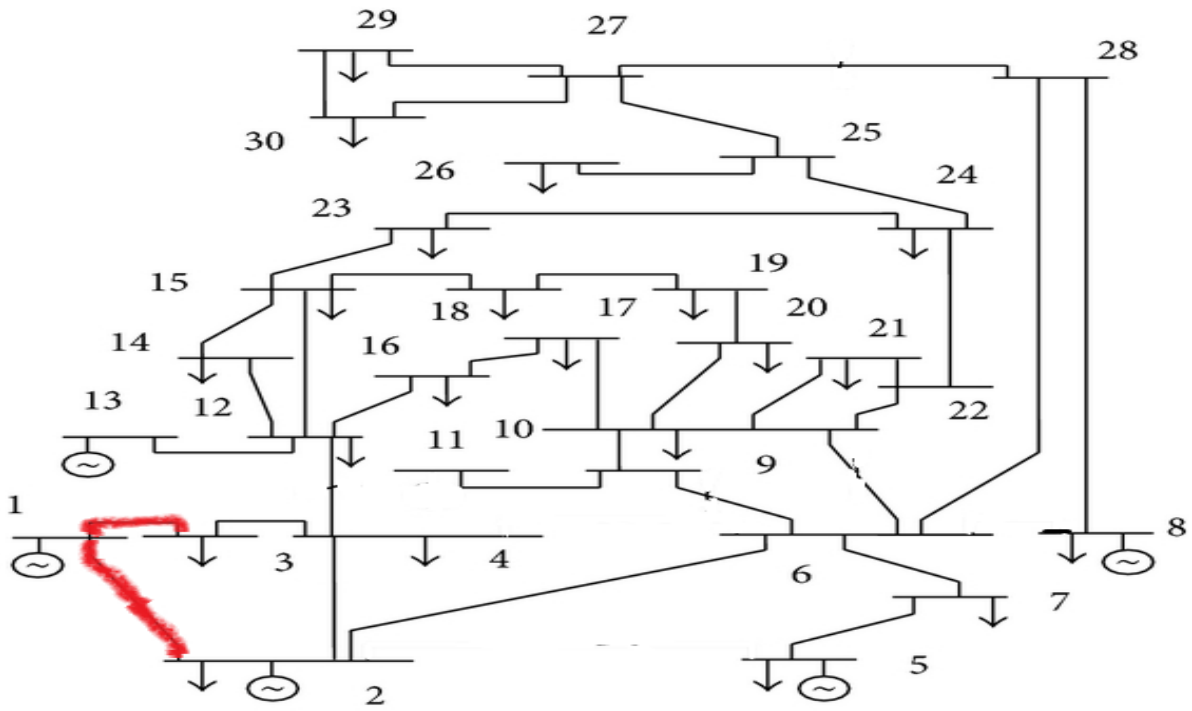

Figure 5.1 Test line (1-2 and 1-3) for ATC calculation

The line for which ATC has calculated i.e. generating to load end has been highlighted in Fig 5.1. Bus 1 is the generating bus so; weather conditions has been considered for the area of bus 1 (generator bus has been considered in the Spiti area of Himachal Pradesh, India) change in ATC of the line for a full day has been shown in Fig 5.4 to Fig 5.9 and the data for wind speed, ambient temperature has been tabulated in Table 5.5 and Table 5.6 .

5.2 Variation in current flow considering DLR

Actual current flow in the line is 0.8311 p.u. considering the DLR method for calculation of dynamic current the mean dynamic current for whole day has been 0.7925 p.u. for 45^0 and 0.8639 p.u. at 90^0 so, by considering the DLR current power transfer has been also increased Fig 5-1 shows the variation in current with considering the DLR and compare that with static rating.

5.3 Losses with and without considering DLR method

Losses for the line without DLR is 0.0133 and after considering the effect of DLR the mean losses for a whole day has been 0.0123 which means with the consideration of dynamic conditions on the system or line it has been possible to minimize the losses on the system or line. Fig 5-2 shows the variation in losses with considering the DLR and compare that losses with static rating.

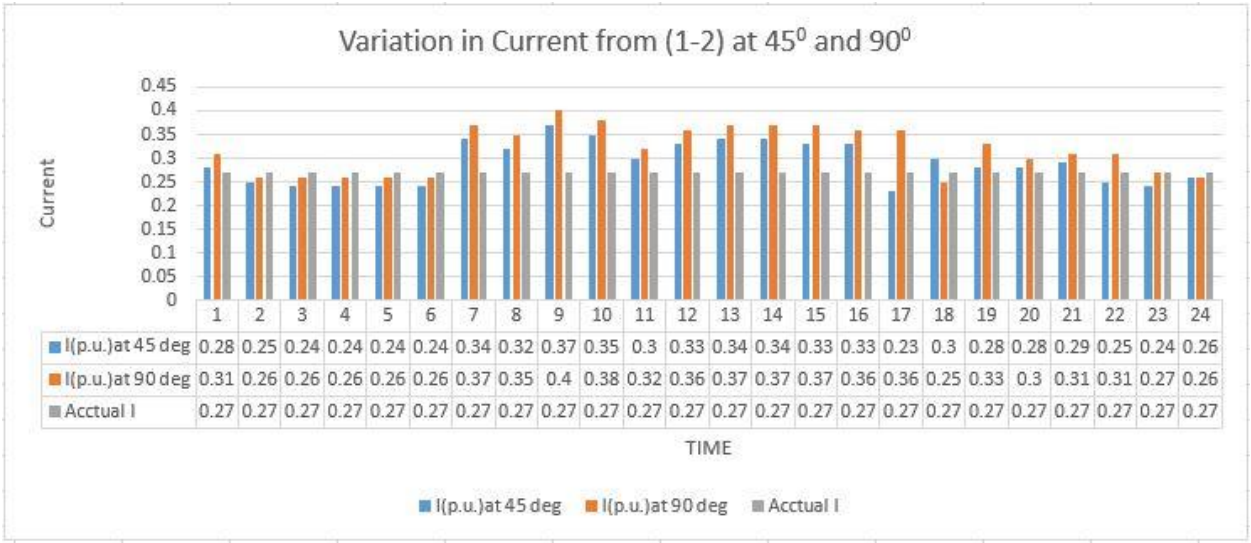

	1	2	3	4	5	6	7	8	9	10	11	12	13	14	15	16	17	18	19	20	21	22	23	24
I(p.u.)at 45 deg	0.28	0.25	0.24	0.24	0.24	0.24	0.34	0.32	0.37	0.35	0.3	0.33	0.34	0.34	0.33	0.33	0.23	0.3	0.28	0.28	0.29	0.25	0.24	0.26
I(p.u.)at 90 deg	0.31	0.26	0.26	0.26	0.26	0.26	0.37	0.35	0.4	0.38	0.32	0.36	0.37	0.37	0.37	0.36	0.36	0.25	0.33	0.3	0.31	0.31	0.27	0.26
Acctual I	0.27	0.27	0.27	0.27	0.27	0.27	0.27	0.27	0.27	0.27	0.27	0.27	0.27	0.27	0.27	0.27	0.27	0.27	0.27	0.27	0.27	0.27	0.27	0.27

Figure 5.2 Variations in current flow from line (1-2) for a whole day

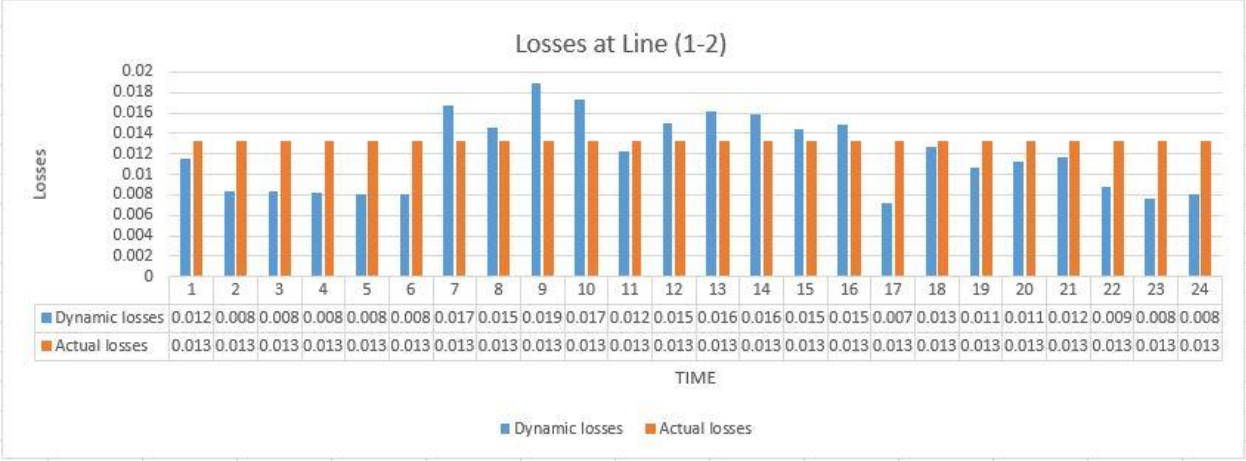

Figure 5.3 Losses in the system from line (1-2) considering DLR method

Table 5.5 Comparison of ATC from bus 1-2 for MOOSE and ZEBRA

Time	Ws(m/s)	Ta(^{0}C)	ATC at Φ = 45^0(ZEBRA)	ATC at Φ = 90^0(ZEBRA)	ATC at Φ = 45^0(MOOSE)	ATC at Φ = 90^0(MOOSE)
1	2	16.4000	81.2546	86.8856	83.9210	85.6324
2	1	17.0000	67.5214	74.0021	70.0015	73.0221
3	1	16.9000	67.2191	73.0437	69.2610	72.1120
4	2	17.2000	78.6906	85.7442	81.0228	84.8004
5	2	18.7000	77.5923	84.5589	79.8887	83.4953
6	2	19.0000	77.3706	84.3196	79.6596	83.2315
7	2	21.1000	75.7976	82.6230	78.0349	81.3589
8	2	22.9000	74.4193	81.1374	76.6111	79.7151
9	2	24.7000	73.0116	79.6211	75.1567	78.0332
10	5	24.4000	91.4534	99.9556	94.0862	98.2626
11	3	24.0000	81.0779	88.5096	83.4380	86.9411
12	2	28.8000	69.6858	76.0424	71.7192	74.0457
13	2	31.5000	67.3953	73.5810	69.3509	71.2866
14	2	32.4000	66.6123	72.7403	68.5411	70.3408
15	5	32.0000	68.2496	75.4582	72.3861	75.2115

16	8	31.9000	94.4048	97.3370	97.0816	98.5550
17	2	29.0000	69.5190	75.8631	71.5468	73.8451
18	4	28.5000	82.7603	90.4527	85.1414	88.3478
19	1	26.5000	60.8112	66.1783	62.6301	64.4808
20	1	24.0000	62.5543	68.0430	64.4347	66.5642
21	2	21.5000	75.4937	82.2955	77.7211	80.9968
22	1	19.2000	65.7507	71.4680	67.7422	70.3695
23	3	16.4000	87.2918	95.2303	89.8509	94.3465
24	1	13.6000	69.2617	75.2380	71.3730	74.5305

5.4 Results for ATC of line considering the DLR

ATC from bus (1-2) (Comparison between **moose** and **zebra** conductors)

ATC for different type of conductors i.e. moose and zebra has been calculated and the results for both conductors at different wind angle has been shown in Fig 5.3 to 5.6 and weather data has been tabulated in table 5-5.

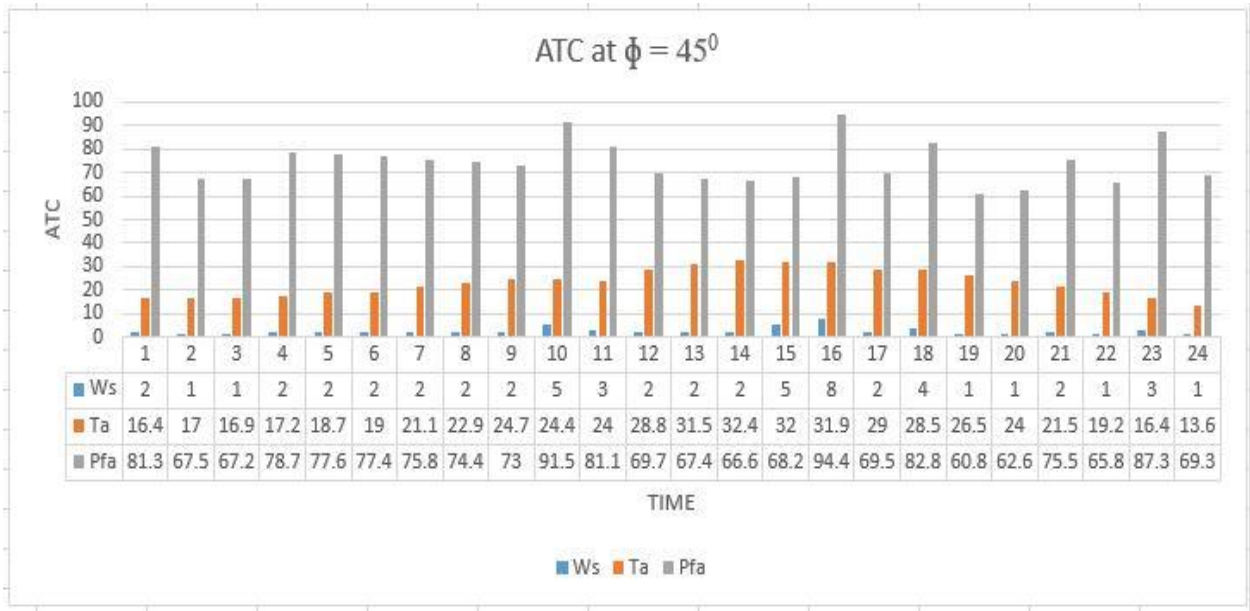

	1	2	3	4	5	6	7	8	9	10	11	12	13	14	15	16	17	18	19	20	21	22	23	24
Ws	2	1	1	2	2	2	2	2	2	5	3	2	2	2	5	8	2	4	1	1	2	1	3	1
Ta	16.4	17	16.9	17.2	18.7	19	21.1	22.9	24.7	24.4	24	28.8	31.5	32.4	32	31.9	29	28.5	26.5	24	21.5	19.2	16.4	13.6
Pfa	81.3	67.5	67.2	78.7	77.6	77.4	75.8	74.4	73	91.5	81.1	69.7	67.4	66.6	68.2	94.4	69.5	82.8	60.8	62.6	75.5	65.8	87.3	69.3

Figure 5.4 Hourly Representation of ATC from line 1-2 at 45^0(ZEBRA)

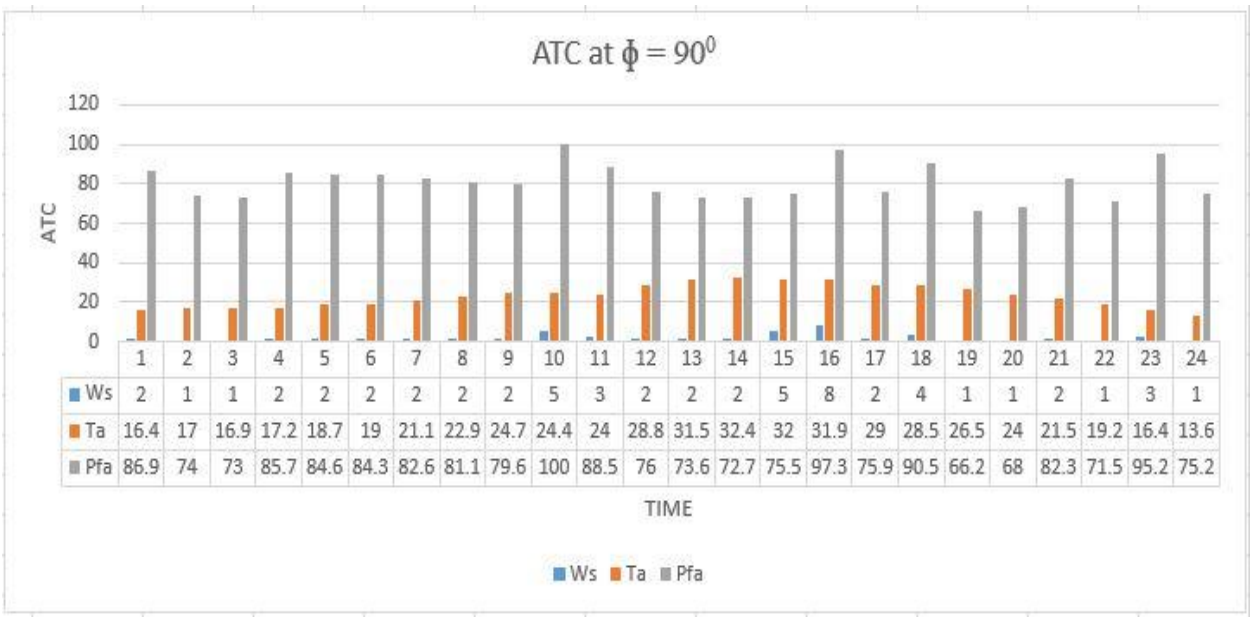

Figure 5.5 Hourly Representation of ATC from line 1-2 at 90^0(ZEBRA)

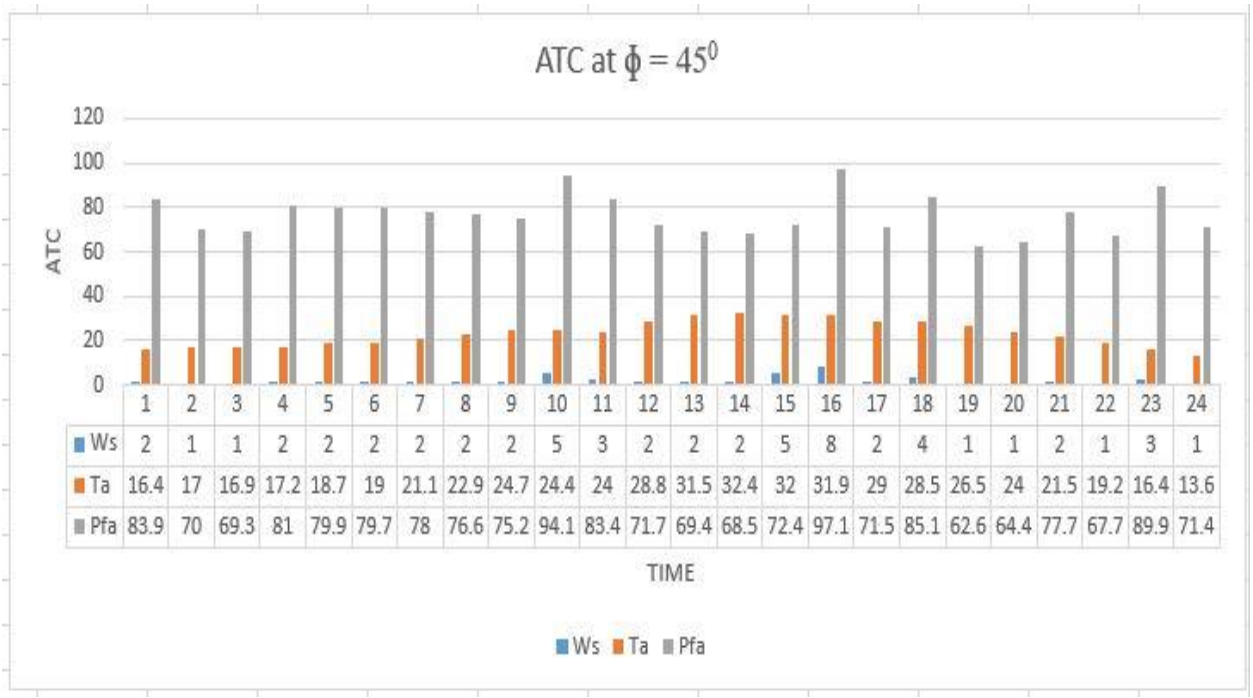

Figure 5.6 Hourly Representation of ATC from line 1-2 at 45^0(MOOSE)

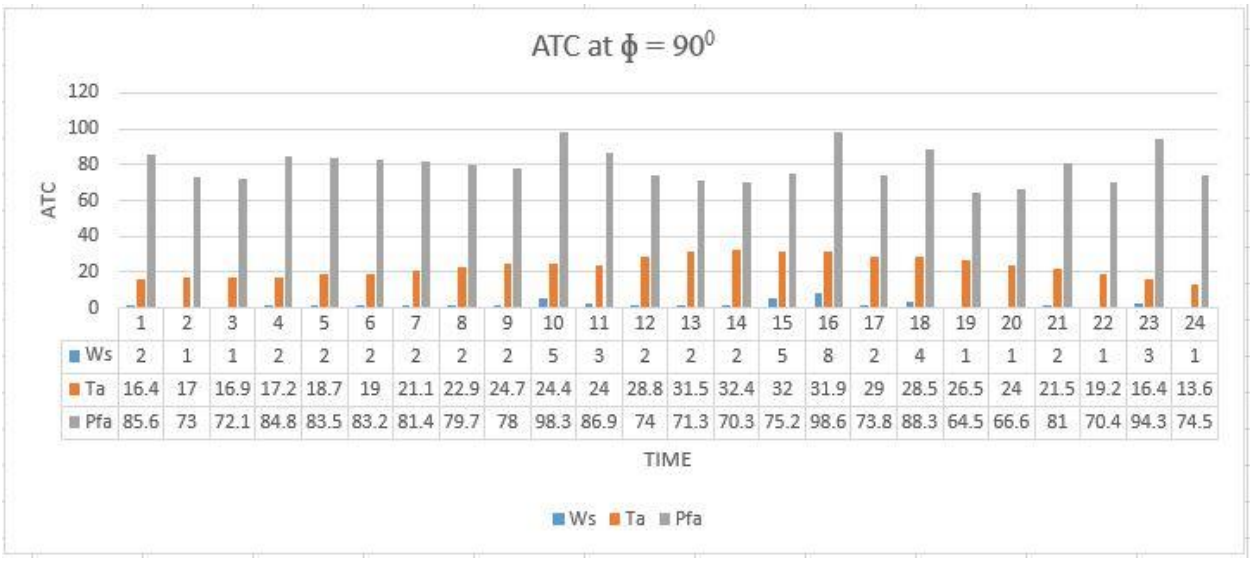

Figure 5.7 Hourly Representation of ATC from line 1-2 at 90^0(MOOSE)

The power carrying capability of the transmission lines has increased as the temperature has been decreased and wind speed has increased. The relation between diameter of the conductor and the variation of the ATC has been found. The direct relationship between the ATC and the diameter of conductor is shown in table 5-5.

ATC from bus (1-3)

Table 5.6 Available transfer capability from bus 1-3

Time	Ws(m/s)	Ta(^{0}C)	ATC at $\Phi = 45^0$	ATC at $\Phi = 90^0$
1	1	7.5000	37.6214	39.8243
2	2	8.6000	38.4074	41.6498
3	1	8.4000	33.1226	35.7683
4	1	8.8000	33.0505	35.6903
5	1	9.4000	32.9420	35.5729
6	1	10.5000	32.7418	35.3565
7	1	11.6000	32.5399	35.1384
8	5	12.6000	46.3027	50.4175
9	4	13.9000	43.6240	47.4597
10	7	14.9000	49.4711	53.9297
11	6	15.8000	47.4374	51.6865

Time	Ws(m/s)	Ta(^{0}C)	ATC at $\Phi = 45^0$	ATC at $\Phi = 90^0$
12	3	16.6000	40.1817	43.6608
13	5	18.8000	44.6176	48.5832
14	6	19.4000	46.4029	50.5600
15	6	20.3000	46.1403	50.2741
16	5	20.4000	44.1708	48.0972
17	5	19.3000	44.4785	48.4319
18	1	17.4000	31.4472	33.9588
19	6	15.2000	45.2671	47.5504
20	3	14.3000	40.7362	44.2631
21	2	12.8000	37.5133	40.6796
22	2	10.0000	38.1122	41.3294
23	2	7.5000	38.6374	41.8995
24	1	5.3000	33.6744	36.3652

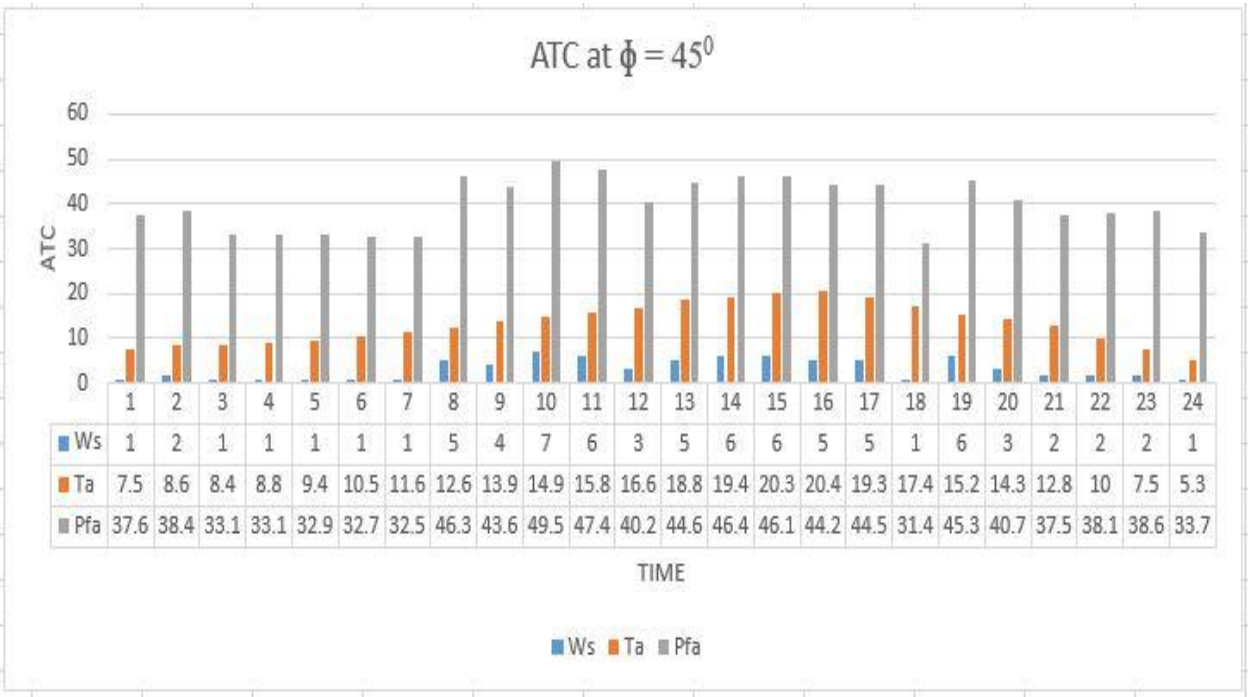

Figure 5.8 Hourly Representation of ATC from line 1-3 at 45^0

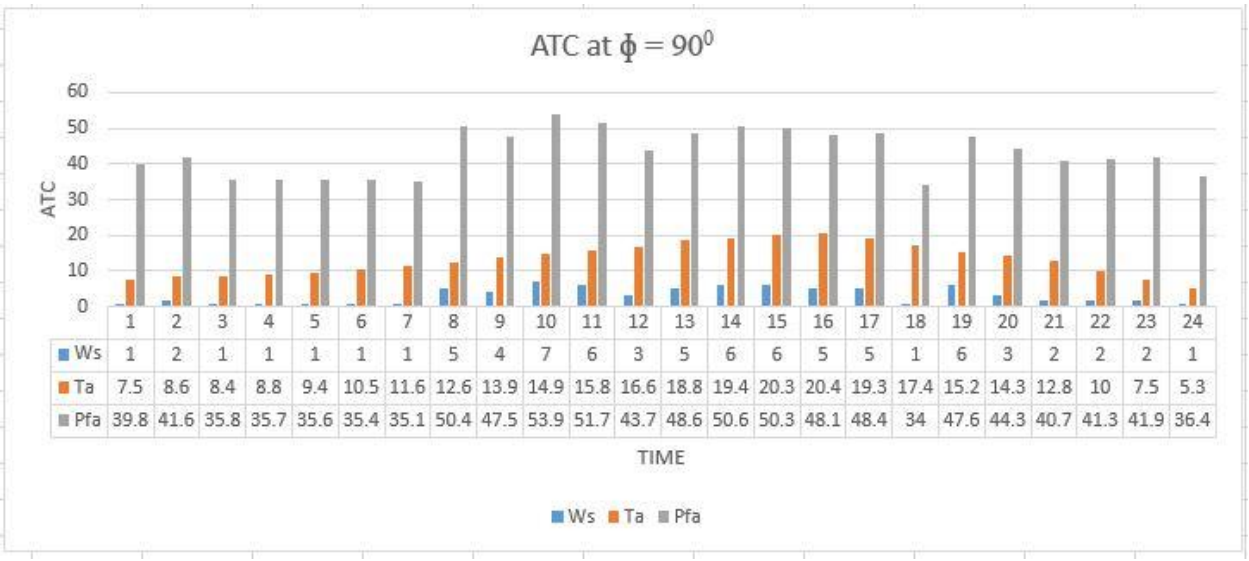

	1	2	3	4	5	6	7	8	9	10	11	12	13	14	15	16	17	18	19	20	21	22	23	24
Ws	1	2	1	1	1	1	1	5	4	7	6	3	5	6	6	5	5	1	6	3	2	2	2	1
Ta	7.5	8.6	8.4	8.8	9.4	10.5	11.6	12.6	13.9	14.9	15.8	16.6	18.8	19.4	20.3	20.4	19.3	17.4	15.2	14.3	12.8	10	7.5	5.3
Pfa	39.8	41.6	35.8	35.7	35.6	35.4	35.1	50.4	47.5	53.9	51.7	43.7	48.6	50.6	50.3	48.1	48.4	34	47.6	44.3	40.7	41.3	41.9	36.4

Figure 5.9 Hourly Representation of ATC from line 1-3 at 90^0

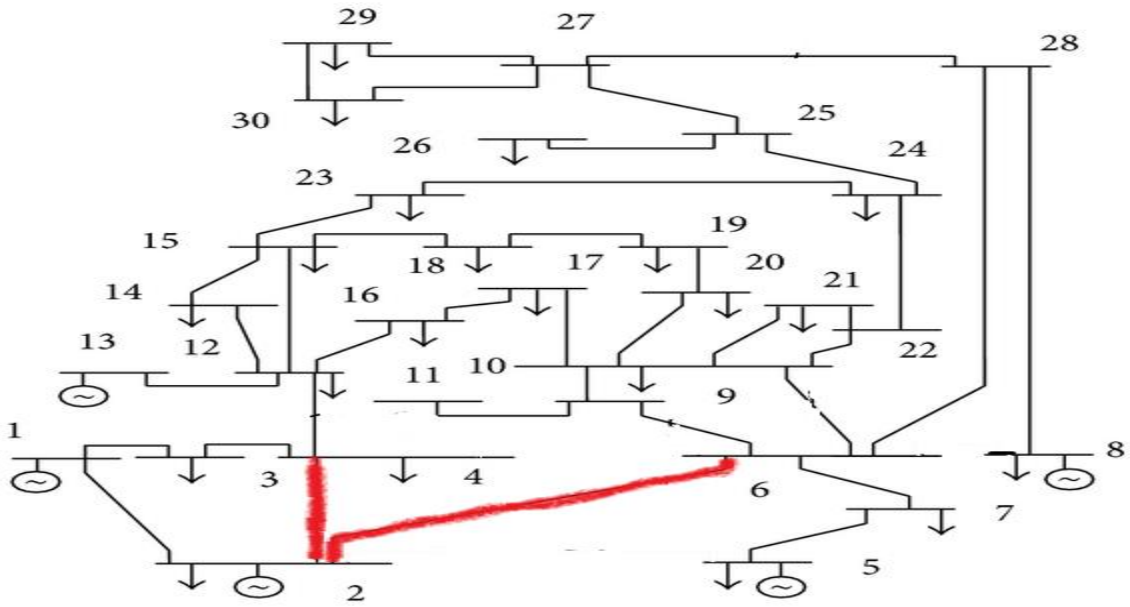

Figure 5.10 Test line (2-4 and 2-6) for ATC calculation

The line for which ATC has calculated i.e. generating to load end has been highlighted in Fig 5.10. Bus 2 is the generating bus so; weather conditions has been considered for the area of bus 2 (the generator bus has been considering in the Kullu area of Himachal Pradesh, India) change in ATC

of the line for a full day has been shown in Fig 5.11 to Fig 5.14 and the data for wind speed, ambient temperature has been tabulated in Table 5.7

ATC from bus (2-4) and (2-6)

Table 5.7 Available transfer capability from bus 2-4 and 2-6

Time	Ws(m/s)	Ta(^{0}C)	ATC at $\Phi = 45^0$ (2-4)	ATC at $\Phi = 90^0$ (2-4)	ATC at $\Phi = 45^0$ (2-6)	ATC at $\Phi = 90^0$(2-6)
1	1	7.5000	21.3045	22.5361	19.5287	23.8621
2	2	8.6000	22.1570	24.0275	19.6891	21.3512
3	1	8.4000	19.1082	20.6345	16.9799	18.3361
4	1	8.8000	19.0666	20.5895	16.9429	18.2962
5	1	9.4000	19.0040	20.5218	16.8873	18.2360
6	1	10.5000	18.8885	20.3969	16.7847	18.1251
7	1	11.6000	18.7721	20.2711	16.6812	18.0133
8	5	12.6000	26.7117	29.0855	23.7365	25.8459
9	4	13.9000	25.1664	27.3792	22.3633	24.3296
10	7	14.9000	28.5396	31.1117	25.3607	27.6464
11	6	15.8000	27.3663	29.8176	24.3182	26.4964
12	3	16.6000	23.1805	25.1876	20.5986	22.3821
13	5	18.8000	25.7396	28.0273	22.8726	24.9056
14	6	19.4000	26.7696	29.1678	23.7879	25.9190
15	6	20.3000	26.6180	29.0028	23.6532	25.7724
16	5	20.4000	25.4819	27.7470	22.6436	24.6564
17	5	19.3000	25.6594	27.9400	22.8014	24.8280
18	1	17.4000	18.1417	19.5906	16.1210	17.4085
19	6	15.2000	25.4108	26.4231	23.7713	25.1693
20	3	14.3000	23.5004	25.5351	20.8829	22.6909
21	2	12.8000	21.6412	23.4678	19.2307	20.8539

Time	Ws(m/s)	Ta(^{0}C)	ATC at $\Phi = 45^0$ (2-4)	ATC at $\Phi = 90^0$ (2-4)	ATC at $\Phi = 45^0$ (2-6)	ATC at $\Phi = 90^0$(2-6)
22	2	10.0000	21.9867	23.8426	19.5378	21.1870
23	2	7.5000	22.2897	24.1715	19.8070	21.4792
24	1	5.3000	19.4265	20.9789	17.2628	18.6422

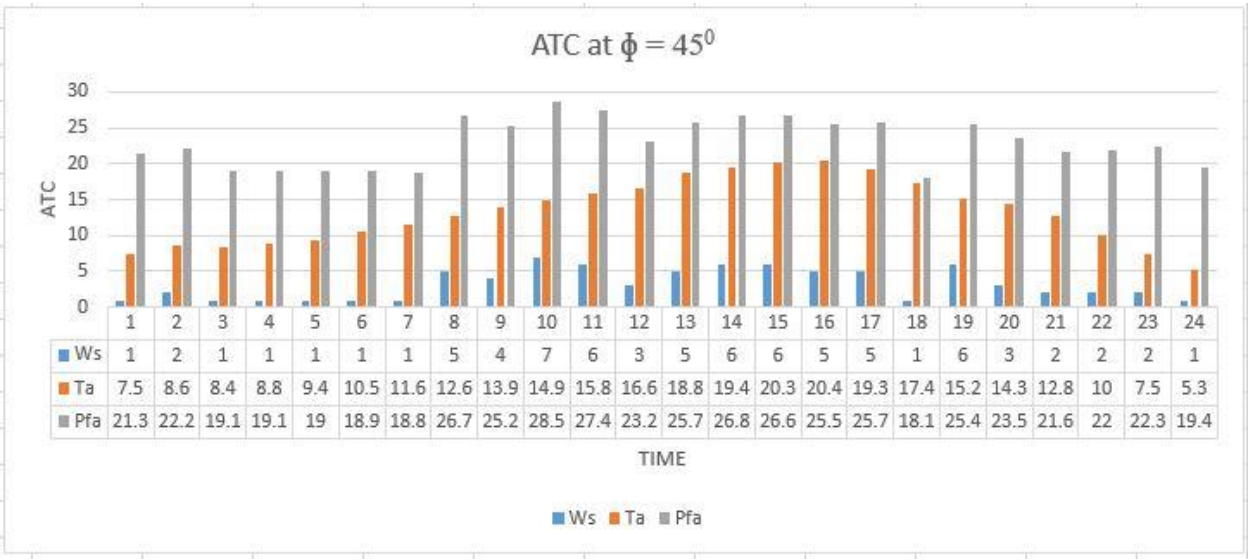

	1	2	3	4	5	6	7	8	9	10	11	12	13	14	15	16	17	18	19	20	21	22	23	24
Ws	1	2	1	1	1	1	1	5	4	7	6	3	5	6	6	5	5	1	6	3	2	2	2	1
Ta	7.5	8.6	8.4	8.8	9.4	10.5	11.6	12.6	13.9	14.9	15.8	16.6	18.8	19.4	20.3	20.4	19.3	17.4	15.2	14.3	12.8	10	7.5	5.3
Pfa	21.3	22.2	19.1	19.1	19	18.9	18.8	26.7	25.2	28.5	27.4	23.2	25.7	26.8	26.6	25.5	25.7	18.1	25.4	23.5	21.6	22	22.3	19.4

Figure 5.11 Hourly Representation of ATC from line 2-4 at 45^0

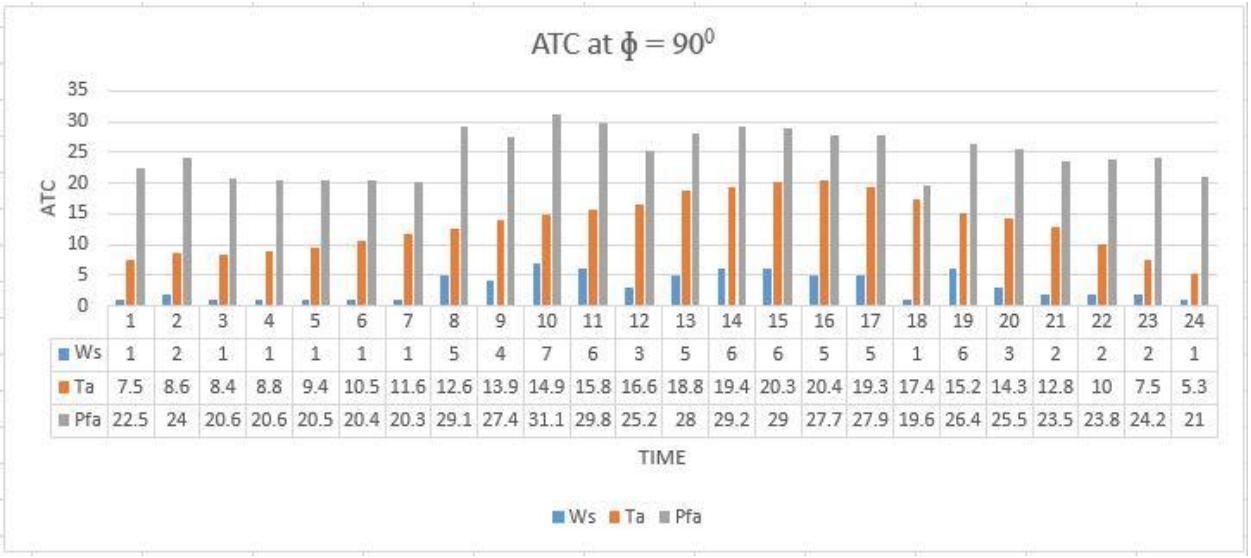

	1	2	3	4	5	6	7	8	9	10	11	12	13	14	15	16	17	18	19	20	21	22	23	24
Ws	1	2	1	1	1	1	1	5	4	7	6	3	5	6	6	5	5	1	6	3	2	2	2	1
Ta	7.5	8.6	8.4	8.8	9.4	10.5	11.6	12.6	13.9	14.9	15.8	16.6	18.8	19.4	20.3	20.4	19.3	17.4	15.2	14.3	12.8	10	7.5	5.3
Pfa	22.5	24	20.6	20.6	20.5	20.4	20.3	29.1	27.4	31.1	29.8	25.2	28	29.2	29	27.7	27.9	19.6	26.4	25.5	23.5	23.8	24.2	21

Figure 5.12 Hourly Representation of ATC from line 2-4 at 90^0

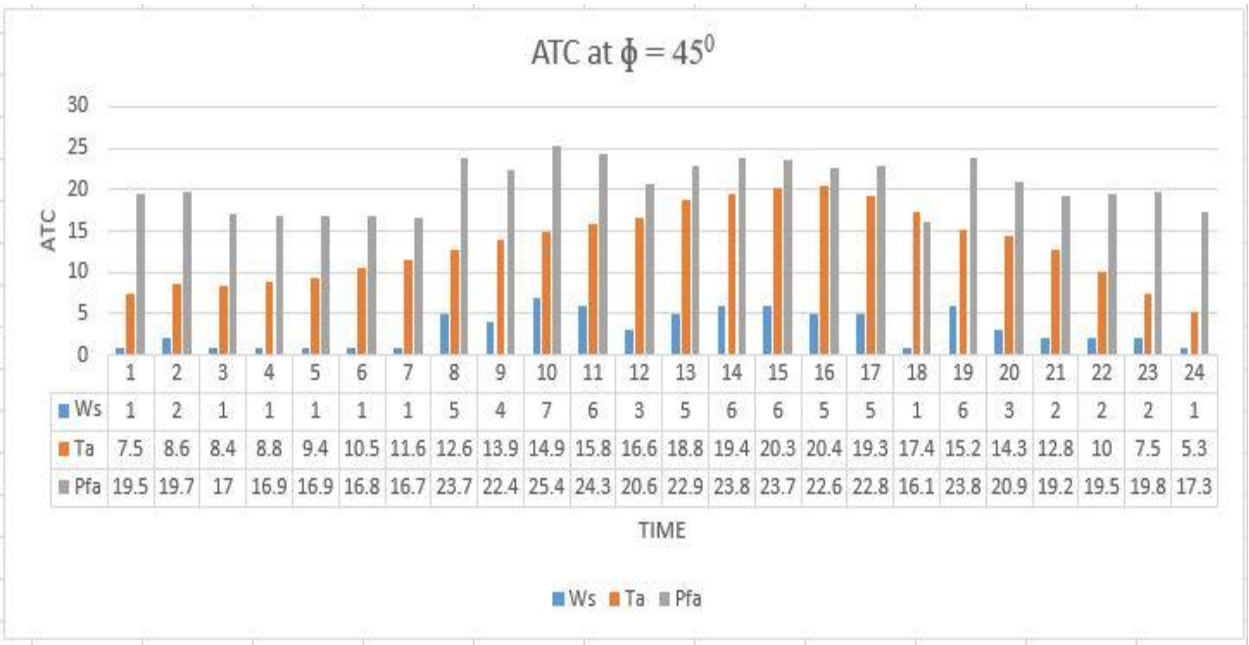

	1	2	3	4	5	6	7	8	9	10	11	12	13	14	15	16	17	18	19	20	21	22	23	24
Ws	1	2	1	1	1	1	1	5	4	7	6	3	5	6	6	5	5	1	6	3	2	2	2	1
Ta	7.5	8.6	8.4	8.8	9.4	10.5	11.6	12.6	13.9	14.9	15.8	16.6	18.8	19.4	20.3	20.4	19.3	17.4	15.2	14.3	12.8	10	7.5	5.3
Pfa	19.5	19.7	17	16.9	16.9	16.8	16.7	23.7	22.4	25.4	24.3	20.6	22.9	23.8	23.7	22.6	22.8	16.1	23.8	20.9	19.2	19.5	19.8	17.3

Figure 5.13 Hourly Representation of ATC from line 2-6at 45^0

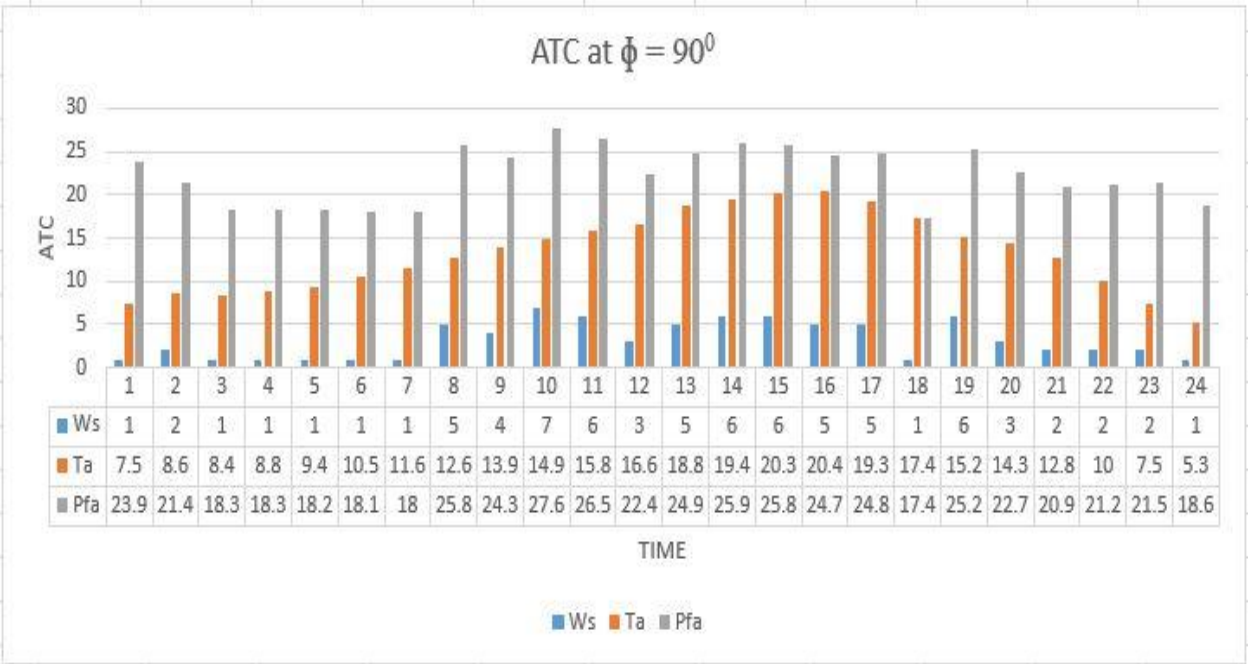

	1	2	3	4	5	6	7	8	9	10	11	12	13	14	15	16	17	18	19	20	21	22	23	24
Ws	1	2	1	1	1	1	1	5	4	7	6	3	5	6	6	5	5	1	6	3	2	2	2	1
Ta	7.5	8.6	8.4	8.8	9.4	10.5	11.6	12.6	13.9	14.9	15.8	16.6	18.8	19.4	20.3	20.4	19.3	17.4	15.2	14.3	12.8	10	7.5	5.3
Pfa	23.9	21.4	18.3	18.3	18.2	18.1	18	25.8	24.3	27.6	26.5	22.4	24.9	25.9	25.8	24.7	24.8	17.4	25.2	22.7	20.9	21.2	21.5	18.6

Figure 5.14 Hourly Representation of ATC from line 2-6 at 90^0

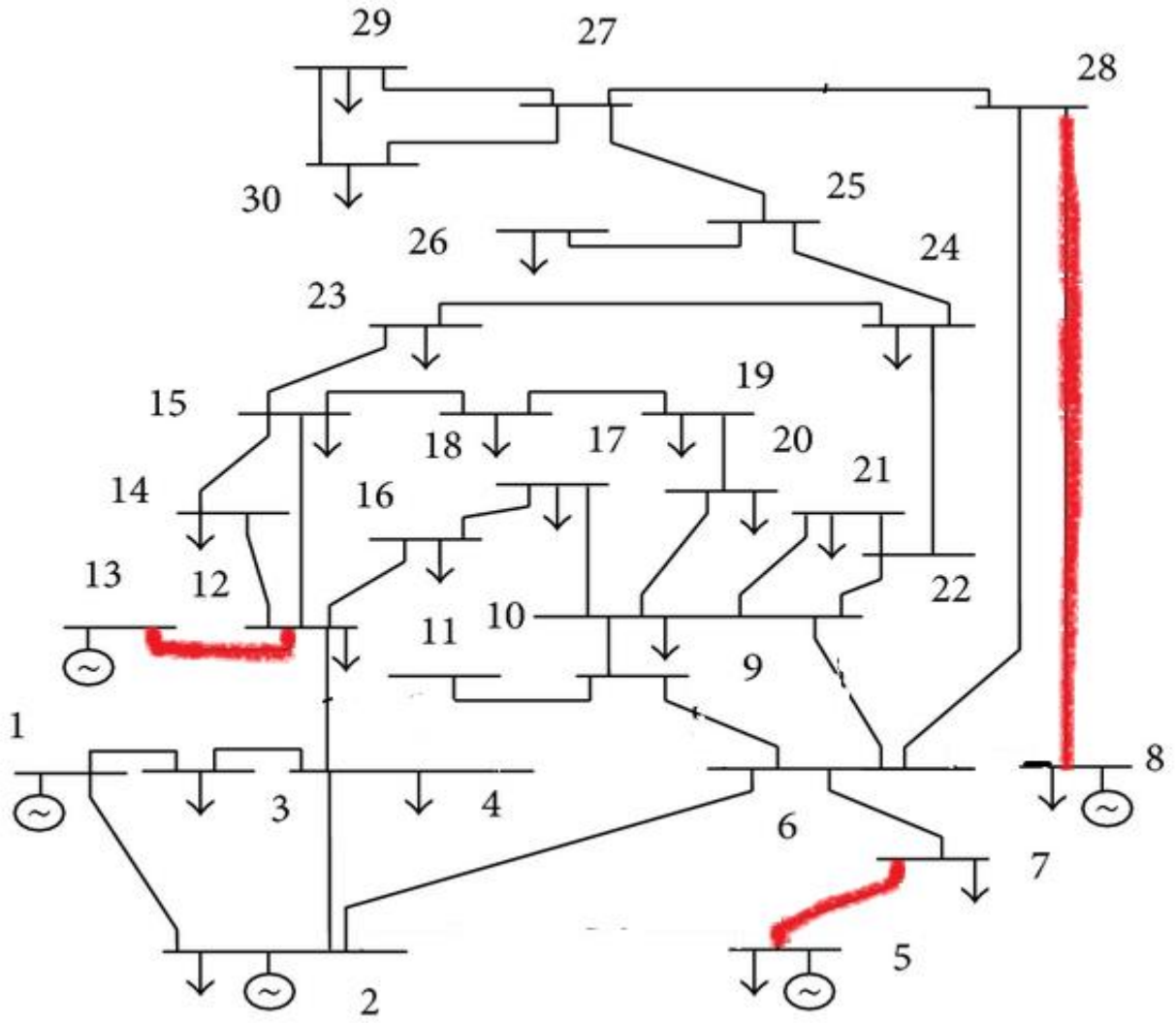

Figure 5.15 Test lines (5-7, 12-13 and 8-28) for ATC calculation

The lines for which ATC has calculated i.e. generating to load ends has been highlighted in Fig 5.15. Bus 5, 8 and 13 are the generating bus so; weather conditions has been considered for the areas of bus 5, 8 and 13 (the generator buses has been considered in the area of Kullu for bus 5, Spiti for bus 8 and Lahaul for bus 13) change in ATC of the lines for a full day has been shown in Fig 5.16 to Fig 5.21 and the data for wind speed, ambient temperature has been tabulated in Table 5.9 for line (5-7), Table 5.10 for line (12-13) and Table 5.11 for line (8-28).

ATC from bus (5-7)

Table 5.8 Available transfer capability from bus 5-7

Time	Ws(m/s)	Ta(^{0}C)	ATC at $\Phi = 45^0$	ATC at $\Phi = 90^0$
1	2	15.4000	14.4325	15.8835
2	1	17.0000	11.5832	12.8693
3	1	16.9000	11.3042	12.3052
4	2	17.2000	13.2721	14.4808
5	2	18.7000	13.0644	14.2571
6	2	19.0000	13.0223	14.2119
7	2	21.1000	12.7240	13.8909
8	2	22.9000	12.4618	13.6091
9	2	24.7000	12.1933	13.3207
10	5	24.4000	15.3423	16.7877
11	3	24.0000	13.5817	14.8477
12	2	28.8000	11.5559	12.6369
13	2	31.5000	11.1140	12.1636
14	2	30.0000	12.5611	14.2035
15	2	32.4000	10.9623	12.0014
16	8	31.9000	15.6755	17.1805
17	2	29.0000	11.5238	12.6025
18	4	28.5000	13.7847	15.0888
19	1	26.5000	10.0778	10.9958
20	1	24.0000	10.4133	11.3534
21	2	21.5000	12.6662	13.8288
22	1	19.2000	11.0248	12.0063
23	3	16.4000	14.7575	16.1168
24	1	13.6000	11.6915	12.7200

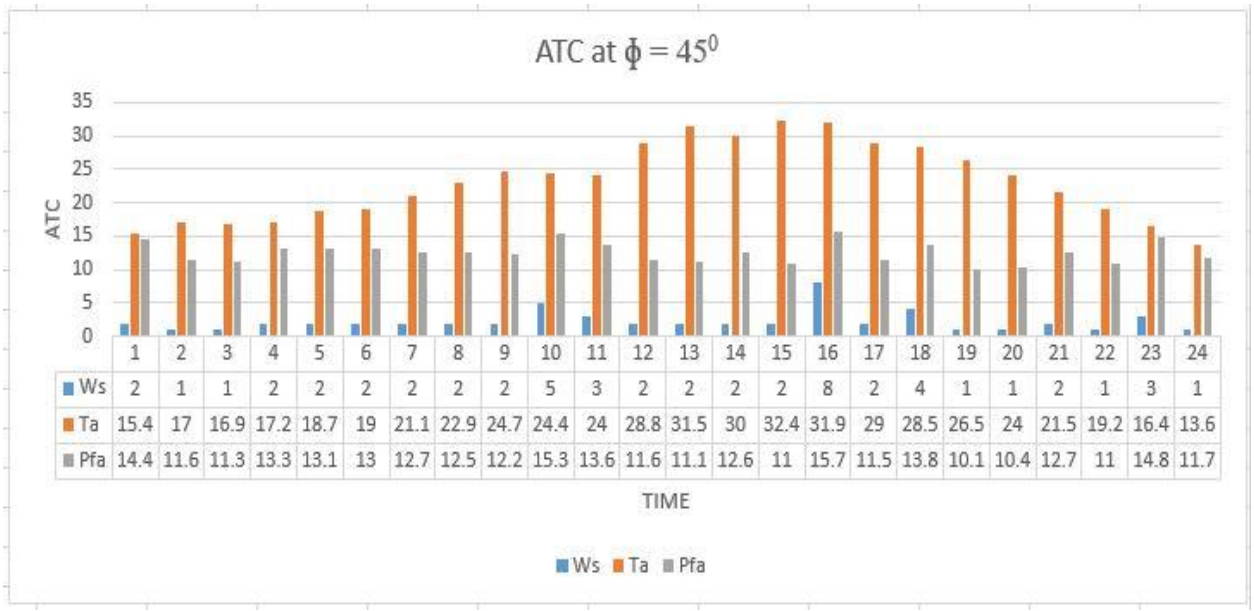

	1	2	3	4	5	6	7	8	9	10	11	12	13	14	15	16	17	18	19	20	21	22	23	24
Ws	2	1	1	2	2	2	2	2	2	5	3	2	2	2	2	8	2	4	1	1	2	1	3	1
Ta	15.4	17	16.9	17.2	18.7	19	21.1	22.9	24.7	24.4	24	28.8	31.5	30	32.4	31.9	29	28.5	26.5	24	21.5	19.2	16.4	13.6
Pfa	14.4	11.6	11.3	13.3	13.1	13	12.7	12.5	12.2	15.3	13.6	11.6	11.1	12.6	11	15.7	11.5	13.8	10.1	10.4	12.7	11	14.8	11.7

Figure 5.16 Hourly Representation of ATC from line 5-7 at 45^0

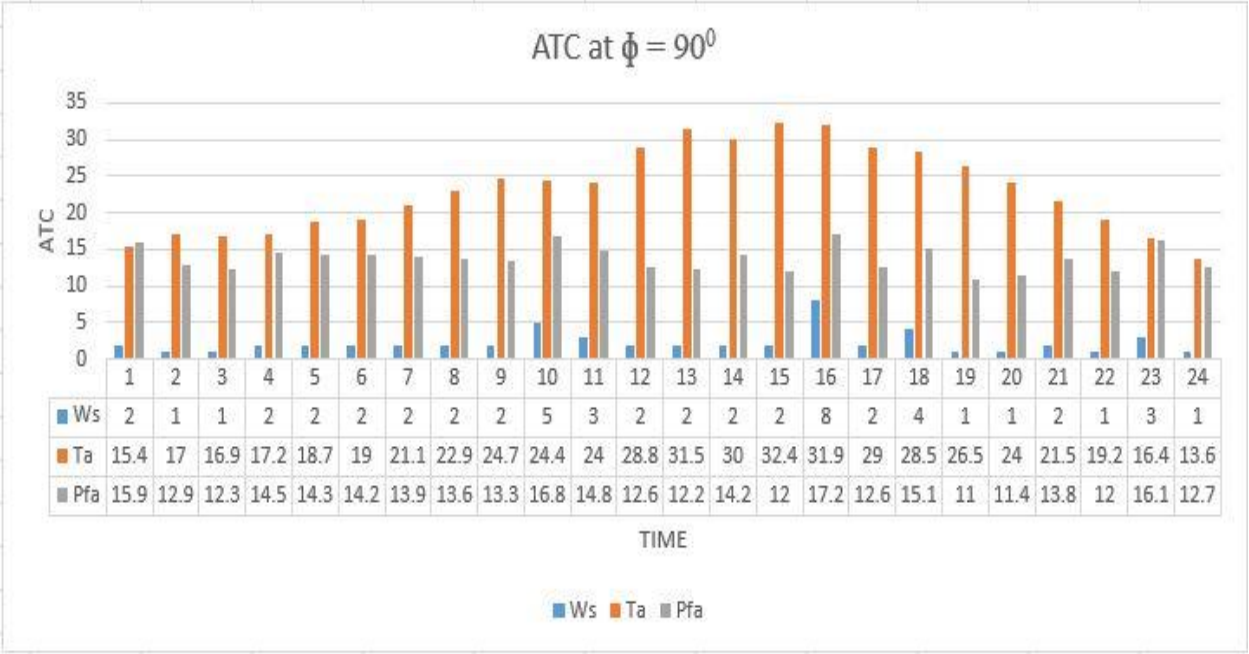

	1	2	3	4	5	6	7	8	9	10	11	12	13	14	15	16	17	18	19	20	21	22	23	24
Ws	2	1	1	2	2	2	2	2	2	5	3	2	2	2	2	8	2	4	1	1	2	1	3	1
Ta	15.4	17	16.9	17.2	18.7	19	21.1	22.9	24.7	24.4	24	28.8	31.5	30	32.4	31.9	29	28.5	26.5	24	21.5	19.2	16.4	13.6
Pfa	15.9	12.9	12.3	14.5	14.3	14.2	13.9	13.6	13.3	16.8	14.8	12.6	12.2	14.2	12	17.2	12.6	15.1	11	11.4	13.8	12	16.1	12.7

Figure 5.17 Hourly Representation of ATC from line 5-7 at 90^0

ATC from bus (12-13)

Table 5.9 Available transfer capability of from bus 12-13

Time	Ws(m/s)	Ta(^{0}C)	ATC at $\Phi = 45^0$	ATC at $\Phi = 90^0$
1	2	15.4000	15.2683	16.3273
2	1	17.0000	13.2544	14.5623
3	1	16.9000	12.8066	13.9406
4	2	17.2000	15.0360	16.4053
5	2	18.7000	14.8006	16.1519
6	2	19.0000	14.7530	16.1007
7	2	21.1000	14.4150	15.7370
8	2	22.9000	14.1180	15.4177
9	2	24.7000	13.8138	15.0910
10	5	24.4000	17.3813	19.0188
11	3	24.0000	15.3867	16.8210
12	2	28.8000	13.0917	14.3163
13	2	31.5000	12.5910	13.7802
14	3	30.0000	14.2891	15.2246
15	2	32.4000	12.4192	13.5964
16	8	31.9000	17.7588	19.4638
17	2	29.0000	13.0553	14.2774
18	4	28.5000	15.6167	17.0941
19	1	26.5000	11.4171	12.4572
20	1	24.0000	11.7972	12.8623
21	2	21.5000	14.3496	15.6666
22	1	19.2000	12.4900	13.6019
23	3	16.4000	16.7188	18.2587

Time	Ws(m/s)	Ta(^{0}C)	ATC at $\Phi = 45^0$	ATC at $\Phi = 90^0$
24	1	13.6000	13.2453	14.4105

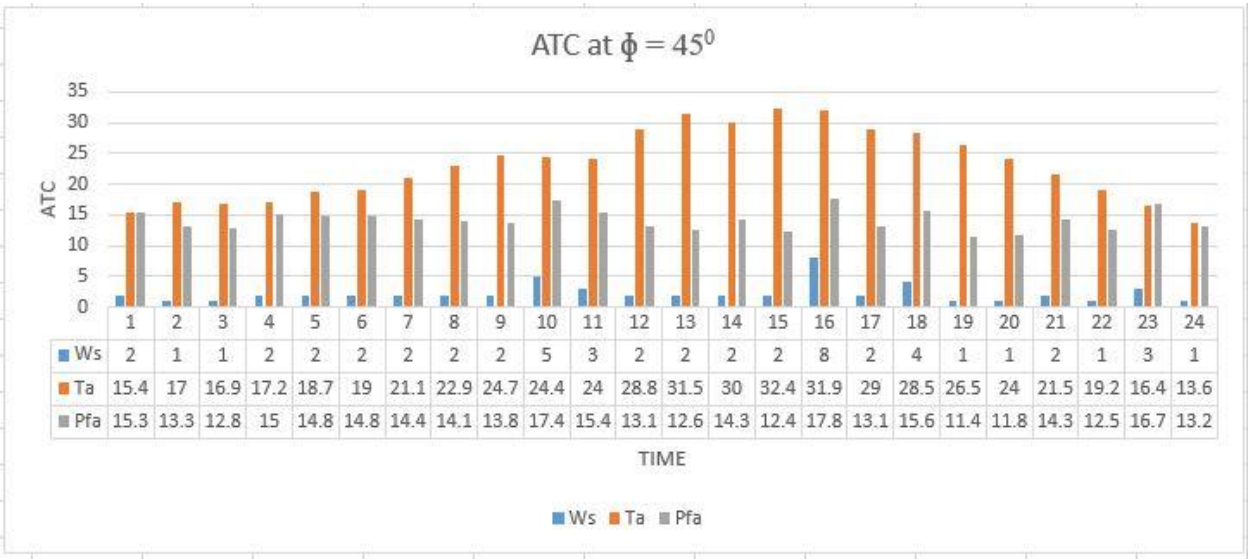

	1	2	3	4	5	6	7	8	9	10	11	12	13	14	15	16	17	18	19	20	21	22	23	24
Ws	2	1	1	2	2	2	2	2	2	5	3	2	2	2	2	8	2	4	1	1	2	1	3	1
Ta	15.4	17	16.9	17.2	18.7	19	21.1	22.9	24.7	24.4	24	28.8	31.5	30	32.4	31.9	29	28.5	26.5	24	21.5	19.2	16.4	13.6
Pfa	15.3	13.3	12.8	15	14.8	14.8	14.4	14.1	13.8	17.4	15.4	13.1	12.6	14.3	12.4	17.8	13.1	15.6	11.4	11.8	14.3	12.5	16.7	13.2

Figure 5.18 Hourly Representation of ATC from line 12-13 at 45^0

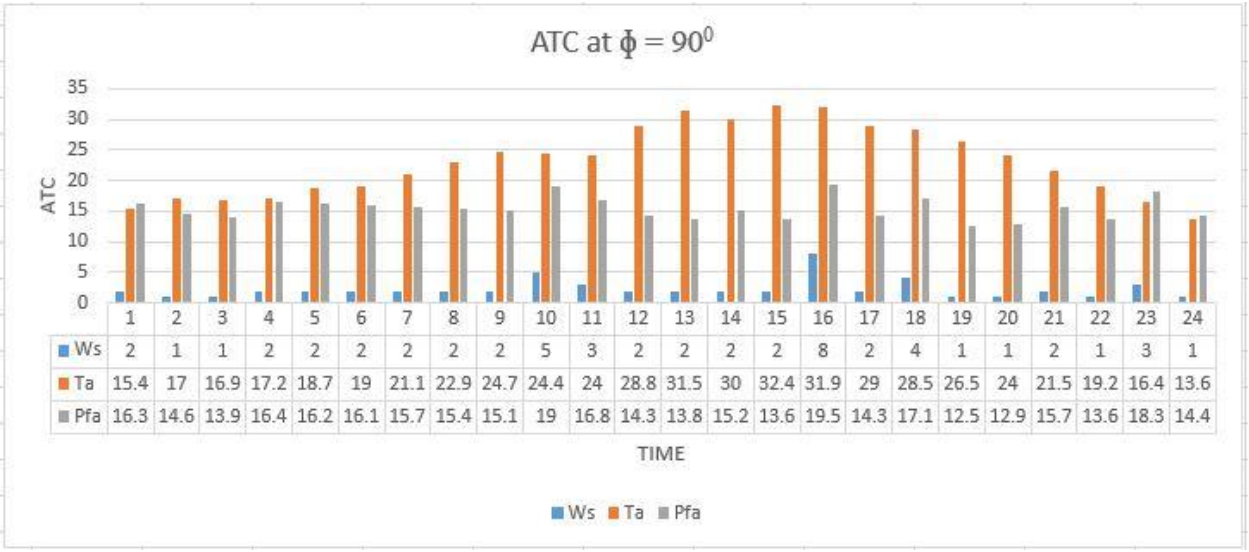

	1	2	3	4	5	6	7	8	9	10	11	12	13	14	15	16	17	18	19	20	21	22	23	24
Ws	2	1	1	2	2	2	2	2	2	5	3	2	2	2	2	8	2	4	1	1	2	1	3	1
Ta	15.4	17	16.9	17.2	18.7	19	21.1	22.9	24.7	24.4	24	28.8	31.5	30	32.4	31.9	29	28.5	26.5	24	21.5	19.2	16.4	13.6
Pfa	16.3	14.6	13.9	16.4	16.2	16.1	15.7	15.4	15.1	19	16.8	14.3	13.8	15.2	13.6	19.5	14.3	17.1	12.5	12.9	15.7	13.6	18.3	14.4

Figure 5.19 Hourly Representation of ATC from line 12-13 at 90^0

ATC from bus (8-28)

Table 5.10 Available transfer capability from bus 8-28

Time	Ws(m/s)	Ta(^{0}C)	ATC at $\Phi = 45^0$	ATC at $\Phi = 90^0$
1	2	18.3000	8.2065	9.4325
2	1	17.0000	9.8562	10.5562
3	1	16.9000	9.2025	10.0173
4	2	17.2000	10.8045	11.7884
5	2	18.7000	10.6353	11.6063
6	2	19.0000	10.6011	11.5695
7	2	21.1000	10.3582	11.3082
8	2	22.9000	10.1448	11.0788
9	2	24.7000	9.9263	10.8440
10	5	24.4000	12.4897	13.6664
11	3	24.0000	11.0565	12.0871
12	2	28.8000	9.4073	10.2873
13	2	31.5000	9.0476	9.9021
14	3	30.0000	11.5422	12.6623
15	2	32.4000	8.9241	9.7700
16	8	31.9000	12.7610	13.9861
17	2	29.0000	9.3812	10.2593
18	4	28.5000	11.2217	12.2834
19	1	26.5000	8.2040	8.9514
20	1	24.0000	8.4772	9.2425
21	2	21.5000	10.3112	11.2576
22	1	19.2000	8.9750	9.7740
23	3	16.4000	12.0137	13.1202

Time	Ws(m/s)	Ta(^{0}C)	ATC at $\Phi = 45^0$	ATC at $\Phi = 90^0$
24	1	13.6000	9.5178	10.3550

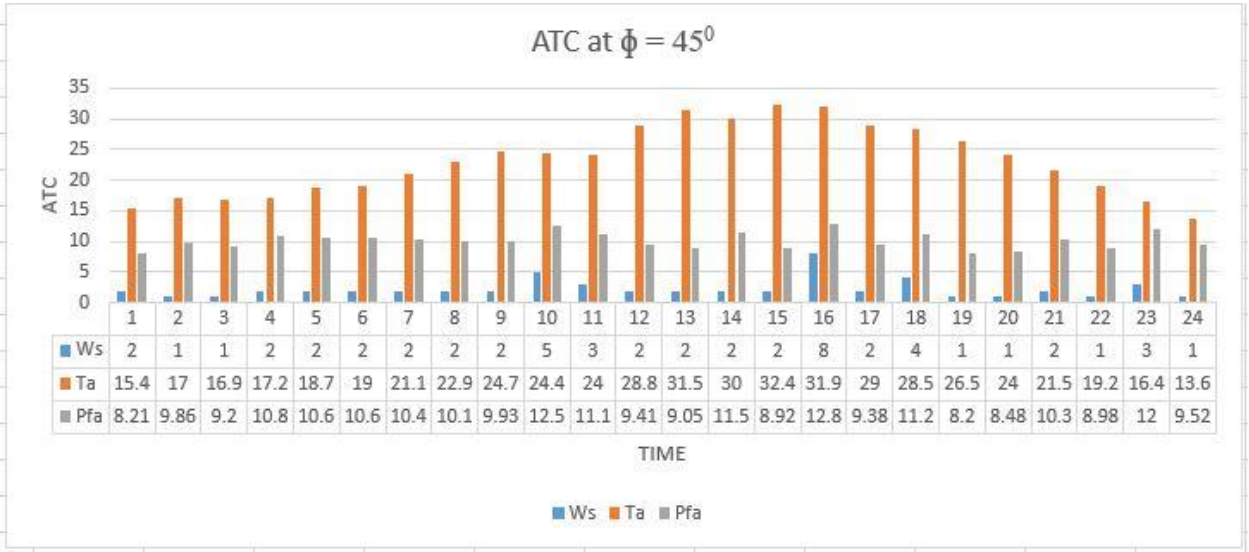

	1	2	3	4	5	6	7	8	9	10	11	12	13	14	15	16	17	18	19	20	21	22	23	24
Ws	2	1	1	2	2	2	2	2	2	5	3	2	2	2	2	8	2	4	1	1	2	1	3	1
Ta	15.4	17	16.9	17.2	18.7	19	21.1	22.9	24.7	24.4	24	28.8	31.5	30	32.4	31.9	29	28.5	26.5	24	21.5	19.2	16.4	13.6
Pfa	8.21	9.86	9.2	10.8	10.6	10.6	10.4	10.1	9.93	12.5	11.1	9.41	9.05	11.5	8.92	12.8	9.38	11.2	8.2	8.48	10.3	8.98	12	9.52

Figure 5.20 Hourly Representation of ATC from line 8-28 at 45^0

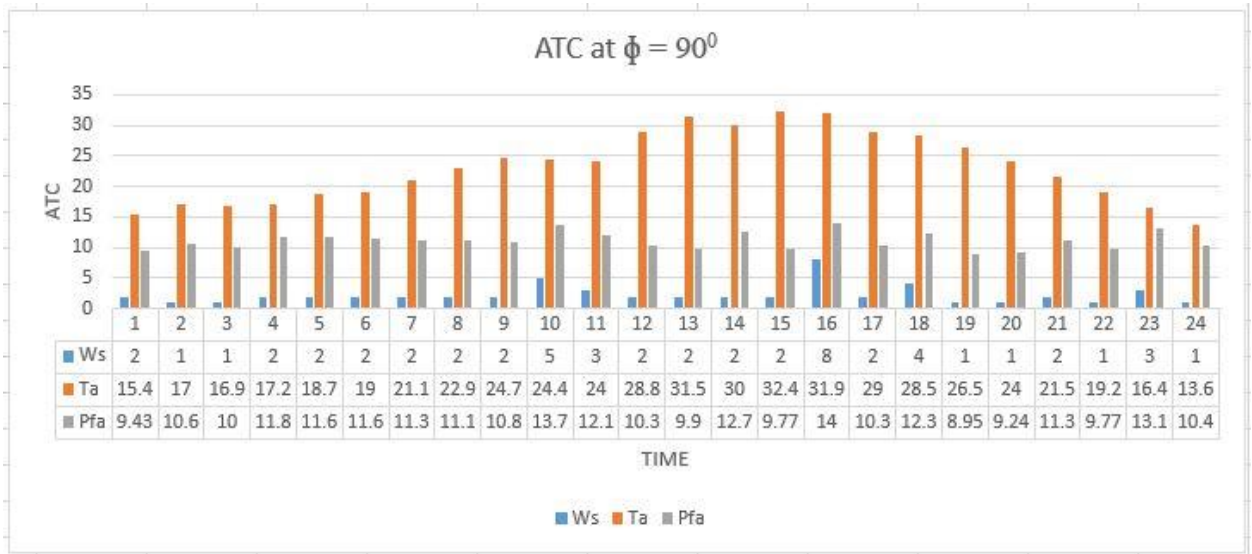

	1	2	3	4	5	6	7	8	9	10	11	12	13	14	15	16	17	18	19	20	21	22	23	24
Ws	2	1	1	2	2	2	2	2	2	5	3	2	2	2	2	8	2	4	1	1	2	1	3	1
Ta	15.4	17	16.9	17.2	18.7	19	21.1	22.9	24.7	24.4	24	28.8	31.5	30	32.4	31.9	29	28.5	26.5	24	21.5	19.2	16.4	13.6
Pfa	9.43	10.6	10	11.8	11.6	11.6	11.3	11.1	10.8	13.7	12.1	10.3	9.9	12.7	9.77	14	10.3	12.3	8.95	9.24	11.3	9.77	13.1	10.4

Figure 5.21 Hourly Representation of ATC from line 8-28 at 90^0

Chapter6. Conclusion and Future work

6.1 Conclusion

The IEEE standard 738 equations has been used for, implementation of predicted or real weather conditions on transmission line system will lead to a efficient solution for power transfer. The main focus of this work has been on showing the effect of change in wind angle with conductor axis which further lead to the improvement in ATC of the transmission lines. Modified IEEE 6-bus and 30-bus system has been used to demonstrate the effect of dynamic weather conditions on the ATC level. The single line diagram for both the bus systems are shown in respective chapters. In order to evaluate the available transfer capability, the effect of dynamic weather conditions has been considered only on the generator buses to the load buses known as source and sink buses. It is better to take the real time weather condition or predicted weather conditions to forecast the accurate power carrying capability of line at any time. It should be noticed that if overall temperature of the area has been decreases the capacity of the thermal limit of the line has been increases. Hence the power carrying capability of the line will also increase. The wind speed and direction of wind with conductor axis are also the main factors and affect the ATC of the line and thermal capacities of the line, also it is shown that only few lines (Generation bus- to -Load bus) are limited in a specific power interchange. In other words, DLR method, based on environmental conditions predictions has been only necessary for limited lines. A MATLAB code has been developed to verify the dynamic line ampacity of an overhead transmission line, with considering the predicted change in ambient temperature and wind speed. The wind angle direction also affects the power carrying capability of the transmission lines or ATC of the line. To showing the effect of change in wind angle on ATC of line a 6-bus system and 30-bus system has been taken as the test systems. The effect of DLR method has been only considered on the buses those are directly connected with generator buses. The effect of the wind angle has been divided into two criterions worst wind angle i.e. $45^0$and best wind angle i.e. 90^0. Then see the effect of both the wind angles respectively on the ATC of the transmission lines while considering the predicted weather data and plot the results which show that with increase in temperature, decrease in wind speed and bad wind angle the ATC of the line has been also poor and at that time the losses in the line will also

increase but when wind speed has been increased and wind angle has been considered good then ATC of the line will increased. At a very low temperature (0^0 to 8^0), high wind speed (6m/s to 15m/s) and wind angle of 90^0 the ATC of the line will exceed the TTC (Total Transfer capability) of the line which shows the decrease in the losses of the line.

6.2 Future Work

This thesis work has been mainly focused on power carrying capability of line based on dynamic ampacity of the line which has been calculated with the help of dynamic line rating (DLR) method. The DLR method is implemented on the different lines (consider the moose and zebra conductor) of a bus system for a whole day with one-hour gap, because of the technical and economic advantages of this system as concluded from this thesis the usage of this system is extended to a larger extent. Although the work has been successfully implemented there is still lot of future scope left in this work which can be listed as follows.

- The results for IEEE standard 738 and CIGER can be compared to choose the best standard.
- Dynamic rating of transformers is also possible to identified in response to upgrade the system or upgrade the ratings of line (based on dynamic line rating method).
- Real time monitoring of wind direction angle with conductor axis is also the good scope of work to estimate the accurate power carrying capability of transmission lines.

References

[1]. Bahadoorsingh, S., L. Bhairosingh, M. Ganness, and C. Sharma. "Improving overhead transmission line usage efficiency on a caribbean island power system." In *T&D Conference and Exposition, 2014 IEEE PES*, pp. 1-5. IEEE, 2014.

[2]. Fernandez, E., I. Albizu, M. T. Bedialauneta, A. J. Mazon, and P. T. Leite. "Dynamic line rating systems for wind power integration." In *Power Engineering Society Conference and Exposition in Africa (PowerAfrica), 2012 IEEE*, pp. 1-7. IEEE, 2012.

[3] Mahmoudian, M., and G. R. Yousefi. "ATC improvement and losses estimation considering dynamic transmission line ratings." In *Electrical Engineering (ICEE), 2012 20th Iranian Conference on*, pp. 404-409. IEEE, 2012.

[4] Abdalla, Omar H., Rashid Al-Badwawi, Hilal Al-Hadi, Hisham Al-Riyami, and Ahmed Al-Nadabi. "Weather-Based Ampacity of Overhead Transmission Lines." In *The 4th General Conference of Arab Union of Electricity and Exhibition, 7-9 January 2013, Doha, Qatar*. 2013.

[5] Yip, Tony, Chang An, Graeme Lloyd, Martin Aten, and B. Ferri. "Dynamic line rating protection for wind farm connections in Integration of Wide-Scale Renewable Resources into the Power Delivery System." In *CIGRE/IEEE PES Joint Symposium*. 2009.

[6] Albizu, Igor, et al. "Influence of the conductor temperature error on the overhead line ampacity monitoring systems." IET Generation, Transmission & Distribution 5.4 (2011): pp. 440-447.

[7]. Alvarez, J. Rodriguez, and C. M. Franck. "Evaluation of the accuracy of a thermal rating model to estimate the temperature of operational transmission lines." CIGRE Science & Engineering (2016).

[8] Bockarjova, Marija, and Goran Andersson. "Transmission line conductor temperature impact on state estimation accuracy." In *Power Tech, 2007 IEEE Lausanne*, pp. 701-706. IEEE, 2007.

[9] Cigr'e Working Group B2.12, Guide for selection of weather parameters for bare overhead conductor ratings, Cigre Brochure 299, August 2006

[10] A. K. Deb, Power line ampacity system: theory, modeling, and applications. Boca Raton: CRC Press, 2000

[11] IEEE, “Standard for calculating the current-temperature of bare overhead conductors,” IEEE Std 738-2006 (Revision of IEEE Std 738-1993), pp. c1–59, 30 2007 Conductors. New York. 1993.

[12] Miura, Masaki, Takuya Satoh, Shinichi Iwamoto, and Ikuo Kurihara. "Application of dynamic rating to evaluation of ATC with thermal constraints considering weather conditions." In *Power Engineering Society General Meeting, 2006. IEEE*, pp. 6-pp. IEEE, 2006.

[13] “Progress of National Reliability Council for Electricity(NRCE)”, Government of India, Ministry of power, central electricity authority.

[14] Merante, Marco. "Application of dynamic rating to improve transportation capability of the power systems connected to wind power plants." (2016).

[15] D. A. Douglass and A. Edris, “Field Studies of Dynamic Thermal Rating Methods for Overhead Lines,” pp. 842–851, 1999

[16] Douglass, Dale A., et al. "Dynamic thermal ratings realize circuit load limits." IEEE Computer Applications in Power 13.1 (2000): pp. 38-44.

[17]. Mai, RuiKun, Ling Fu, and Xu HaiBo. "Dynamic line rating estimator with synchronized phasor measurement." In *Advanced Power System Automation and Protection (APAP), 2011 International Conference on*, vol. 2, pp. 940-945. IEEE, 2011.

[18] Mousavi-Seyedi, Seyed Sina, Farrokh Aminifar, Sina Azimi, and Zahra Garoosi. "On-line assessment of transmission line thermal rating using PMU data." In *Smart Grid Conference (SGC), 2014*, pp. 1-6. IEEE, 2014.

[19] Merrell, John, Tacoma Power, Mike P. Diedesch, and Jared R. Johnson. "Dynamic Line Ratings for the Cowlitz-LaGrande Transmission Lines." Washington State University, 2008.

[20] H. D. Chiang, A. J. Flueck, K. S. Shah, and N. Balu, “CPFLOW: A Practical Tool for Tracing Power System Steady-State Stationary Behavior Due to Load and Generation Variation.,” IEEE Trans. Power Systems, May 1995, pp. 623-634.

[21] Wijethunga, A. H., J. V. Wijayakulasooriya, and J. B. Ekanayake. "Effect of sampling rate of weather parameters on the dynamic line rating." In *Industrial Instrumentation and Control (ICIC), 2015 International Conference*, pp. 663-668. IEEE, 2015.

[22] Black, W. Z. and Rehberg, R. L., “Simplified model for steady-state and real-time ampacity of overhead conductors,” IEEE Transactions on Power Apparatus and Systems, vol. 104, Oct. 1985, pp 29-42

[23] Black, W. Z. and Byrd, W. R., “Real-time ampacity model for overhead lines,” IEEE Transactions on Power Apparatus and Systems, vol. PAS-102, No. 7, July 1983, pp. 2289-2293.

[24] Aluminum Electrical Conductor Handbook, 2nd ed. Washington, DC: The Aluminum Association, 1982.

[25] Douglass, D. A., Kirkpatrick, L. A. and Rathbun, L. S., “AC resistance of ACSR-Magnetic and temperature effects,” IEEE Transactions on Power Apparatus and Systems, vol. PAS-104, no. 6, pp. 1578-1584, June, 1985.

[26] Davis, M. W., “A new thermal rating approach: the real time thermal rating system for strategic overhead conductor transmission lines, Part II.” IEEE Transactions on Power Apparatus and Systems, vol. PAS97, pp. 810-825, Mar./Apr. 1978.

[27] Heating, Ventilating and Air-Conditioning Guide. New York: American Society of Heating, Refrigerating, and Air-Conditioning Engineers, 1956.

[28] Indian metrological data [online] Available: http://www.imdaws.com/ViewAWSData.aspx

[29] Cigr´e Working Group B2.36, Guide for Application of Direct Real-Time Monitoring Systems Cigr´e Brochure 498, June 2012.

Appendix

Symbols	Description	Practice Value	Units
	Conductor Attributes		
D	Diameter of Conductor	31.77- moose, 28.6- zebra	mm
Tlow	AC resistance for minimum conductor	25	°C
R(Tlo w)	AC resistance at T_{low}	$7.283x10^{-5}$	Ωm^{-1}
Thigh	AC resistance for maximum conductor	75	°C
R(Thigh)	AC resistance at T_{high}	$8.688x10^{-5}$	Ωm^{-1}
	Geographical Parameters		
Z_1	Line azimuth	90	°
He	Elevation of conductor from sea level	100	m
	Atmospheric Parameters		
T_a	Ambient temperature of air	variable	°C
T_c	Maximum Temperature of conductor	as per cond.	°C
α	Emissivity	0.8	
ε	Solar absorptivity	0.6	
lat	Degrees of Latitude	variable	°c
V_w	Wind speed	variable	ms^{-1}
N	Day of year	Predicted or real time	

t	Time of day	hourly	
Solar parameters			
Ω	Hour angle	-15	^{0}c
Zc	Solar azimuth	Depend upon hour angel	
Hc	Solar altitude	calculated	